

Some pages of this thesis may have been removed for copyright restrictions.

If you have discovered material in Aston Research Explorer which is unlawful e.g. breaches copyright, (either yours or that of a third party) or any other law, including but not limited to those relating to patent, trademark, confidentiality, data protection, obscenity, defamation, libel, then please read our [Takedown policy](#) and contact the service immediately (openaccess@aston.ac.uk)



Development of an in-vitro animal model to evaluate novel pharmaceutical approaches to DED management

FRANCESCO MENDUNI

Doctor of Philosophy

ASTON UNIVERSITY

December 2018

©Francesco Menduni, 2018

Francesco Menduni asserts his moral right to be identified as the author of
this thesis

This copy of the report has been supplied on the condition that anyone who
consults it is understood to recognise that its copyright rests with its author
and that no quotation from the thesis and no information derived from it may
be published without appropriate permission or acknowledgement.

ASTON UNIVERSITY

English Abstract

School of Life and Health Sciences
Biomedical Engineering

Doctor of Philosophy

Development of an in-vitro animal model to evaluate novel pharmaceutical approaches to DED management

by Francesco MENDUNI

In the ophthalmic field, multifactorial pathologies such as Dry Eye Disease (DED) and cataract are largely studied in living animal models that can fail to precisely mirror the complexity of these conditions in humans. Recent advances in biomedical technologies have improved the reliability of *in-vitro/ex-vivo* animal alternatives, and to date, the corneal and crystalline lens tissue have been independently maintained physiologically stable for 10 days.

This thesis details the development of a novel and complete *ex-vivo* anterior eye model, which is capable of sustaining both the cornea and crystalline lens in a physiologically stable state in loco for 7 days. The platform is based on porcine eyes, which represent a high quality and reliable human tissue source substitute, and being slaughterhouse waste, also perfectly align the project with the 3Rs principle of replacing, refining and reducing living animal experimentation. The model is modular and scalable, allowing for the maximisation of experimental reliability, and the minimisation of waste and energy use. In addition, the whole system is designed to be fitted in a laminar flow cabinet, avoiding external biological contamination, and is easily transportable between tissue engineering laboratories, maximising accessibility.

The model was validated estimating cell viability over time. Stromal fibroblasts were found to be viable up to the seventh day of culture, and corneal and crystalline lens tissue maintained their transparency over the culturing period. Dry Eye Disease was successfully induced in the model by irrigating the ocular surface every 40s, and validated using impression cytology technique. Moreover, due to the unique presence in loco of the crystalline lens, the model was also used as a platform to perfect cataract surgery and successfully implant intraocular lenses (IOLs).

The novel and complete *ex-vivo* anterior eye model developed in this thesis provides further insights into pre-clinical anterior segment investigations in ophthalmology, taking a step forward toward bridging the existing gap between *in-vitro* and *in-vivo* biomedical technologies.

Keywords: Ex-vivo; Ex-vitro; Organ culture; Cornea; Crystalline lens; Dry Eye

UNIVERSIDAD COMPLUTENSE MADRID

Spanish Abstract

Facultad de Óptica y Optometría
Departamento de Optometría y Visión

Doctorado en Óptica, Optometría y Visión

Desarrollo de un modelo animal in-vitro para evaluar nuevos fármacos para el tratamiento de ojo seco.

Doctorando Francesco MENDUNI

Dentro del campo oftalmológico, patologías multifactoriales como Enfermedad del Ojo Seco (EOS) y Cataratas son ampliamente estudiadas a través de modelos animales que no reproducen con exactitud estas condiciones en humanos debido a su complejidad. Los recientes avances en la tecnología biomédica han mejorado la fiabilidad de modelos animales in-vitro/ex-vivo, y hasta el momento, el tejido de la córnea y cristalino se han mantenido fisiológicamente estables de forma independiente durante 10 días.

Esta tesis describe el desarrollo de un nuevo y completo modelo de ojo anterior ex vivo, que es capaz de mantener tanto la córnea como el cristalino en un estado fisiológico estable durante 7 días. La plataforma se basa en ojos porcinos, que representan una fuente alternativa al tejido humano de alta calidad y fiable, y al tratarse de residuos de matadero, también alinea perfectamente el proyecto con el principio 3Rs de reemplazar, refinar y reducir la experimentación con animales vivos. El modelo es modular y escalable, permitiendo la maximización de la fiabilidad experimental y la minimización de los residuos y el uso de energía. Además, todo el sistema está diseñado para instalarse en un gabinete de flujo laminar, evitando la contaminación biológica externa, y facilitando su transporte entre los laboratorios de ingeniería de tejidos, aumentando así la accesibilidad del mismo.

El modelo fue validado estimando la viabilidad celular en el transcurso del tiempo. Se encontró que los fibroblastos estromales eran viables hasta el séptimo día de cultivo, y el tejido corneal y cristalino mantuvieron su transparencia durante el período de cultivo. La enfermedad del ojo seco se indujo con éxito en el modelo mediante irrigación de la superficie ocular cada 40 s, y se validó utilizando la técnica de citología de impresión. Además, debido a que la posición del cristalino no se ha alterado, el modelo también se utilizó como plataforma para perfeccionar la cirugía de cataratas e implantar con éxito lentes intraoculares (LIOs).

El novedoso y completo modelo de ojo anterior ex-vivo desarrollado en esta tesis proporciona información adicional sobre investigaciones pre-clínicas del segmento anterior en oftalmología, dando un paso adelante para reducir las diferencias existentes entre las tecnologías biomédicas in-vitro e in-vivo.

Palabras clave: Ex-vivo; Ex-vitro; Cultivo Órganos; Cornea; Lente cristalina; Ojo Seco.

“Ad Maiora Semper”

Acknowledgements

This thesis represents the most important and arduous goal of my life so far, and I would have never been able to achieve it without the help and love of the people that have constantly supported me along these three long years.

In primis, I would like to thank my supervisors: Prof. James Wolffsohn, my greatest professional inspiration, Prof. Leon Davies, for his guidance in my first year and his continuous support, and Dr. Antonio Fratini for the important opportunities given to me within the Biomedical Engineering degree course at Aston.

Secondly, I would like to thank all the people I was lucky enough to meet at Aston University. Graham, for having taught me all the secrets of the mechanical workshop with love and passion. Ipek, Gibran, Maria, Tecla, Patrick, Virginia, Fiona, Radovan, Samir, Isotta e Fabio, for all the coffees, launches and happy moments shared in the office. A special thank goes to Ipek for having got my back every day, and to Gibran for having turned the long hours in the wetlab into enjoyable moments.

I thank the whole EDEN group for all the unforgettable experiences lived together around the world. They could have never picked a better acronym for our group. In particular, I would like to thank Dr. David Madrid Costa for the attention and care given us in every meeting.

I thank Giovanni and Luca, for having shared with me the journey of creating something that goes well beyond selling olive oil in UK. It is rare to find such good friends in such a short period of time, and for this I feel blessed. Giovanni, it will be an honour to be on your side in such an important day of your life.

I thank Lucia and Massimiliano, for having been unforgettable examples of friendship and family that will always inspire me.

I thank Antonio, a real older brother for me. If we did not meet that famous afternoon, I could have never been here today. I will always be grateful to you for this incredible experience. Thanks for having believed in me.

I thank Paolo, Tecla, Filippo, Gloria, Giacomo, Alberto, Silvia, Diandra e Sasan for having made Birmingham a less grey place to live by organising great dinners, parties and beers out.

I thanks my lifelong friends, Gennaro, Andrea, Damiano, Giovanni, Mirko e Gaetano, for having proved me that the friendship is something that does not suffer from time or distance. I am blessed to have you as brothers.

I thank mum, dad, Monica, uncle Antonio, grandpa Franco and grandma Ida, for having taught me the value of the family. I would always be grateful to you.

I thank Anna, for having been on my side every day regardless the huge struggle of the distance. I can't wait for the 28/08/19 to come - you will make me the happiest man on the earth. I love you.

Finally, I would like to thank grandma Tina and grandpa Nicola, for having guided and protected me when I was a child, and for continuing to do so from up there.

Acknowledgements

Questa tesi rappresenta il traguardo più importante ed impegnativo della mia vita, e non sarei mai stato capace di raggiungerlo senza l'affetto e la guida delle persone che mi sono state vicine durante questi tre lunghi anni.

In primis, ringrazio i miei relatori di tesi. Prof. James Wolffsohn, per essere semplicemente la mia più grande fonte di ispirazione professionale, Prof. Leon Davies, per la sua accorta guida durante il mio primo anno di dottorato, e Dr. Antonio Fratini per le importanti opportunità datemi nel corso di laurea di Ingegneria Biomedica ad Aston.

In secondo luogo, vorrei ringraziare tutte le persone che ho avuto la fortuna di incontrare ad Aston durante questo cammino. Ringrazio Graham, per avermi trasmesso la sua grande esperienza con amore e passione. Ringrazio Ipek, Gibran, Maria, Tecla, Patrick, Virginia, Fiona, Radovan, Samir, Isotta e Fabio, per gli innumerevoli caffè, pranzi e momenti felici che hanno reso l'ufficio una vera e propria seconda casa. Tra tutti, un grazie speciale va ad Ipek, per aver avuto una parola di conforto anche nei momenti più bui, e a Gibran per aver reso piacevoli anche le lunghe ore passate in laboratorio.

Ringrazio tutto il gruppo EDEN per le indimenticabili esperienze vissute in giro per il mondo. Non avrebbero potuto scegliere acronimo migliore per il nostro gruppo. In particolare, ringrazio Dr. David Madrid Costa per la cura e attenzione mostratami in ogni incontro.

Ringrazio Giovanni e Luca, per aver dato vita ad un qualcosa di speciale che va ben oltre il vendere specialità pugliesi e napoletane in terra inglese. E' raro stringere un'amicizia così bella in così poco tempo, e per questo mi sento fortunato. Giovanni, sarà un onore poter essere al tuo fianco in un giorno così importante della tua vita.

Ringrazio Lucia e il "signore di Roma" Massimiliano, per essere stati veri esempi di amicizia e famiglia che porterò sempre con me.

Ringrazio Antonio, per essere diventato un vero e proprio fratello maggiore. Se non ci fossimo incontrati quel famoso pomeriggio, tutto questo non sarebbe mai potuto succedere. Ti sarò per sempre grato per avermi dato questa fantastica possibilità e aver creduto in me.

Ringrazio Paolo, Tecla, Filippo, Gloria, Giacomo, Alberto, Silvia, Diandra e Sasan per aver alleviato il grigiore di Birmingham a ritmo di cene, feste e piacevoli birrette.

Ringrazio i miei amici di sempre, Gennaro, Andrea, Damiano, Giovanni, Mirko e Gaetano, per avermi confermato che l'amicizia vera non ha tempo e distanza. Sono fortunato ad avere dei fratelli come voi.

Ringrazio mamma, papà, Monica, zio Antonio, nonno Franco e Nonna Ida per avermi insegnato il valore della famiglia. Ve ne sarò immensamente grato.

Ringrazio Anna, per la forza e il coraggio con la quale sei stata al mio fianco, nonostante la distanza. Il 28/08/19 mi renderai l'uomo più felice del mondo. Ti amo.

Infine ringrazio Nonna Tina e Nonno Nicola, per avermi guidato e protetto da bambino, e per continuarlo a fare da lassù.

Contents

English Abstract	2
Spanish Abstract	3
Acknowledgements	5
1 Introduction	13
2 The Historical Evolution of Ex-Vivo Ocular Surface Models: a Systematic Review	17
2.1 Introduction	17
2.2 Methods	18
2.2.1 Data	18
2.2.2 Study Selection	19
2.3 Results	19
2.3.1 Corneal permeation chamber(s)	21
2.3.2 Corneal perfusion model(s)	25
Perfusion models based on whole eyeball	26
Perfusion models based on isolated corneoscleral buttons	28
2.3.3 Corneal wound healing model(s)	34
2.3.4 Artificial anterior chamber(s)	38
2.3.5 Crystalline lens model(s)	41
2.4 Discussion	42
3 Optimisation of the Porcine Ocular Tissue Storage for Biomedical Research	47

3.1	Introduction	47
3.2	Methods	48
3.3	Results	51
3.4	Discussion	54
4	Anatomical Biometry of the Porcine Eyeball	58
4.1	Introduction	58
4.2	Methods	59
4.3	Results	61
4.3.1	Corneal curvature	61
4.3.2	Corneal thickness	62
4.3.3	Anterior chamber angle and depth	64
4.3.4	Corneal diameters	64
4.3.5	Endothelial cell density (ECD)	65
4.4	Discussion	65
5	The Aston Biological Anterior Eye Model	70
5.1	Introduction	70
5.2	The organ storage system	72
5.2.1	Modular perfusion chamber	72
	Suction module	73
	Perfusion module	74
	Mounting protocol	75
5.2.2	Environmental control system	78
	Endothelial perfusion	78
	Epithelial irrigation	79
5.3	Biological evaluation	84
5.3.1	Long term survival	85
5.3.2	Dry eye replication	88
5.4	Discussion	91
6	A Novel Training Platform for Ocular Surgery	94
6.1	Introduction	94

6.2	Methods	97
6.2.1	Wet Lab for animal tissue handling setup	97
6.2.2	Perfusion chamber re-engineering	98
6.2.3	Cataract surgery	100
6.2.4	Inducing cataract in porcine eyes	101
6.3	Surgical Results	102
6.3.1	Non cataractous eyes	102
6.3.2	Cataractous eye	106
6.3.3	Trainee feedback	107
6.4	Discussion	108
7	Conclusions	112
A	Risk and COHSS assessments	153
B	Non Cataractous eye surgery feedback	179
C	Cataractous eye surgery feedback	181

List of Abbreviations

ACD	A nterior C hamber D epth
BCOP	B ovine C orneal O paCity and P ermeability
BR	B icarbonate- R inger's S olution
BSS	B alanced S alt S olution
BSS Plus	B alanced S alt S olution P lus
CAD	C omputer A ided D esign
CCC	C ontinuous C urvilinear C apsulorhexis
CCD	C harge C oupled D evice
CCT	C entral C orneal T hickness
CIC	C onjunctival I mpression C ytology
DED	D ry E ye D isease
DMA	D ynamic M echanical A nalysis
DMEM	D ulbecco's M odified E agle M edium
DPBS	D ulbecco's P hosphate- B uffered S aline
EEBA	E uropean E ye B ank A ssociation
ECD	E ndothelial C ell D ensity
FBS	F etal B ovine S erum
FR	F low R ate
GBR	G lutathione B icarbonate- R inger's S olution
HAH	H uman A queous H umour
HCEC	H uman C orneal E pithelial C ells
HEPES	4 -(2- H ydroxy E thyl)-1- P iperazine E thane S ulfonic A cid
HVH	H uman V itreous H umour

ICE	Isolated Chicken Eye
IOL	IntraOcular Lens
IOP	IntraOcular Pressure
LASIK	Laser ASsisted In situ Keratomileusis
LEC	Lens Epithelial Cells
LFS	Laser Fluorescence Spectroscopy
LR	Lactated Ringer's Solution
MEM	Minimum Essential Medium
MGD	Meibomian Gland Dysfunction
MM	Main Medium
OCT	Optical Coherence Tomography
OVD	Ophthalmic Viscosurgical Device
PAH	Porcine Aqueous Humour
PBS	Phosphate-Buffered Saline
PCB	Printed Circuit Board
PCO	Posterior Capsule Opacification
PCR	Posterior Capsule Rupture
PID	Proportional Integral Derivative
PMMA	Poly-Methyl-MethAcrylate
PTFE	PolyTetraFluoroEthylene
SC	Sodium Chloride
SD-OCT	Spectral Domain OCT
SOP	Standard Operating Procedure
SPDR	Single Pole Double Throw
T	Temperature
TF	Time Frame
TFT	Thin Film Transistor
TM	Trabecular Meshwork

List of Figures

1.1	DED: a growing reality degrading quality of life and vision.	14
2.1	Flow of study selection.	20
2.2	Schematic diagram of the pressure apparatus introduced by Stanworth and Naylor (1950).	21
2.3	Schematic diagram of the diffusion chamber introduced by Donn et al. (1959).	22
2.4	Schematic diagram of the perfusion chamber introduced by McCarey et al. (1973).	23
2.5	Schematic diagram of the corneas mounting method introduced by Dik- stein and Maurice (1972).	24
2.6	Diagram of the pDEM set up introduced by Choy et al. (2004).	28
2.7	Experimental setup of short-term Ex Vivo Eye Irritation Test, Spoler et al. (2010).	29
2.8	Schematic diagram of the perfusion system introduced by Johnson and Tschumper (1987).	31
2.9	Schematic diagram of the anterior pulsatile perfusion model introduced by Ramos & Stamer (2008).	33
2.10	Schematic diagram of the organ culture model introduced by Foreman et al. (1996).	35
2.11	Schematic diagram of the corneal organ culture introduced by Desh- pande et al. (2015).	36

2.12 Schematic diagram of the corneal perfusion chamber introduced by Zhao et al. (2006).	37
2.13 Schematic diagram of the corneal bioreactor introduced by Guindolet et al. (2017).	38
2.14 Schematic diagram of the Barron artificial anterior chamber, Bower & Rocha (2007).	40
2.15 Schematic diagram of a lens stretcher.	42
2.16 Historical evolution of the anterior eye modelling life span.	46
3.1 Enucleation of the porcine eyeball, and its transportation in air or storage solution.	49
3.2 Pachymetry on porcine eyeball.	50
3.3 Exterior view of the LAKK-M system, which includes a diagnostics block for data processing, a light-guide cable, a pulse oximeter and calibrated light filters.	51
3.4 Experimental setup of LFS on porcine eyeballs.	51
3.5 Exemplary pictures of porcine eyes immediately after enucleation, and corneas after dissection.	52
3.6 Effect of initial storage on corneal thickness.	52
3.7 Representative transmission spectra of six porcine corneas and four porcine crystalline lenses.	53
3.8 Dynamic mechanical traces of two porcine corneas pre and post storage in supplemented DMEM for 36 hours.	54
3.9 Spectroscopic data of 13 porcine eyes analysed using LAKK-M system, and associated biomarkers.	54
3.10 Peak of the backscattered signal received from the 13 porcine corneas analysed using LAKK-M system.	55
3.11 Fluorescent peaks of different biomarkers in 13 porcine corneas. A (Collagen), B (Elastin), C (NADH), D (Pyridoxine).	56
3.12 Pre-scalded eye, with intact corneal epithelium, and with injury.	57
4.1 Representative Visante AS-OCT image of an examined porcine eyeball.	61
4.2 Setup for scanning slit confocal examination of porcine eyeballs.	62

4.3	Steepest and flattest meridian data distribution of porcine eyes.	62
4.4	Central corneal thickness data distribution (Visante OCT) and associated Gaussian fitting.	63
4.5	Porcine corneal thickness profile.	63
4.6	Anterior chamber angle and depth data distribution of porcine eyes. . .	64
4.7	Shortest and longest corneal diameter data distribution of porcine eyes.	65
4.8	Representative confocal image of the endothelial cell layer of an examined porcine eyeball.	65
4.9	Exemplary 3D topography of a porcine cornea.	67
5.1	Number of publications per year with the keywords ex vivo model in the title.	71
5.2	Aston organ storage system scheme.	72
5.3	Evolution of the prototyping phase of the suction module.	73
5.4	Suction module design and manufacturing.	74
5.5	Perfusion module design and manufacturing.	75
5.6	Schematic description of the procedure devised to mount a porcine anterior segment in the perfusion chamber.	75
5.7	Exemplary image of the SD-OCT setup to image porcine eyes.	77
5.8	Experimental image of four porcine anterior segments mounted in the Aston biological anterior eye model and perfused with transparent DMEM at 37°C at 1ml/min, under 18-20 mmHg.	79
5.9	3D rendering of the automated spray system.	80
5.10	DC Motor Direction control scheme using two SPDT relays.	81
5.11	Electronic design scheme of the automated epithelial irrigation system. .	82
5.12	Electronic enclosure rendering and connecting shield PCB of the Aston Biological Anterior Eye Model.	82
5.13	Experimental overview of the Aston Biological Anterior Eye Model fitted in the laminar flow cabinet.	83
5.14	Representative NIBUT images on a porcine eye.	84
5.15	3D-stack image of a porcine cornea at stromal level.	85

5.16	Excitation (- -) and Emission (-) spectra of Calcein AM and Ethidium Homodimer-1.	86
5.17	Live/Dead 2D images of a porcine cornea at day 0 and day 7.	87
5.18	Higher magnification representative image of corneal fibroblasts obtained using confocal microscopy.	87
5.19	Transparent cornea and crystalline lens after 7 days of storage in the Aston biological anterior eye model.	88
5.20	Examples of CIC filter papers stained and permanently fixed.	89
5.21	Ocular surface samples before the mounting procedure (A), after two hours of irrigation every 20s (B) and 40s (C).	90
6.1	Percentage of cataract operations complicated by PCR for Independent Surgeons (I.S.), Junior Trainees (J.T.) and Senior Trainees (S.T.).	96
6.2	Exemplary pictures of the working area for ophthalmic surgery training in the Aston wet lab.	98
6.3	Tissue adhesive and glued porcine anterior segment to perfusion chamber.	99
6.4	A non-horizontal corneal incision using the original perfusion chamber. The surgeon did not have enough space to access the cornea as in a real-life cataract surgery. The angle of the corneal incision was evaluated using ImageJ software.	99
6.5	Modified perfusion chamber allowing greater tissue exposure to the surgeon while practicing cataract surgery.	100
6.6	Horizontal corneal incision using modified perfusion chamber.	100
6.7	Trainee preparing a porcine eye for cataract surgery.	101
6.8	Cataract surgery on a porcine eye: sutureless clear corneal incision.	102
6.9	Cataract surgery on a porcine eye: anterior chamber filling with OVD.	103
6.10	Cataract surgery on a porcine eye: anterior capsule tearing for continuous curvilinear capsulorrhexis (CCC).	103
6.11	Cataract surgery on a porcine eye: capsular opening obtained by continuous curvilinear capsulorrhexis (CCC).	104

6.12	Cataract surgery on a porcine eye: hydrodissection and hydrodelin- eation of the nucleus.	104
6.13	Cataract surgery on a porcine eye: phacoemulsification of the nucleus.	105
6.14	Cataract surgery on a porcine eye: : IOL insertion in the capsular bag. . .	105
6.15	Cataract surgery on a porcine eye: remaining OVD is removed with the lens remaining well centred.	106
6.16	Pictures before and after cataract induction in porcine globes by mi- crowave heating for 5s, 7s and 10s.	106
6.17	Porcine globe 24hr after being treated for cataract induction.	107
6.18	Back-side view of an IOL implanted in the Aston Biological Eye Model.	110
7.1	Advancing bioengineering for the improvement of human health and wellbeing requires multidisciplinary collaboration.	116

List of Tables

1.1	Definitions of the 3Rs: Replacement, Reduction and Refinement.	15
2.1	Key parameters of main permeation studies from 1959 to 2008.	23
2.2	Key parameters of main studies based on the model developed by Dik- stein and Maurice in 1972.	25
2.3	Key parameters of main perfusion models based on the whole eyeball. .	27
2.4	Key parameters of main perfusion models based on isolated human cor- neoscleral buttons.	30
2.5	Key parameters of main perfusion models based on animal isolated cor- neoscleral buttons.	32
2.6	Chemical composition of human aqueous humour, vitreous humour, LR, BSS, BSS Plus and MEM.	45
2.7	Summary of the key parameters to control for creating an ex-vivo model of the cornea or crystalline lens.	46
4.1	Key aspects of previous studies analysing the porcine eyeball parameters.	60
4.2	Comparison of mean porcine eye parameters experimentally obtained and estimated average human eye parameters according to the scien- tific literature.	68
5.1	Parameters of the Ganymede Series SD-OCT, Thorlabs.	77
5.2	Anterior chamber depth (ACD) measured in eight porcine eyes before and after the mounting procedure using OCT.	77
5.3	Central Corneal Thickness (CCT) measured in eight porcine eyes before and after the mounting procedure using OCT.	78

5.4	Main parameters of the endothelial perfusion system.	79
5.5	12V DC linear actuator specification.	81
5.6	Excitation and Emission peaks of Calcein AM and Ethidium Homodimer- 1.	86
6.1	Challenging scenarios for cataract surgery and their prevalence esti- mated from scientific literature.	97
6.2	Summary of the trainee's feedbacks on the cataract surgery performed on the Aston Biological Anterior Eye model.	107

If you find a need, fulfil the gap.

Lailah Gifty Akita

1

Introduction

Pathological ocular conditions such as Dry Eye Disease (DED) and cataract hold important and disruptive ramifications in terms of patient function, satisfaction, and quality of life (Craig, Nelson, Azar, Belmonte, Bron, Chauhan, de Paiva, Gomes, Hammitt, Jones, Nichols, Novack, Stapleton, Willcox, Wolffsohn & Sullivan 2017, Rao et al. 2011). Governments are constantly striving for new and better treatments to combat eye disease and sight loss, however, less than 2% of all UK medical research funding is directed at ocular disease (Pezzullo et al. 2018). Consequently, there is a real need for increasing value for money in medical research and intervention/management strategies. As such, multidisciplinary approaches which engage multiple centres in different countries, where scientists work together innovatively at the frontier of research in engineering, biology, chemistry and medicine to design novel products and procedures are of significant value in solving today's medical challenges.

DED affects at least 344 million people worldwide (Figure 1.1), and is one of the most

frequent causes of patient visits to eye care practitioners (Craig, Nelson, Azar, Belmonte, Bron, Chauhan, de Paiva, Gomes, Hammitt, Jones, Nichols, Nichols, Novack, Stapleton, Willcox, Wolffsohn & Sullivan 2017). The latest DEWS TFOS report defines DED as "a multifactorial disease of the ocular surface characterised by a loss of homeostasis of the tear film, and accompanied by ocular symptoms, in which tear film instability and hyperosmolarity, ocular surface inflammation and damage, and neurosensory abnormalities play etiological roles." (Craig, Nichols, Akpek, Caffery, Dua, Joo, Liu, Nelson, Nichols, Tsubota & Stapleton 2017). Hyperosmolarity of the tear film and inflammation of the ocular surface are the main mechanisms of the disease, however, fully understanding the epidemiology and best management of DED continues to be a challenge. Due to the significant corneal consequences of DED, human eye research is often limited, and as such, animal eye models have been extensively used to simulate the condition in research studies (Chan et al. 2014).



FIGURE 1.1: Dry Eye Disease (DED): a growing reality degrading quality of life and vision.

To date, *in-vivo* animal models have been used widely in multidisciplinary biological and medical research as a means of investigating physiological mechanisms and for the evaluation and refinement of novel therapies prior to first-in-human clinical trials (Barre-Sinoussi & Montagutelli 2015). In the field of ophthalmology, a large proportion of such models have been used to evaluate the effect on the ocular tissues from administered molecules in terms of factors such as irritation and toxicity. However, as far as the ocular surface is concerned, these models remain limited as they do not reproduce the complexity and chronicity of frequent and debilitating conditions such as DED or Meibomian Gland Dysfunction (MGD) (Barre-Sinoussi & Montagutelli 2015,

Barabino & Dana 2004).

50 years ago, the 3Rs principle (Table 1.1) was developed as an attempt to provide a framework for conducting humane animal research (Kirk 2018), and since then, the scientific community has largely moved away from *in-vivo* towards *in-vitro* studies. Technological advances over this period have produced repeatable and reliable *in-vitro* platforms which have made it now possible to investigate the extrinsic parameters of ocular surface diseases such as tear film deficiency or environmental stress in a fraction of the time, at a much reduced cost, and with greater predictive relevance for humans (Choy, Cho, Benzie, Choy & To 2004).

TABLE 1.1: Definitions of the 3Rs: Replacement, Reduction and Refinement.

Principle	Description
Replacement	Use of technologies or approaches directly replacing or avoiding the use of animals in experiments where they would otherwise have been used.
Reduction	Application of methods minimising the number of animals used per experiment or study consistent with the scientific aims.
Refinement	Use of technologies or approaches directly replacing or avoiding the use of animals in experiments where they would otherwise have been used.

In-vitro cell lines have proved particularly valuable for pharmacological screening, and for characterising and examining the physiological behaviour of individual cell types. However, they do have clear limitations in terms of replicating the complex interactions that occur between the different structures of a living organ, especially in the eye (Shafaie et al. 2016). For this reason, *ex-vivo* models may be a more promising prospect for replicating a natural eye environment, and also have the potential for replacing or minimising the use of laboratory animals (Stanworth & Naylor 1950, Guindolet et al. 2017).

Though recent work has provided a means to maintain the cornea (Guindolet et al.

2017) or crystalline lens (Cleary et al. 2010) in a physiologically stable state for up to seven days, an *ex-vivo* complete anterior eye model that is capable of preserving both of these structures in loco for a similar time frame is elusive. As such, this thesis has been written to describe a multidisciplinary collection of studies which centre on using up-to-date biomedical engineering technology to develop and test a complete *ex-vivo* anterior eye model. The ultimate aim of this work was to generate a scientific platform which would have multiple future applications and be ultimately translatable to human donor eyes and, therefore, could play a pivotal role in bridging the existing gap between *in-vitro* and *in-vivo* anterior segment investigations in ophthalmology.

This thesis begins with a systematic and detailed literature review (Chapter 2). This was initially conducted to deduce the most appropriate parameters to ensure that physiological eye conditions were replicated as closely and accurately as possible. From this knowledge, an optimal preservation technique was developed to maximise corneal transparency and minimise biological tissue deterioration in a porcine eye model (Chapter 3). The anatomical biometry of the porcine eyeball was also extensively characterised to generate reproducible baseline data (Chapter 4). Chapter 5 describes how this knowledge was applied to develop a new *ex-vivo* anterior eye model for assessing tear stability and ocular surface damage. Furthermore, the evaluation of the instrument at tissue and cellular level will also be detailed. The final experimental chapter (Chapter 6) will address how the instrument was re-engineered to provide a novel and reliable training platform for cataract surgery. The final chapter (Chapter 7) will provide a summary of the research project, will review the answers to the research questions posed, will comment on study limitations and will make recommendations for future investigations.

2

The Historical Evolution of Ex-Vivo Ocular Surface Models: a Systematic Review

2.1 Introduction

The human eye is a masterpiece of engineering characterised by highly specialised structures functionally linked to allow vision. Among all these structures, the tear film and ocular surface play a key role in the maintenance of adequate vision as they refract light through the lens and onto the retina for photoreceptor activation, while protecting the eye from injury and external pathogens (Gipson 2007).

Ocular pathologies like Dry Eye Disease (DED), which selectively affect these parts of the eye of millions of people throughout the world, are currently largely studied observing overt clinical signs in animal models that fail to precisely mirror the complexity of these conditions (Craig et al., 2017). As a consequence, many human

clinical trials do not result in acceptable safe and efficacious advances, making the progress slow and incremental (Barabino & Dana 2004). However, recent advances in biomedical technologies have improved the reliability of alternative techniques for ocular investigation, providing economic and logistical advantages for animal alternatives. These techniques include *ex-vivo* models of deceased animal tissue and *in-vitro* cell culture models (Shafaie et al. 2016). Although the use of cell culture models is particularly valuable in the early stages of investigation (e.g. screening potential pharmacologic agents or novel biomaterials), it has clear limitations in replicating the complex anatomy and physiology of the ocular surface. Therefore, investigators have developed *ex-vivo* models that could store the ocular surface in its physiological state, maintaining structural integrity (Guindolet et al. 2017).

This chapter systematically reviews *ex-vivo* models of the ocular surface from the earliest reported to 2018, discussing the key features required to best replicate the anterior eye.

2.2 Methods

This systematic review was conducted in accordance with the procedures developed by the Cochrane Collaboration (Higgins & Green 2011) and the Preferred Reporting Items for Systematic reviews and Meta-Analyses (PRISMA) guidelines (Moher et al. 2009).

2.2.1 Data

Three electronic databases were searched from the earliest date: Web of ScienceTM Core Collection, MEDLINE and Scopus. English language restriction was applied. The following search strategy was designed for Web of ScienceTM Core Collection and it was modified to search MEDLINE and Scopus:

1. artificial-anterior-chamber;
2. isolated-corne*;

3. trabecular-meshwork NEAR/3 culture*;
4. (in-vitro OR ex-vitro OR ex-vivo) NEAR/3 (eye NEAR/3 model);
5. culture* NEAR/3 (anterior-chamber OR anterior-segment);
6. perfus* NEAR/3 (anterior-chamber OR anterior-segment) OR (perfus* NEAR/1 corne*).

Keywords used have been specifically selected to comprise all the different ways in which scientists have been naming the different in vitro models of the anterior eye along the years. Additionally, a hand search of reference lists of the retrieved papers was completed. The electronic sources were last searched on 1st August 2018.

2.2.2 Study Selection

Included in this review were *ex-vivo* models that used enucleated eyeballs, or components thereof, for the short or long-term maintenance of normal physiological and biochemical functions of the ocular surface. Therefore, excluded from this review were studies based on the following models:

- Cell line models;
- Static organ culture;
- In vivo models;
- Phantom models (e.g. Finite Element Methods models, acrylic glass models);
- Models of organs different from the eye (e.g. kidney, vessels, mammary cancer);

Titles and abstracts resulting from the literature searches were reviewed, according to the eligibility criteria stated above. Full-text copies of all relevant articles were obtained for further assessment and inclusion in the review.

2.3 Results

A total of 4066 titles and abstracts were identified from the electronic searches as of August 2018, Figure 2.1. After removing the duplicates, titles and abstracts were screened

and 483 studies were identified as potentially relevant for this review. Finally, a full-text review identified 275 eligible articles.

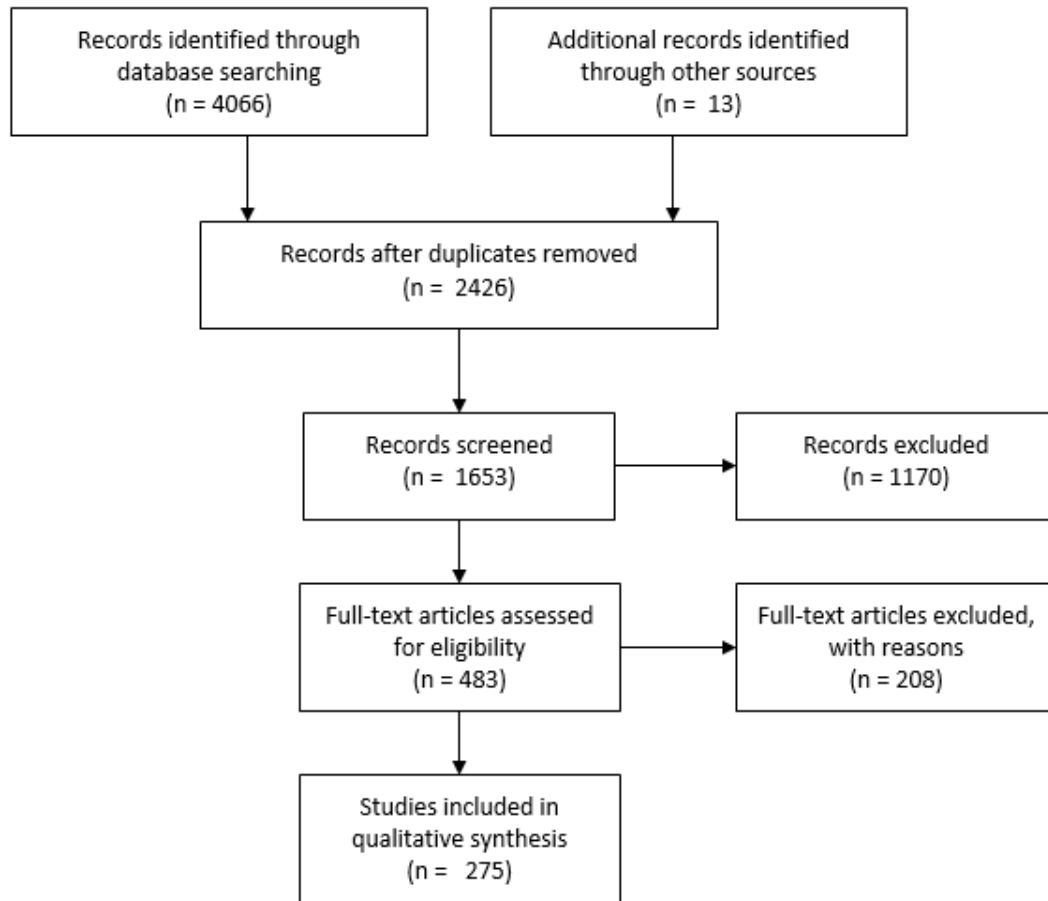


FIGURE 2.1: Flow of study selection. 4079 titles and abstracts were identified through database and online searching. After removing the duplicates and screening titles and abstract 483 studies were reviewed. Finally, 275 studies were included in the review after full-text examination.

The original concept of eye modelling dates as far back as the 4th c. BC, when Aristotle highlighted the chick as the greatest model to use for studying eye development in his Book II of *Generation of Animals*. However, it is only in the 1950s that Stanworth and Naylor devised the first artificial chamber in which the birefringence of the isolated cornea could be studied under near-physiological conditions in polarised light (Stanworth & Naylor 1950).

In particular, the isolated cornea was clamped between two chambers filled with

Ringer's solution (Figure 2.2), and polarised light from a slit lamp source was collimated onto the corneal specimen. As the purpose of the study was the pure evaluation of corneas physical properties, this apparatus far from satisfied the requirement of maintaining the isolated tissue in a physiological condition.

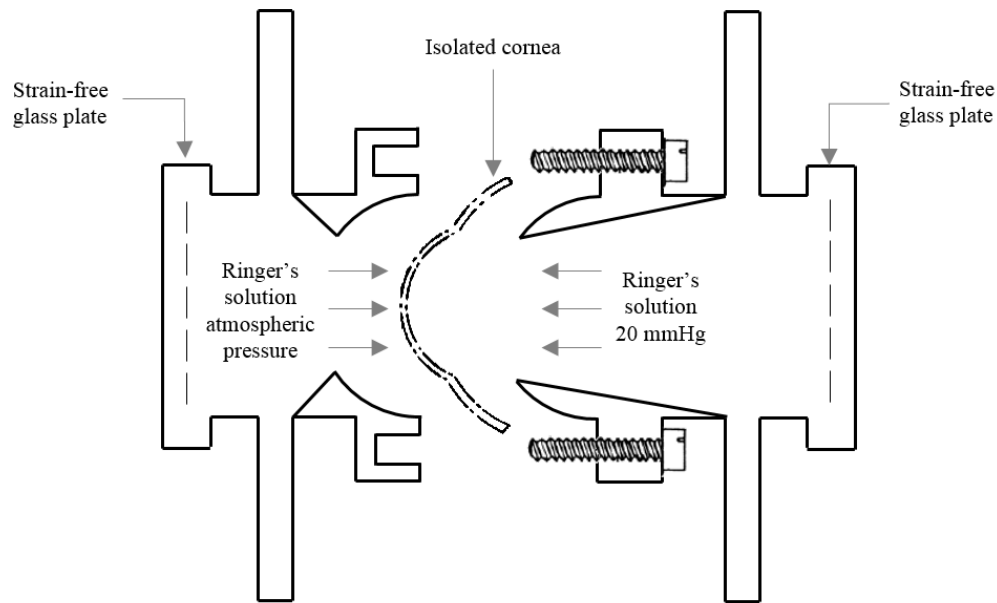


FIGURE 2.2: Schematic diagram of the pressure apparatus introduced by Stanworth and Naylor (1950). It consisted of two chambers between which the isolated cornea was clamped. Strain-free glass plates close the apparatus at the front and the back, so that both chambers could be filled with any required fluid at any desired pressure. Figure redrawn by the PhD author.

2.3.1 Corneal permeation chamber(s)

A crucial step forward was made around 10 years later by Donn and his research group (Donn et al. 1959). Basing their chamber model on the one developed by Ussing and Zerahn for the frog skin (Ussing & Zerahn 1951), the authors were able to maintain the isolated rabbit cornea viable for up to 8 hours, while studying its permeability. Corneal viability was assessed by performing potential, resistance and conductance measurement across the excised tissue, Figure 2.3.

This work pioneered the use of horizontal diffusion cells for studying drug permeation and ionic diffusion across corneas, which is the reason why these models have

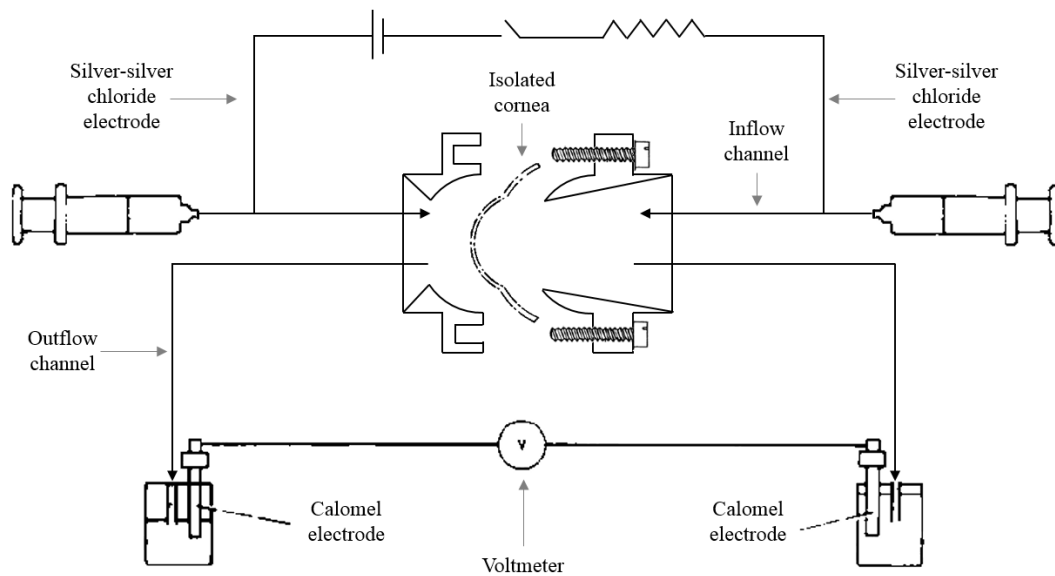


FIGURE 2.3: Schematic diagram of the diffusion chamber introduced by Donn et al. (1959). It consisted of two Lucite chambers between which the isolated cornea was clamped. Motor-driven syringes were used to perfuse artificial aqueous humour into the chambers. The potential difference across the cornea was measured connecting the outflow beakers by means of Calomel electrodes to a voltmeter. Corneal resistance was calculated passing a known current through the cornea via the inflow tubes and evaluating changes in potential. Figure redrawn by the PhD author.

been labelled as corneal permeation chamber(s) in this review. Several researchers modified the design of these chambers over the years to try to replicate in vivo conditions more closely. For example, in 1990 Richman et al. introduced an additional infusion pump for controlling tear film turnover and varying the contact time of the cornea with the drug (Richman & Tang-Liu 1990), and Madhu et al. combined the chamber with quantitative high performance liquid chromatography to assess both corneal and scleral permeability in human ocular tissues (Madhu et al. 1998).

The main parameters of these studies are summarised in Table 2.1, which identifies that the time frame of these models was limited to 11 hours. This is mainly due to the fact that the corneal hydration was not satisfactorily maintained normal during the period under study. In fact, some studies reported grossly opaque corneas by the end of the experiments, but still relatively stable electrical parameters over the experimental period (Ploth & Hogben 1967).

TABLE 2.1: Key parameters of main permeation studies from 1959 to 2008. / = not reported, BR = Bicarbonate-Ringer's Solution.

Source	IOP [mmHg]	MM	T [°C]	FR [μ l/min]	Tissue	TF [hr]
Donn et al. 1959	18	BR	35	/	Rabbit	8
Green 1965	/	BR	35	/	Rabbit	2
Klyce 1972	15	BR	34	/	Rabbit/Frog	2
Klyce et al. 1973	/	BR	34	/	Rabbit	6
Fischer et al. 1974	/	/	/	/	Rabbit	/
Graves et al. 1976	15	/	35	/	Frog	1
Klyce 1977	10-30	BR	35	/	Rabbit	11
Mark & Maurice 1977	11	BR	35	5000	Rat	7
Spinowitz & Zadunaisky 1979	/	BR	35	/	Frog	/
Candia & Podos 1981	/	BR	23-24	/	Frog	7
Rojanasakul & Robinson 1990	/	/	35	/	/	/
Richman & Tang-Liu 1990	/	BR	35	/	Rabbit	2
Kwok & Klyce 1992	/	BR	37	/	Rabbit	2
Madhu et al. 1998	/	BR	35	/	Human	4
Valls et al. 2008	13-19	BR	35	/	Rabbit	2.5

To overcome this limitation, researchers around the world started to devise models for the maintenance of normal corneal hydration. In these models, functional and ultrastructural changes in isolated cornea during perfusion were studied by means of specular microscopy, an imaging technique that added a new dimension to corneal storage studies as it enabled researchers to dynamically profile corneal thickness while observing the endothelial morphology (Maurice 1968). An example of this apparatus is shown in Figure 2.4.

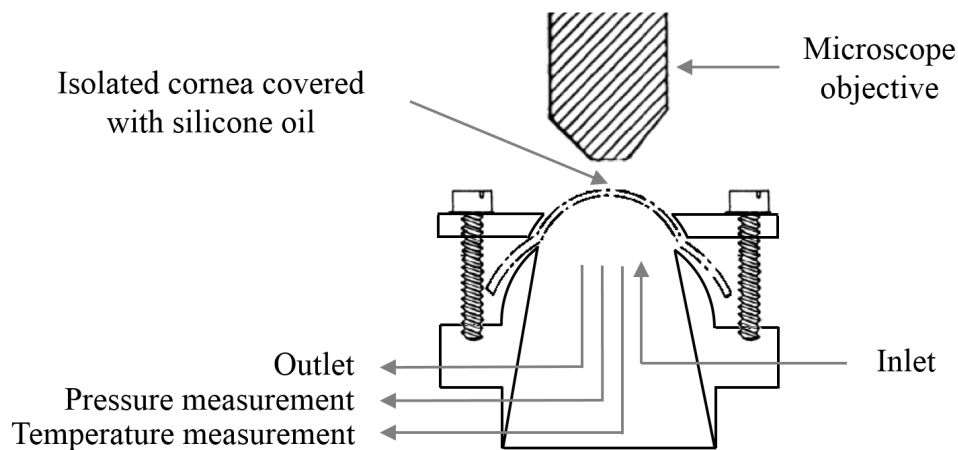


FIGURE 2.4: Schematic diagram of the perfusion chamber introduced by McCarey et al. (1973). The isolated cornea was mounted in a vertical chamber enclosed in a brass water-jacket and mounted under a specular microscope. Endothelial perfusion was performed at $30 \mu\text{l/min}$ under a pressure of 15 mmHg. The corneal epithelium was covered with medical grade silicone oil for microscopic examination. Figure redrawn by the PhD author.

The first successful model of this type was devised by Mishima and Kudo in 1967. They excised rabbit corneas, mounted them in small Plexiglas perfusion chambers, and followed changes in their thickness while incubated. With this system, the authors were able to carry out a perfusion of both the posterior and the anterior surfaces of the cornea, and to extend the time frame to over 10 hours (Mishima & Kudo 1967). A step further was made in 1972 by Dikstein and Maurice, who developed an improved method of mounting the cornea and determining its thickness (Figure 2.5) (Dikstein & Maurice 1972). In particular, their techniques and perfusion medium were simpler than those of Mishima and Kudo and, although they only achieved a preparation lifespan of 5-6 hr, this seemed to allow a fuller reversal of the cornea swelling in the period of study.

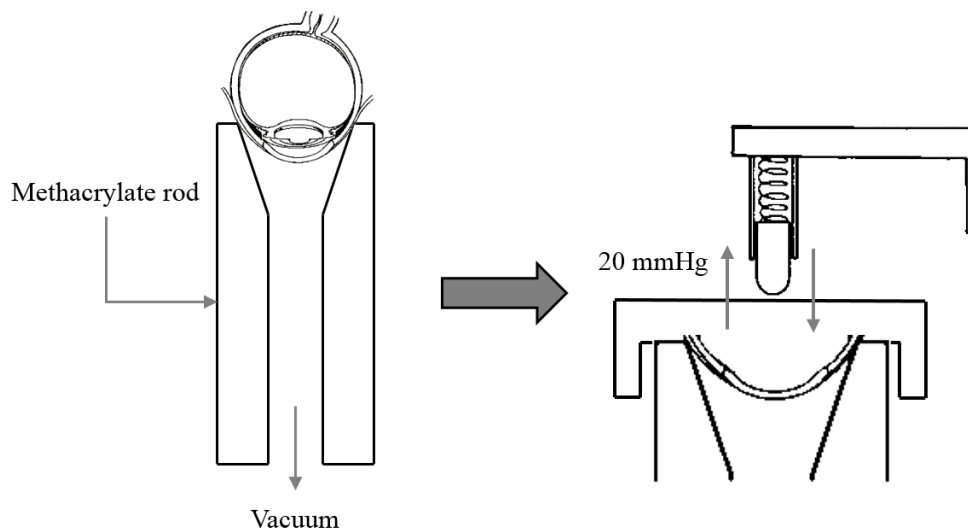


FIGURE 2.5: Schematic diagram of the corneas mounting method introduced by Dikstein and Maurice (1972). The cornea was pressed on to a cannulated methacrylate rod and was held in place by a light suction during the dissection. The perfusion chamber was then pressed down to form a seal, and the perfusion fluid was circulated through the inside of the chamber under a positive pressure of 20 mmHg. Figure redrawn by the PhD author.

This model was extensively used by other authors not only for showing the existence of a correlation between corneal swelling rate, endothelial pattern, and cellular integrity (McCarey et al. 1973), but also to evaluate the effect of different irrigating solution on the cornea (Yagoubi et al. 1994), or to explore contact lens adhesion (Rae &

TABLE 2.2: Key parameters of main studies based on the model developed by Dikstein and Maurice in 1972. / = not reported, BSS = Balanced Salt Solution, BR = Bicarbonate-Ringer's Solution, SC = Sodium Chloride, LR = Lactated Ringer's Solution, GBR = Glutathione Bicarbonate-Ringer's Solution.

Source	IOP [mmHg]	MM	T [°C]	FR [μ l/min]	Tissue	TF [hr]
Mishima & Kudo 1967	15-20	Kei No.4	34	36-46	Rabbit	10
Dikstein & Maurice 1972	11	BSS	36	10	Rabbit	6
McCarey et al. 1973	15	BR	34	30	Rabbit	6.5
McCarey et al. 1976	15	SC	34	60	Rabbit	5
Nyberg et al. 1977	/	/	/	/	Rabbit	3
O'Brien & Edelhauser 1977	15	BR	34	/	Rabbit	/
Van Horn et al. 1977	15	BR	37	/	Rabbit/Human	5
Whikehart & Edelhauser 1978	15	LR/BR	37	/	Rabbit	5
Stern et al. 1981	15	GBR	37	20.6	Rabbit	3
Hull et al. 1982	15	BR	37	/	Rabbit	3
Hull et al. 1985	15	BR	37	16.6	Rabbit	3
Watsky et al. 1990	/	GBR	/	/	Rabbit	2
Wilson & Chalmers 1990	20	GBR	35	100	Rabbit	2.5
Rae & Huff 1991	11-18.5	M199	/	17-25	Rabbit	3
Doughty 1992	11	BSS	35	25	Rabbit	2.5
Srinivas & Maurice 1992	11	BSS	/	60	Rabbit	6
Yagoubi et al. 1994	11	TC199	35	41	Rabbit	7.5
Riley et al. 1998	/	BR	/	100	Rabbit	1
Thiel et al. 2001	18	BSS Plus	35	17	Porcine	14
Holley et al. 2002	15-20	BSS Plus	37	0.07	Rabbit/Human	4
Thiel et al. 2002	18	BSS Plus	35	17	Porcine/Human	14
Brereton et al. 2005	18	BSS Plus	35	17	Porcine	10
Dawson et al. 2007	15-55	BSS Plus	37.5	0.07	Human	5
Doughty & Bergmanson 2008	29.5	BSS/HEPES	37	66	Sheep	10

Huff 1991). The main parameters of several studies based on this model are reported in Table 2.2 . Independently from what has been analysed with these models, all these studies involved the use of human or animal material and clamping of the corneoscleral button into a special holder where the posterior chamber could be perfused with medium and an appropriate pressure gradient could be applied. For this reason, these systems were successful for evaluating the corneal endothelium, though no evaluation was made of the corneal epithelium or stroma.

2.3.2 Corneal perfusion model(s)

The concept of perfusing isolated tissue has also been extensively used to study glaucoma. Elevated Intraocular Pressure (IOP) constitutes the primary risk for the development of the most common form of glaucoma, primary open-angle glaucoma (Sommer et al. 1991). IOP is determined by a dynamic equilibrium between aqueous humour production and outflow and high IOP can theoretically be caused by either an excessive production of aqueous humour or reduction of its outflow or a combination of both (Johnstone & Grant 1973). With regards to this, the trabecular

meshwork (TM)/Schlemms canal outflow pathway system constitutes the main route by which the aqueous humour exits the anterior chamber of the eye (Bill & Phillips 1971). During the years, several models have been developed and evolved to closely replicate the in vivo state of the aqueous humour outflow, from both a histologic and molecular perspective. These models utilise either the whole eyeball or isolated corneoscleral preparations, and they have been included in this review since they might be optimised to achieve the final objective of producing a complete *ex-vivo* anterior eye model.

Perfusion models based on whole eyeball

Whole eyeball models are based on the aqueous perfusion of enucleated whole eyes as a convenient and direct means for quantitative evaluation of facility of aqueous outflow.

The first successful quantitative aqueous perfusion on enucleated whole eyes long after death was performed by Grant in 1963. He developed a specific fitting by which he was able to perform evaluation on the whole eyeball for a period of 5 hours. During its procedure, globes were placed in a silicone rubber mould which enveloped the posterior segment to the equator. The anterior half was covered with absorbent paper saturated with perfusion solution. A 5 mm corneal trephination was performed in all eyes to permit insertion of a stainless steel corneal perfusion fitting (Grant 1963).

Following Grants studies, researchers all over the world emulated these experiments to evaluate aqueous outflow functions not only in the human eye, but also in bovine, monkey and porcine eyes. Details of these studies are summarised in Table 2.3.

Among these studies, Choy et al. demonstrated an *ex-vivo* model of DED for the first time in 2004, using freshly enucleated porcine eyes (Choy, Cho, Benzie, Choy & To 2004). With this model, researchers were able to simulate DED conditions of different severity changing blinking intervals and/or volume of "lacrimation". For achieving so, they fixed the entire eyeball in a plastic holder, with the nictitating membrane placed just above the cornea, and by using a movable mechanical arm, they could

TABLE 2.3: Key parameters of main perfusion models based on the whole eyeball. / = not reported, Vrb = Variable, BSS = Balanced Salt Solution, PBS = Phosphate-Buffered Saline, DPBS = Dulbecco's Phosphate-Buffered Saline, DMEM = Dulbecco's Modified Eagle Medium, BR = Bicarbonate-Ringer's Solution.

Source	IOP [mmHg]	MM	T [°C]	FR [μ l/min]	Tissue	TF [hr]
Grant 1963	/	/	34	/	/	5
Kupfer & Ross 1971	11.5-16	Saline	/	/	Human	/
Johnstone & Grant 1973	-2-50	PBS	/	/	Human	2.5
Epstein et al. 1978	25	DPBS	22	/	Human	4
Epstein et al. 1982	25	DPBS	22	/	Monkey/Bovine	4
Moses et al. 1982	25-40	Saline	/	/	Human	/
Nguyen et al. 1988	15	H ₂ O ₂	/	1000	Bovine	3
Johnson et al. 1993	15	DPBS	34	/	Bovine	5
Epstein et al. 1997	/	DPBS	25	/	Bovine/Porcine	5
Epstein et al. 1999	15	DPBS	25	/	Porcine	5
Overby et al. 2002	15	DPBS	34	/	Bovine	5
McDonnell et al. 2003	Vrb	BSS	/	/	Human/Rabbit	/
Choy, Cho, Benzie, Choy & To 2004	/	DPBS	21-23	/	Porcine	4
Choy, Shun, Cho, Benzie & Choy 2004	/	DPBS	/	/	Porcine	4
Fyffe et al. 2005	/	DMEM	20	/	Porcine	/
Kompella et al. 2006	/	PBS	37	/	Bovine	1
Lu et al. 2008	15	DPBS	34	/	Bovine	3
Choy et al. 2008	/	DPBS	21-23	/	Porcine	4
Johnson et al. 2010	10	DPBS	34	/	Porcine	1
Spoler et al. 2010	10	BR	32	/	Rabbit	6
Kray et al. 2011	10	BR Plus	32	/	Rabbit	6
Zhu et al. 2013	7-30	DPBS	34	/	Bovine	/
Chan et al. 2014	7-30	DPBS	22-24	/	Porcine	/
Hunter et al. 2014	Vrb	DMEM	22-24	2.5	Human	/
Johannesson et al. 2014	20-40	Saline	/	/	Porcine	/
Wang et al. 2014	/	Barany's Medium	40	/	Porcine	/

sweep the membrane over the cornea surface simulating blinking (Figure 2.6).

Six years later, Spoler et al. used a short-term approach of the Ex Vivo Eye Irritation Test to mimic DED and monitored corneal desiccation by two dimensional quantitative Optical Coherence Tomography (OCT) analysis (Figure 2.7) (Spoler et al. 2010). Moreover, by using three dimensional OCT analysis, they were also able to analyse deep structural disorders in the cornea, visualising damages within the epithelium and the anterior stroma (Kray et al. 2011).

What is interesting in all these models is that the time frame in which the tissue remains physiologically stable is limited to 5 hours. This is linked to the increasing mortality rate of endothelial cells due to the non-efficient corneal perfusion. For this reason, these *ex-vivo* studies have mainly been used to analyse topical drug application as high solute uptake is desired in a short time with eye drops. However, this limited experimental time frame of only several hours makes these models not successful tools for studying pathologies such as DED, for which a detailed analysis of corneal regeneration following corneal drying under different treatment conditions is

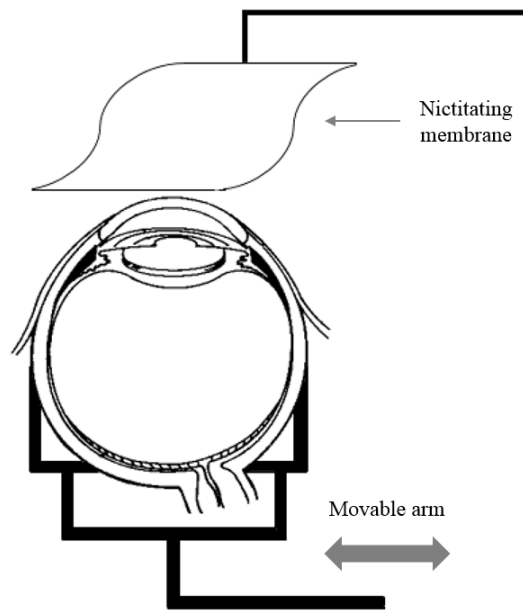


FIGURE 2.6: Diagram of the pDEM set up introduced by Choy et al. (2004). The whole porcine eyeball with conjunctiva tissue, lacrimal gland and the nictitating membrane was fixed in a movable arm. The nictitating membrane was swept over the corneal surface upon movement of the movable in order to replicate blinking. Figure redrawn by the PhD author.

essential. To expand the usable time scale for experiments, researchers developed alternative *ex-vivo* eye models based on isolated corneoscleral preparations, particularly focusing on the trabecular meshwork.

Perfusion models based on isolated corneoscleral buttons

Johnson and Tschumper introduced the most successful *ex-vivo* model of the TM in 1987. They were able to maintain human cells of the outflow pathway functional at the molecular level for a period of 21 days (Johnson & Tschumper 1987). In particular, after bisecting the globe at the equator, they removed vitreous and lens under sterile conditions. After clamping the anterior segment in a modified Petri dish, they perfused the eye with Dulbeccos Modified Eagle Medium (DMEM) with a mixture of antibiotics at a normal human flow rate of $2.5 \mu\text{l}/\text{min}$ (Figure 2.8). Explants were cultured at 37°C in an atmosphere of $5\% \text{CO}_2$ and variations in IOP were continuously monitored without altering the culture by connecting a pressure transducer to a second access cannula built into the dish.

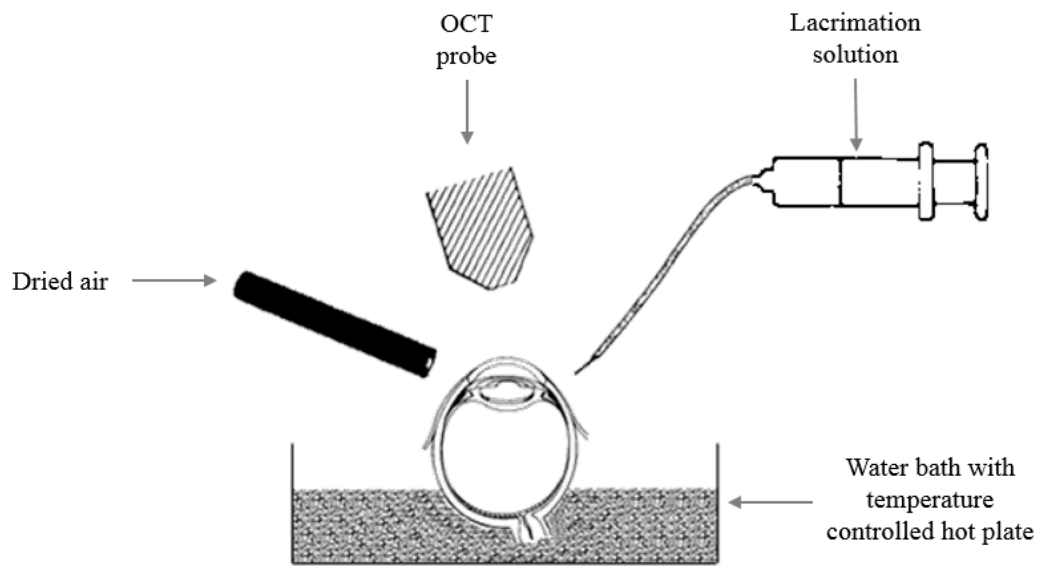


FIGURE 2.7: Experimental setup of short-term Ex Vivo Eye Irritation Test, Spoler et al. (2010). Rabbit eyeballs were placed into a temperature-controlled water bath. Lacrimation was simulated by using a perfusion pump for applying single drops of Ringers solution at a defined interval onto the corneal surface. A gas hose with internal diameter of 3.0 mm was used to flush dried air at variable flow rate over the cornea, simulating different environmental conditions. Figure redrawn by the PhD author.

By using this method, researchers were not only able to prove that trabecular cells require a minimum perfusion rate of approximately $1 \mu\text{l}/\text{min}$ for long-term survival (Johnson 1996), but were also able to study gene transfer in human donor tissue, facilitating the evaluation of a correlation of the effects of specific altered protein concentrations with changes in outflow function (Borras et al. 1998). Moreover, this model was used to investigate Human Corneal Epithelial Cells (HCEC) transplantation (Patel et al. 2009), and to determine the influence of TM bypass stent on human outflow facility (Bahler et al. 2012). The main characteristics of several studies that used this method to characterise the regulation of outflow facility in isolated perfused human eyes are presented in (Table 2.4).

These models were based on human donor eyes, which are limited by their availability and high cost. More important, healthy human donor eyes are prioritised for corneal transplantation, therefore, those available for research are generally not of the

TABLE 2.4: Key parameters of main perfusion models based on isolated human corneoscleral buttons. / = not reported, Vrb = Variable, DMEM = Dulbecco's Modified Eagle Medium, MEM = Minimum Essential Medium.

Source	IOP [mmHg]	MM	T [°C]	FR [μ l/min]	TF [d]
Johnson & Tschumper 1987	vrb	DMEM	37	2.5	28
Johnson & Tschumper 1989	vrb	DMEM	37	2.5	28
Buller et al. 1990	vrb	DMEM	37	2.5	7
Johnson et al. 1990	vrb	DMEM	37	2.5	21
Tschumper et al. 1990	vrb	/	/	2.5	21
Clark et al. 1995	vrb	DMEM	/	2	21
Johnson 1996	vrb	DMEM	37	0.5-10	21
Johnson 1997	vrb	DMEM	37	2.5	14
Borras et al. 1998	vrb	DMEM	37	2.5	7
Borras et al. 1999	vrb	DMEM	37	3-4.5	5
Fautsch et al. 2000	vrb	DMEM	37	2.5	10
Clark et al. 2001	vrb	MEM	37	2.5	10
Pang et al. 2001	vrb	DMEM	37	2.5	18 hr
Borras et al. 2002	vrb	DMEM	37	3	7
Loewen et al. 2002	vrb	DMEM	37	2.5	5
Vittitow et al. 2002	vrb	DMEM	37	3-4	7
Vittitow & Borras 2002	vrb	DMEM	37	3-4	3
Perruccio et al. 2003	vrb	DMEM	37	2.5	8
Santas et al. 2003	vrb	DMEM	37	2.5	3
Fautsch et al. 2003	vrb	DMEM	37	2.5	21
Bahler, Fautsch, Hann & Johnson 2004	vrb	DMEM	37	2.5	28
Bahler, Hann, Fautsch & Johnson 2004	vrb	DMEM	37	2.5	/
Bahler, Smedley, Zhou & Johnson 2004	vrb	DMEM	37	2.5	5
Gonzalez et al. 2004	vrb	DMEM	37	3	/
Gottanka et al. 2004	vrb	DMEM	37	3	15
Liton, Liu, Challa, Epstein & Gonzalez 2005	vrb	DMEM	37	3	4
Liton, Luna, Challa, Gonzalez & Epstein 2005	vrb	DMEM	37	3	/
Rao et al. 2005	vrb	DMEM	37	3	4
Fautsch et al. 2006	vrb	DMEM	37	2.5	4
Fleenor et al. 2006	vrb	DMEM	37	2.5	6
Stamer et al. 2007	vrb	DMEM	37	2.5	7
Wan et al. 2007	vrb	DMEM	37	2.5	8
Wordinger et al. 2007	vrb	DMEM	37	2.5	8
Bahler et al. 2008	vrb	DMEM	37	2.5	3
Perruccio et al. 2008	vrb	DMEM	37	2.5	8
Ramos & Stamer 2008	vrb	DMEM	37	2.5	6
Stamer et al. 2008	vrb	DMEM	37	2.5	8
Patel et al. 2009	vrb	MEM	37	2.5	7
Spiga & Borras 2010	vrb	DMEM	37	3-6	6
Chowdhury et al. 2011	vrb	DMEM	37	2.5	10
Bahler et al. 2012	vrb	DMEM	37	2.5	3
Keller et al. 2013	8	DMEM	37	vrb	7
Oh et al. 2013	vrb	DMEM	37	2.5	9
Chowdhury et al. 2015	vrb	DMEM	37	2.5	1
Vranka et al. 2015	8.8	DMEM	/	vrb	/
Abu-Hassan et al. 2015	8.34	DMEM	37	vrb	10

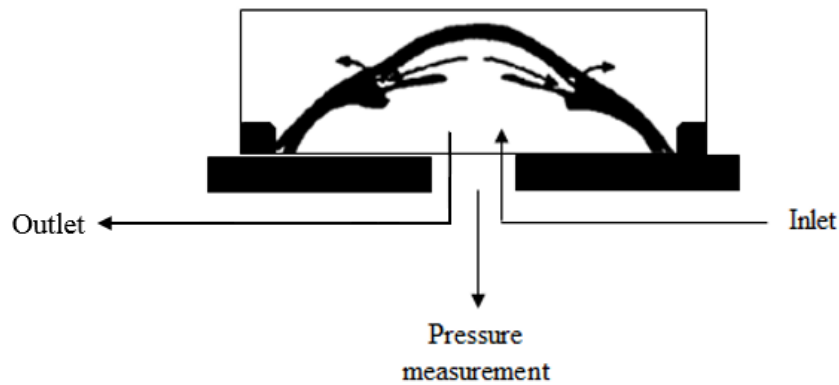


FIGURE 2.8: Schematic diagram of the perfusion system introduced by Johnson and Tschumper (1987). It consisted of a modified culture dish (made of acrylic plastic) with a tight-fitting O-ring to seal the dissected eye, creating a "closed eye". Cell culture medium was infused at $2.5 \mu\text{l}/\text{min}$ using a syringe pump, and pressure within the eye was monitored by inserting a pressure transducer into the second cannula. Figure redrawn by the PhD author.

best quality. For this reason, researchers have looked for animal alternatives, which are inexpensive and readily available. In particular, Ericksonlamy et al. were able to demonstrate in 1988 that trabecular meshwork cells maintain their morphological integrity at constant outflow resistance in the perfused anterior segment of the bovine eye (Ericksonlamy et al. 1988). In fact, for anatomical reasons, only in the bovine eye can the ciliary muscle be easily detached from the trabecular meshwork, allowing a complete dissociation of effects of ciliary muscle and trabecular meshwork on outflow regulation. On the other hand, Hu et al. characterised the monkey anterior segment organ culture system (Hu et al. 2006).

However, among all these animal alternatives, porcine eyes are the ones that show more features in common with human eye, as will be elucidated in chapter 3 (McMenamin & Steptoe 1991, Menduni et al. 2018). In addition, Bachmann et al. established the applicability of the porcine perfusion model, conducting a detailed morphologic analysis of the porcine outflow system and new ultrastructural investigations of the juxtacanalicular region (Bachmann et al. 2006).

The main characteristics of several perfusion studies in isolated animal corneoscleral buttons are presented in Table 2.5.

TABLE 2.5: Key parameters of main perfusion models based on isolated animal corneoscleral buttons. / = not reported, Vrb: Variable, DMEM = Dulbecco's Modified Eagle Medium, MEM = Minimum Essential Medium, DPBS = Dulbecco's Phosphate-Buffered Saline.

Source	IOP [mmHg]	MM	T [°C]	FR [μ l/min]	Tissue	TF [hr]
Zhou et al. 1998	vrb	DMEM	37	16.7	Bovine	3
Goldwich et al. 2003	vrb	DMEM	37	4.4	Porcine	2
Liu et al. 2005	vrb	MEM	37	2.5	Monkey	7
Bachmann et al. 2006	vrb	DMEM	37	4.5	Porcine	7
Hu et al. 2006	vrb	DMEM	37	2.5	Monkey	8
Webb et al. 2006	vrb	DMEM	37	2.5	Bovine	4
Zhao et al. 2006	18	MEM	35	2.5	Bovine	10
Vaajanen et al. 2007	15	/	/	vrb	Porcine	/
Rao et al. 2008	vrb	DMEM	37	3	Porcine	8
Zhang et al. 2008	vrb	DMEM	37	2.5	Porcine	4
Njie et al. 2008	7.35	DMEM	37	vrb	Porcine	2
Bhattacharya et al. 2009	vrb	DMEM	37	2.5 - 4.5	Porcine/Monkey	10
Scott et al. 2009	15	DPBS	34	vrb	Bovine	4 hr
Syriani et al. 2009	10	DMEM	37	vrb	Bovine	4 hr
Lee et al. 2010	vrb	DMEM	37	2.5	Monkey	4 hr
Birke et al. 2011	vrb	DMEM	37	4.5	Porcine	4
Mao et al. 2011	vrb	DMEM	37	5	Bovine	10
Fujimoto et al. 2012	vrb	DMEM	37	3	Porcine	7
Kumar et al. 2012	7.35	DMEM	37	vrb	Porcine	1
Qiao et al. 2012	7.35	DMEM	37	vrb	Porcine	1
Giovingo et al. 2013	7.36	DMEM	37	vrb	Porcine	3
Pinheiro et al. 2015	vrb	MEM/HEPES	32	6.44	Rabbit	4
Slauson et al. 2015	vrb	DMEM	37	2.5	Monkey	8
Pervan et al. 2016	vrb	DMEM	37	4.5	Porcine	2

Despite the widespread usage of the model introduced by Johnson and Tschumper, few studies have been conducted to investigate or make refinements to the original technique of the culture system itself (Johnson & Tschumper 1989, Johnson 1996). In addition, Bahler et al. examined one puzzling aspect of the model, the initial baseline variable IOP, concluding that the variations in baseline IOP may be caused by cell fragments and debris from dying cells in anterior segment tissues, suggesting to use the cultures only after an initial period of stabilization (Bahler, Fautsch, Hann & Johnson 2004). This reversible phenomenon is generally referred to as "washout", and it lasts several hours, depending on the animal specimen used. Moreover, Fautsch et al. studied protein expression profiles from TM and effluent collected from anterior segment cultured with this model (Fautsch et al. 2003). They found that protein profiles from fresh and cultured TM were quite similar, although the addition of supplements such as Fetal Bovine Serum (FBS) may be required for protein profiles to match those of the in vivo state.

Five years later, Ramos and Stamer (Ramos & Stamer 2008) proposed a modified version of the anterior segment perfusion to isolate and study the resistance generated by the conventional outflow pathway in response to different biomechanical conditions (Figure 2.9). In particular, a positive piston displacement pump was used in combination with a syringe pump to generate IOP oscillations that simulated the ocular pulse found in vivo. Moreover, an additional real-time pressure transducer was located in parallel to the original pressure transducer to monitor and adjust peak-to-peak magnitude of intraocular pulsations. This improvement allowed researchers to study not only how a static increase in IOP can affect outflow tissues, but also the effect of cyclic or dynamic stresses applied to these tissues. In addition, the use of this model demonstrated that, despite physiological and anatomic differences that exist among species, porcine and human anterior segments show similar behaviour in response to cyclic biomechanical stress (Ramos & Stamer 2008).

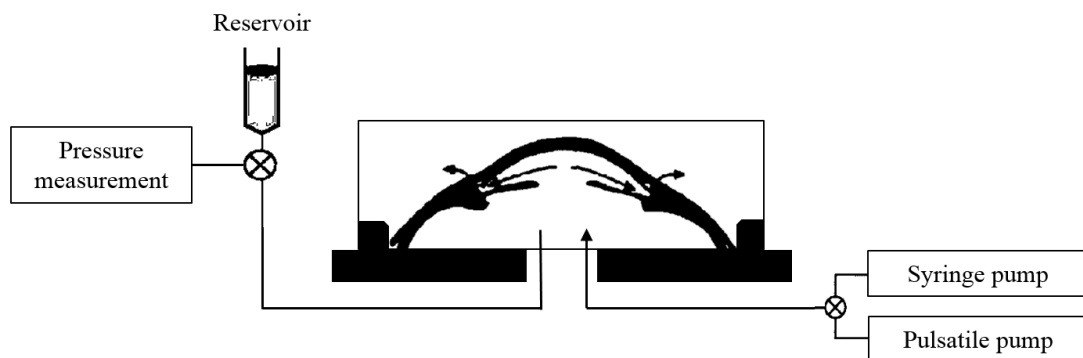


FIGURE 2.9: Schematic diagram of the anterior pulsatile perfusion model introduced by Ramos & Stamer (2008). It was a modified version of the anterior segment perfusion system introduced by Johnson and Tschumper (1987). A positive piston displacement pump was used in combination with a syringe pump to generate IOP oscillations that simulated the ocular pulse found in vivo. Figure redrawn by the PhD author.

However, the main drawback of these systems is that the only site of egress for the perfusate is the trabecular meshwork and the canal of Schlemm. Therefore, the hydrostatic pressure in this system varies with the facility of outflow, leading to variable and often elevated IOP (Johnson 1997). Brunette et al. solved this issue in 1989, adding an outflow cannula that allows a constant level of pressure in the anterior

chamber (Brunette et al. 1989). With this model, endothelial cells on isolated corneas were maintained in a viable and functional state for three weeks, but no epithelial irrigation and evaluation was carried out, making it impossible to study epithelial restoration following corneal wounding.

2.3.3 Corneal wound healing model(s)

Corneal wound healing is indeed a significant clinical issue as it an essential prerequisite for restoring corneal integrity and maintaining vision after eye injury (Ljubimov & Saghizadeh 2015), which is the most common reason for attendance at an emergency department, accounting for 14% of eye department presentations and 8% of eye department hospitalisations (Nash & Margo 1998).

This phenomenon was initially studied in submerged organ culture models, which experienced a reduction in epithelial cell layers, epithelial and stromal oedema together with endothelial and stromal keratocytes deterioration (Vanhorn et al. 1975, Richard et al. 1991). Successively, the air interface organ culture technique was developed and showed to be a more appropriate model for the long-term maintenance of epithelial integrity (Elgebaly et al. 1984, 1987). In fact, using different animal cornea, several types of wounds were studied using this technique, from mechanical (Tanelian & Bisla 1992, Carrington et al. 2006) to alkali burns (Zhao et al. 2009). However, since animals heal differently from humans, researchers have applied this technique to human tissue during the last 25 years (Collin et al. 1995, Foreman et al. 1996, Zagon et al. 2001, Rajan et al. 2005), more faithfully assessing the role of growth factors in corneal wound healing. Of relevance, Foreman et al. showed in 1996 that an *ex-vivo* human corneal model could be used to evaluate epithelial wound healing over a period of 72 hours (Foreman et al. 1996). In detail, wounded human corneas were placed in tissue culture dishes, kept in place by an agar gel and cultured at 37°C in a humidified 5% CO₂ incubator. Moreover, epithelial irrigation was simulated by adding medium dropwise to the surface of the corneal epithelium every 12hr (Figure 2.10).

Six years later, Janin-Manificat et al. extended this model through the use of additional

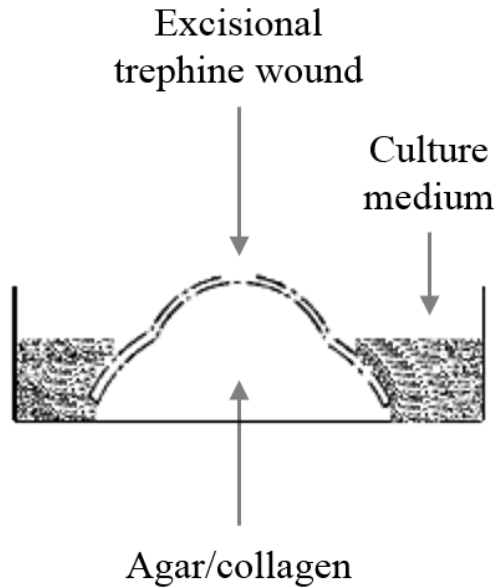


FIGURE 2.10: Schematic diagram of the organ culture model introduced by Foreman et al. (1996). Wounded corneas were placed epithelial-side down into sterile cups containing tissue culture medium. The endothelial corneal concavity was filled with medium containing agar and rat tail tendon collagen. After the mixture set, corneas were inverted and transferred to 60 mm tissue culture dishes and cultured in an incubator with tissue culture medium. Figure redrawn by the PhD author.

wound healing biomarkers and reporting, for the first time, the opacity that is characteristic of corneal scarring or haze (Janin-Manificat et al. 2012). A further improvement was made by Deshpande et al. in 2015 with the introduction of intermittent movement of medium on the epithelium (Figure 2.11). By using this model, researchers found a longer surviving period of the cornea of four weeks and also a more effective recovery from wounding compared to previous authors (Deshpande et al. 2015).

Although fairly simple to set up and with a long life span, these models failed to mimic the situation in vivo in which the cornea is both kept intermittently moist, through the blinking action of the eyelids, and independently perfused at a physiological flow rate.

A more sophisticated system with separate epithelial irrigation and endothelial perfusion was developed by Thiel et al. in 2001. They horizontally mounted porcine corneoscleral preparations in simple chambers ensuring an air interface on the epithelial side and a fluid perfusion on the endothelial side. By using specular microscopy, pachymetry and histological techniques, they maintained the tissue physiologically

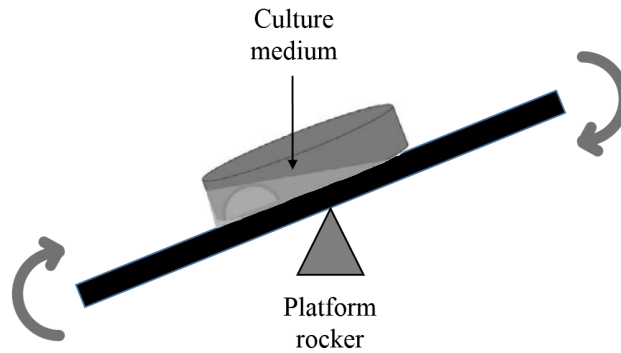


FIGURE 2.11: Schematic diagram of the corneal organ culture introduced by Deshpande et al. (2015). Corneas were placed at the periphery of a 90-mm Petri dish and cultured with culture medium. The Petri dish was placed on a rocking system consisting of an egg incubator, which was subsequently placed on a platform rocker. Figure redrawn by the PhD author.

stable for 14 hours (Thiel et al. 2001). This time frame was limited by the fact that the epithelial irrigation was performed manually. Zhao et al. overcame this limitation in 2006 introducing a perfusion chamber model made of polycarbonate and secured with a clamping sleeve (Figure 2.12), with separate endothelium perfusion and automatic apical surface irrigation systems (Zhao et al. 2006). They evaluated bovine corneoscleral preparations at light ultrastructural level (corneal cell types, including the putative epithelial stem cell population), and they monitored epithelial wound healing and response to penetrating keratoplasty over a period of 10 days.

The most advanced corneal storage method found in the literature was designed in 2017 by Guindolet et al. using porcine corneas (Guindolet et al. 2017). Their corneal bioreactor featured distinct epithelial and endothelial controlled chambers. Minimum essential medium containing 2% FBS was perfused in the endothelial chamber at a rate of $5 \mu\text{l}/\text{min}$, while creating an IOP of 20 mmHg. Epithelium was instead alternating exposed to air and immersed in a specific epithelial culture medium using a controlled peristaltic pump. The whole system was designed to be compatible with current ophthalmology imaging systems, such as slit lamp, OCT systems and specular microscopy, and to be fitted in a CO_2 incubator (Figure 2.13). The authors were able to store porcine corneas for seven days, retaining excellent endothelial cell survival, integrity of the epithelium and limbus, and physiological corneal thickness and shape

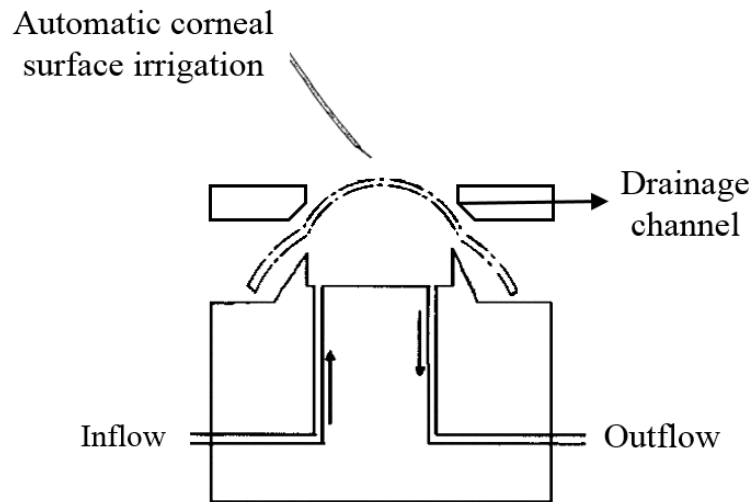


FIGURE 2.12: Schematic diagram of the corneal perfusion chamber introduced by Zhao et al. (2006). It consisted of a perfusion chamber made of polycarbonate, secured with a clamping sleeve. The scleral region of the corneoscleral button was clamped between the main body of the perfusion chamber and clamping sleeve. The endothelium was perfused at $2.5 \mu\text{l}/\text{min}$ under an IOP of 18 mmHg. The epithelium was automatically irrigated using an automatic peristaltic pump. Figure redrawn by the PhD author.

never previously achieved.

This innovative bioreactor enabled direct tissue visualisation through its anterior and posterior transparent windows. However, the mechanical design of the chamber and the presence of the front window would not allow corneal manipulation to perfect donor tissue preparation methods for corneal transplant or to practice surgical techniques.

In respect to this, several artificial anterior chambers have been developed across the years to perfect cataract transplant and lamellar surgery and they have been included in this review to help determine how complete anterior eye models might be optimised to access and manipulate the ocular structures.

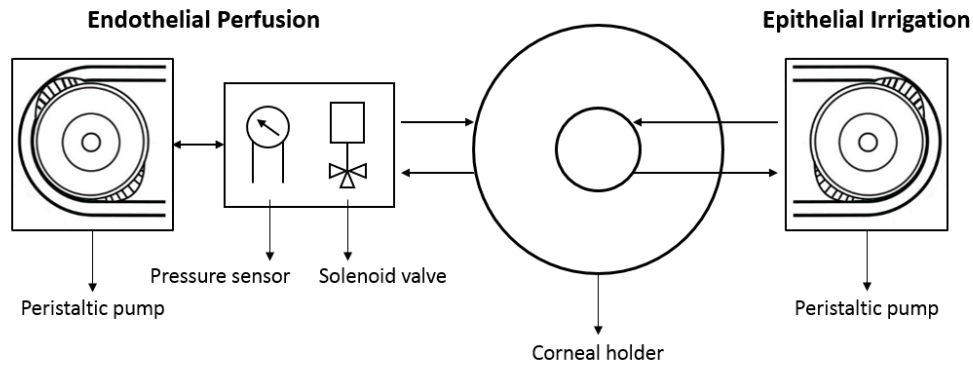


FIGURE 2.13: Schematic diagram of the corneal bioreactor introduced by Guindolet et al. (2017). Fresh endothelial medium was pumped into the anterior chamber using a peristaltic pump controlled by a pressure sensor and a micro solenoid valve. Epithelial medium was independently pumped on the ocular surface every 30s using a separate peristaltic pump. Figure redrawn by the PhD author.

2.3.4 Artificial anterior chamber(s)

The artificial anterior chamber was initially developed by Ward and Nesburn in 1976, when they introduced a new technique for anterior trephination of corneas preserved in McCarty-Kaufman medium (Ward & Nesburn 1976). The ingenious artificial anterior chamber was manufactured with Teflon and stainless steel; its main working components were a black Teflon dome with a flattened top and a stainless steel securing rings. Using this model, researchers were able to eliminate the need to trephine excised corneas from the endothelial side when preparing donor buttons for use in penetrating keratoplasty.

Four years later, this instrument was modified to allow corneoscleral rims to be cut using a microkeratome (Maguen et al. 1980). However, fears about microkeratome use hindered the widespread use and development of this device, which became an effective tool in corneal transplants only after the development of new refractive surgery techniques such as laser in situ keratomileusis (LASIK) (Pallikaris et al. 1990, Buratto et al. 1992).

In fact, in the first years of the 21st century Behrens et al. evaluated the precision and

accuracy of a new artificial anterior chamber model with a metal base in obtaining corneal lenticules for lamellar keratoplasty (Behrens et al. 2001). The device consisted of a stainless steel structure with three screw-type safety rings. The lower ring held a metal device that covered the superficial sclera and maintained a tight fit on the metal base of the chamber to avoid leakage. A second ring in an intermediate position approximated the chamber on the former structure to tighten the sclera from above. Finally, a third ring located superiorly was adjusted to modify the height of the microkeratome plate. The chamber was also connected to an infusion system with a reservoir of saline solution, placed 1.2 m above the chamber level to control IOP. From then on, several authors have used these chambers to mount donor tissue and perfect techniques such as corneal transplant and penetrating, lamellar and endothelial surgery (Azar et al. 2001, Hamaoui et al. 2001, Li, Behrens, Sweet, Osann & Chuck 2002, Li, Ellis, Behrens, Sweet & Chuck 2002, Springs et al. 2002, Wiley et al. 2002, Behrens et al. 2003, Busin 2003, Erb et al. 2004, Ignacio et al. 2005, Sarayba et al. 2005, Ignacio et al. 2006, Pirouzmanesh et al. 2006, Zhu et al. 2006, Bahar et al. 2007).

A further improvement of this technology was made by Bower and Rocha in 2007, with the introduction of the first disposable artificial anterior chamber (Bower & Rocha 2007). It was composed of three pieces: base with tissue pedestal, tissue retainer, and locking ring (Figure 2.14). The base had two ports with silicone tubing that can be used by the surgeon to adjust the pressure injecting or aspirating medium. The Barron artificial anterior chamber, together with the Moria automated lamellar therapeutic keratoplasty system, the Baush and Lomb artificial anterior chamber and the AMADEUS artificial anterior chamber have been extensively used to date, reducing the need to use whole cadaver eyes as surgeons have been given the possibility to use eye bank corneas rather than whole eyes for lamellar dissections (Kaiserman et al. 2007, Sideroudi et al. 2007, Romppainen et al. 2007, Bahar et al. 2008, Mehta et al. 2008, Wu & Yeh 2008, McCauley et al. 2009, Moshirfar et al. 2009, Hwang & Kim 2009, Espana et al. 2011, Krabcova et al. 2011, Rice et al. 2011, Rocha et al. 2011, Sikder et al. 2011, Gatell 2012, Hong et al. 2012, Bhogal et al. 2012, Maier et al. 2012, Tang et al. 2012, Vetter et al. 2012, Bucher et al. 2013, Muraine et al. 2013, Neuburger et al. 2013, Waite et al. 2013, Arafat et al. 2014, Tsatsos 2014, Vaddavalli et al. 2014, Romano et al. 2015, Villarrubia

& Cano-Ortiz 2015, Sharma et al. 2016).

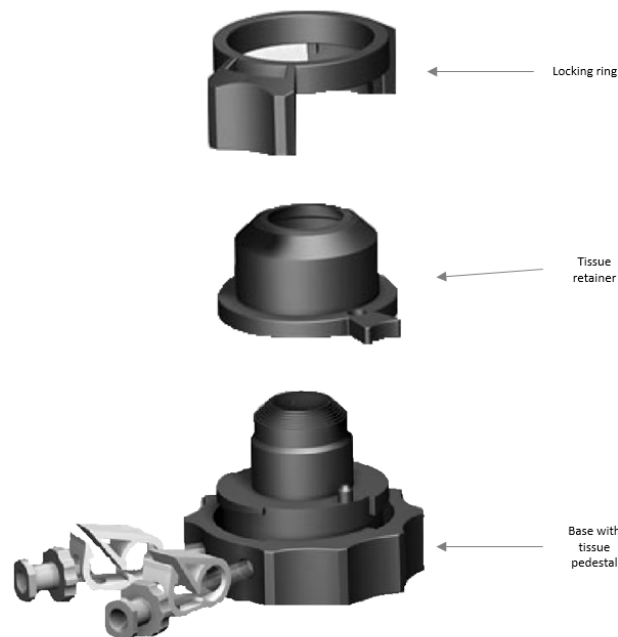


FIGURE 2.14: Schematic diagram of the Barron artificial anterior chamber, Bower & Rocha (2007). The corneoscleral button was placed onto the base, the tissue retainer was carefully placed over the unit and advanced to the bottom of the base. The artificial anterior chamber was then secured by placing the locking ring over the unit and turning it until the locked position was reached. The pressure inside the chamber was controlled using a gravity infusion system. Figure redrawn by the PhD author.

Artificial anterior chambers have greatly contributed to the refinement of corneal transplantation, which is now established as the most successful form of human transplantation (Crawford et al. 2013). Consequently, in a complete anterior eye model corneal tissue should be easily accessible while the specimen is cultured. On the same note, millions of individuals worldwide are visually impaired due to cataract formation, which is the reason why cataract is a major priority in the global initiative to eliminate avoidable blindness by the year 2020 (Rao et al. 2011). Today, cataract is only treated by surgery, which initially restores high quality vision, but then Posterior Capsule Opacification (PCO) develops in a proportion of patients causing a secondary loss of vision (Wormstone et al. 2009). Unfortunately, the biological processes governing PCO formation and how surgical procedures can be developed to improve surgery

outcomes are still unclear. In addition, presbyopia is a ubiquitous concern, which currently affects more than a billion adults worldwide, and this figure is set to rise as over 40% of the global population are expected to be over 40 years of age by 2030 (Frick et al. 2015). Despite over a century of investigation, no physical or pharmacological solution is currently available, since the mechanism of ocular accommodation has not been fully replicated/mimicked. This is mainly due to the fact that the restorative techniques are difficult to develop and refine in *in vivo* models, which provide real data on ocular physiology, but also restrict the ability to measure dynamic intraocular forces and morphometric changes with optimal precision. Therefore, scientists over the past 20-30 years have been developing experimental crystalline lens models that could be used as meaningful tools to improve patient health (Wormstone & Eldred 2016), and they have been included in this review to explore the possibility of combining them with corneal analogues to produce a complete anterior eye model.

2.3.5 Crystalline lens model(s)

Cleary et al. described an *in-vitro* organ culture model for PCO in which the mean time to lens epithelial cell (LEC) confluence was 10 days (Cleary et al. 2010). They introduced a modified dissection technique which retained the ciliary body and zonular fibres in association with the capsular bag by pinning the intact crystalline lens - zonule - ciliary body complex to a silicone ring. After performing cataract extraction, the capsule bag was placed in culture and LEC growth was observed along the days with phase contrast microscopy. However, no mechanical test was performed on the lens tissue to test accommodation.

The most used methods for elasticity measurements on *ex-vivo* lenses are compression techniques (Baradia et al. 2010, Sharma et al. 2011) spinning tests (Fisher 1971, Schumacher et al. 2009), or stretching devices (Fisher 1977). The first two methods exert forces on isolated lenses by indenters or by inducing centrifugal forces, while the stretching device exerts radial forces on the lens via the ciliary body, partly replicating the dynamic *in vivo* action of ocular accommodation. This is accomplished by uniformly increasing the distance of radially arranged arms, to which the ciliary body or sclera is attached. Such a stretching device was introduced for the first time by Fisher

(1977), who measured a decreasing accommodation amplitude of human lenses with age. Thereafter, several groups improved the device, being able to measure an always more complete set of lens parameters, including applied forces, optical power, lens thickness, lens diameter, and radius of curvature, Figure 2.15 (Pierscionek 1993, 1995, Manns et al. 2007, Ehrmann et al. 2008, Reilly et al. 2008, 2009, Kammel et al. 2012). Among these parameters, measuring the applied forces represented a key step forward, as the increase in arm distance is only an indirect measure for the actual force on the ciliary body.

Finally, in 2013, Eppig et al. successfully implanted an accommodative intraocular lens (IOL) into freshly enucleated porcine eyes mounted in a custom-made lens stretcher (Eppig et al. 2013). Using OCT imaging, they were able to measure the accommodative vault and change in geometry only in eyes with an intact vitreous, indicating the importance of the latter for the functionality of accommodative IOLs.

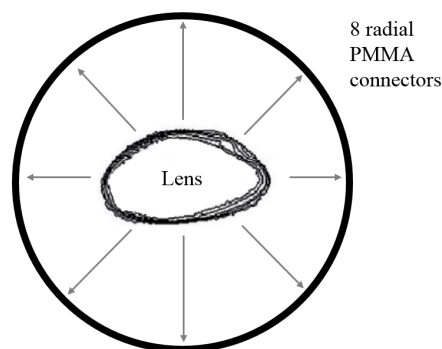


FIGURE 2.15: Schematic diagram of a lens stretcher. After preparing the external ocular surfaces, the tissue is placed in a temperature controlled cell containing buffered solution. Eight PMMA connectors are bonded to the tissue and used to stretch the lens to replicate accommodative action. Figure redrawn by the PhD author.

2.4 Discussion

Every year, up to 100 million animals are used in laboratory experiments all over the world; in 2010, the total number of animals used in the United States was almost 1.37 million, without including rats and mice that make up about 90% of research animals,

but are not covered by the Animal Welfare Act (Shafaie et al. 2016). In 2011, 3.71 million animals were used for research in UK (Doke & Dhawale 2015). To minimise animal experiments, a great amount of research has been dedicated to the development of more economic and ethical alternatives to animal testing, endeavouring to devise *ex-vivo* and *in-vitro* models that could reduce the dependency on live animal testing. In the ophthalmic field, the development of alternative *ex-vivo* ocular models has made important contributions to fundamental applied and preclinical research. However, *ex-vivo* storage of ocular tissues in their physiological state still remains a great challenge for both researchers and eye banks (Guindolet et al. 2017).

This review analysed and compared the most successful *ex-vivo* ocular surface models developed mainly in the past 150 years, in order to deduce the most appropriate parameters that allow physiological eye conditions to be replicated as closely as possible. A successful ocular storage method should maintain the integrity of every structure of the ocular surface and their close interrelationship. Moreover, when studying pathologies such as DED, the operational time frame should also be long enough to be able to evaluate epithelial and endothelial wound healing, and to retain corneal transparency. As evident in the first *ex-vivo* model of DED demonstrated by Choy and colleagues, whole eyeballs have a limited time frame of few hours due to the high mortality rate of cells (Choy, Cho, Benzie, Choy & To 2004). Organ culture of corneoscleral preparations should therefore be the preferred choice to expand the usable time scale of the experimental system.

An additional prerequisite for developing a successful ocular model is the preservation of physiologically stable epithelium and endothelium to take account of the indirect interactions between these two layers (Pai & Glasgow 2010). To preserve the epithelium, the replication of both in vivo air-liquid interface and tear film dynamics is crucial. It has been shown that the air-liquid interface improves epithelial integrity and tight junction formation (Ban et al. 2003), and blinking plays a key role in maintaining the integrity of ocular surface. Mimicking tear replenishment in the eye requires the delivery of a tear analogue to the surface of the *ex-vivo* eye model followed by a period of drying in a recurring fashion under physiological conditions. In the

past, this has been achieved using either rocking platforms to create an intermittent movement of cell medium on the epithelium (Deshpande et al. 2015) or automated systems to drop fluid onto the cornea (Zhao et al. 2006). Recently, Mohammadi et al. proposed a tear replenishment spray system that allows coverage of the corneal surface with a small amount of tear analogue that is sufficient for hydration while it still maintains the air-liquid interface (Mohammadi et al. 2014). By controlling parameters such as spray frequency and/or tear volume, pathologies such as DED could also be mimicked, as decreased blink rate can be associated with the occurrence of its symptoms (Freudenthaler et al. 2003). In addition, tear analogues should be chemically optimised for ensuring an epithelial closure rate comparable to that of clinical observations (Dua & Forrester 1987, Le Sage et al. 2001). Zhao et al. reported epithelial closure rate in bovine corneas comparable to that of clinical observations of healing in human cornea when the epithelial surface was irrigated with Hanks MEM containing 4% FBS at a flow rate of $20 \mu\text{l}/\text{min}$ (Zhao et al. 2006). More recently, Guindolet et al. reinforced this result showing that intermittent air exposure of the epithelium enabled preservation of a stratified and differentiated epithelial layer, guaranteeing also the presence of undifferentiated basal cells expressing stem cell markers (Guindolet et al. 2017).

To preserve the endothelium, the anterior chamber should be distinctly perfused at a physiological flow rate of $\sim 2.5 \mu\text{l}/\text{min}$ (McLaren et al. 2003) and at a controlled temperature of $\sim 37^\circ\text{C}$, creating a pressure 18-20 mmHg higher than atmospheric pressure in the artificial anterior chamber. To ensure constant flow rates and IOP, the model should be engineered to have an inflow and outflow cannula for the endothelial perfusion, to not leave the TM/Schlemms canal as the only site of egress. Moreover, the chemical composition of the endothelium perfusate should be optimised for ensuring endothelial cells preservation and wound healing. Ideally, the medium composition should be equivalent to that of the aqueous humour as regards concentrations of organic and inorganic components. Table 2.6 compares the chemical composition of human aqueous humour, vitreous humour and different media. While BR solution has been reported to be inadequate for maintaining corneal thickness during *in-vitro* perfusion (Mishima & Kudo 1967), MEM containing 2-4% FBS has shown excellent results

TABLE 2.6: Chemical composition of human aqueous humour (HAH), human vitreous humour (HVH), Lactated Ringer's Solution (LR), Balanced Salt Solution (BSS), BSS Plus and Minimal Essential Medium (MEM).

Ingredient	HAH	HVH	LR	BSS	BSS Plus	MEM
Sodium	162.9	144	102	155.7	160	143.43
Potassium	2.2-3.9	5.5	4	10.1	5	5.33
Calcium	1.8	144	3	3.3	1	1.79
Magnesium	1.1	1.3	/	1.5	1	0.81
Chloride	131.6	177	/	128.9	130	124.36
Bicarbonate	20.15	15	/	/	25	26.19
Phosphate	0.62	0.4	/	/	3	1.01
Lactate	2.5	144	28	/	/	123
Glucose	2.7-3.7	3.4	/	/	5.0	5.55
Ascorbate	1.06	2	/	/	/	/
Glutathione	0.0019	/	/	/	0.3	/
Citrate	/	/	/	5.8	/	/
Acetate	/	/	/	28.6	/	/
pH	7.38	/	6-7.2	7.6	7.4	123
Osmolarity (mOsm/Kg)	304	/	277	298	305	280-320

in bovine corneas in term of corneal swelling, without causing any endothelial proliferation (Zhao et al. 2006, Guindolet et al. 2017). Furthermore, the addition of porcine or human aqueous humour to the anterior perfused segment could improve trabecular cell viability and molecular characteristics maintenance (Fautsch et al. 2005). The overall system should be designed to maintain a sterile closed environment and to be compatible with current ophthalmology imaging systems (such as optical coherence tomography, slit lamp, confocal microscope), and the biological tissue used should ideally be cheaply and readily available. While human material for research is dramatically declining (Curcio & Research Tissue Acquisition Working 2006), porcine eyes represent the best substitute for a reliable and high quality tissue source not only with respect to morphologic and biochemical conditions, but also because the variations in age compared with human donor eyes are relatively small (Menduni et al. 2018). Moreover, porcine eyes are discarded from food-industry animals, avoiding the deliberate sacrifice of animals and allowing biochemical and molecular analyses of samples to be performed in adequate statistical extents.

In conclusion, successful *ex-vivo* models of the ocular surface are largely the result of ideas, experimentation and perseverance by researchers over the past approximately 150 years. Nowadays, it is possible to restore a near physiological environment to the cornea or the crystalline lens for up to seven days (Figure 2.16), by ensuring the

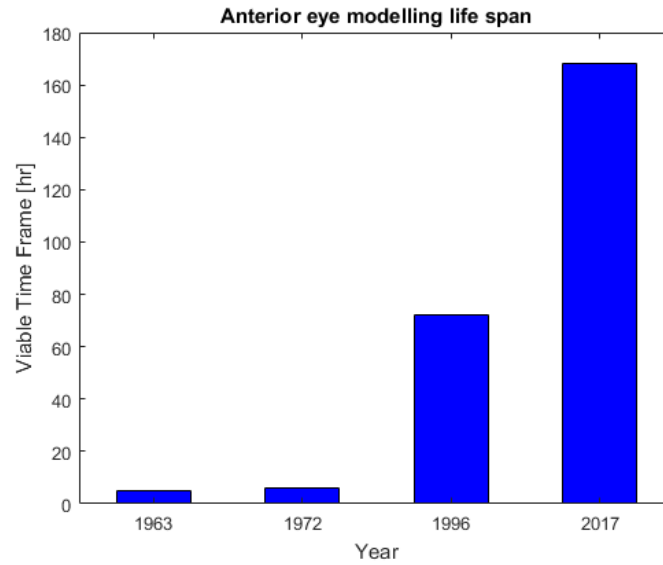


FIGURE 2.16: Historical evolution of the anterior eye modelling life span: Grant (1963), Dikstein & Maurice (1972), Foreman et al. (1996), Guindolet et al. (2017).

TABLE 2.7: Summary of the key parameters to control for creating an ex-vivo model of the cornea or crystalline lens. DMEM = Dulbecco's Modified Eagle Medium, FBS = Fetal Bovine Serum.

Key Parameter	Best Approach
Epithelial Irrigation	Automated Spray System
Tear Substance Chemical Composition	Supplemented DMEM containing 4% FBS
IOP	18 mmHg
Endothelial Perfusion Flow Rate	2.5 $\mu\text{l} / \text{min}$
Endothelial Perfusate Chemical Composition	Supplemented DMEM containing 4% FBS
Animal Tissue	Porcine eye

control of the key parameters summarised in Table 2.7. Though still leaving room for improvement, these models represent cost-effective platforms for preclinical experiments, which are suited for studying irritation, permeation and healing in anterior eye ocular structures independently. The development of a complete anterior eye model, in which the corneal and crystalline lens tissue could be maintained physiologically stable for several days in their natural anatomy may represent a natural step forward for the scientific community. Due to the greater availability of immunoassays and imaging techniques, this model could allow researchers to create a powerful testing platform to elucidate problematics such as the complex relationship between cataract surgery and DED, as well as fostering the creation of an artificial or bioengineered cornea, holy grail of corneal transplantation.

3

Optimisation of the Porcine Ocular Tissue Storage for Biomedical Research

3.1 Introduction

In the ophthalmic field, the *ex-vivo* storage of biological tissue in its physiological state is one of the greatest challenges of both eye bankers and researchers. The pig cornea is the most suitable corneal xenograft due to the considerable similarity to human corneas in terms of refractive power, size and tensile strength (Kim et al. 2016). In addition, porcine tissue can be collected from local abattoirs and used immediately post mortem for preclinical tests, allowing vision science researchers to perform several experiments at reduced cost (Menduni et al. 2018).

In theory, porcine tissue samples represent an unlimited research resource, but in practice porcine corneas in organ culture although remaining metabolically and physiologically active, they lose their shape and transparency and dramatically swell, becoming more than four times thicker and greatly affecting the outcome of research studies (Guindolet et al. 2017). Even if porcine corneal products have been classified as suitable for human clinical trials when processed by standard procedures recommended by the European Eye Bank Association (EEBA) guidelines for technical preparation of the cornea, the translation of the scientific findings is very dependent on the eyeball quality and storage conditions (Kim et al. 2014). Therefore, it is crucial to optimise the preservation technique of porcine eyes to maximise corneal transparency and minimise tissue deterioration.

This chapter evaluated the optimal preservation technique for porcine eyes in respect to corneal transparency and tissue deterioration combining invasive and non-invasive characterisation techniques of biological tissue.

3.2 Methods

Overall, 25 porcine eyeballs were enucleated from a local abattoir within four hours of animal death and transferred to the laboratory either in air ($n = 5$) or in the transport solution ($n = 20$) at 4°C (Figure 3.1). The transport solution consisted of Dulbecco's Modified Eagles Medium (DMEM; Lonza, Berkshire, UK), supplemented with 1% penicillin (10,000 units/ml) and streptomycin (10,000 mg/ml), 1% v/v L-glutamine (Lonza, Berkshire, UK), 10% Foetal Bovine Serum (FBS; Sigma-Aldrich, Dorset, UK) and 20% w/v Dextran ($M_w \sim 250kDa$, Sigma-Aldrich, Dorset, UK) to minimise corneal swelling (Kim et al. 2014). Animals were white domestic pigs aged between 12 to 25 weeks.

Central corneal thickness was obtained in all 20 eyes using ultrasound pachymetry (UP-1000, Nidek, Gamagori, Aichi, Japan), while corneal and crystalline lens transparency were quantified in five eyes transported in air and five eyes transported in the transport solution using spectrophotometry (SpectraMax M2, Molecular Devices

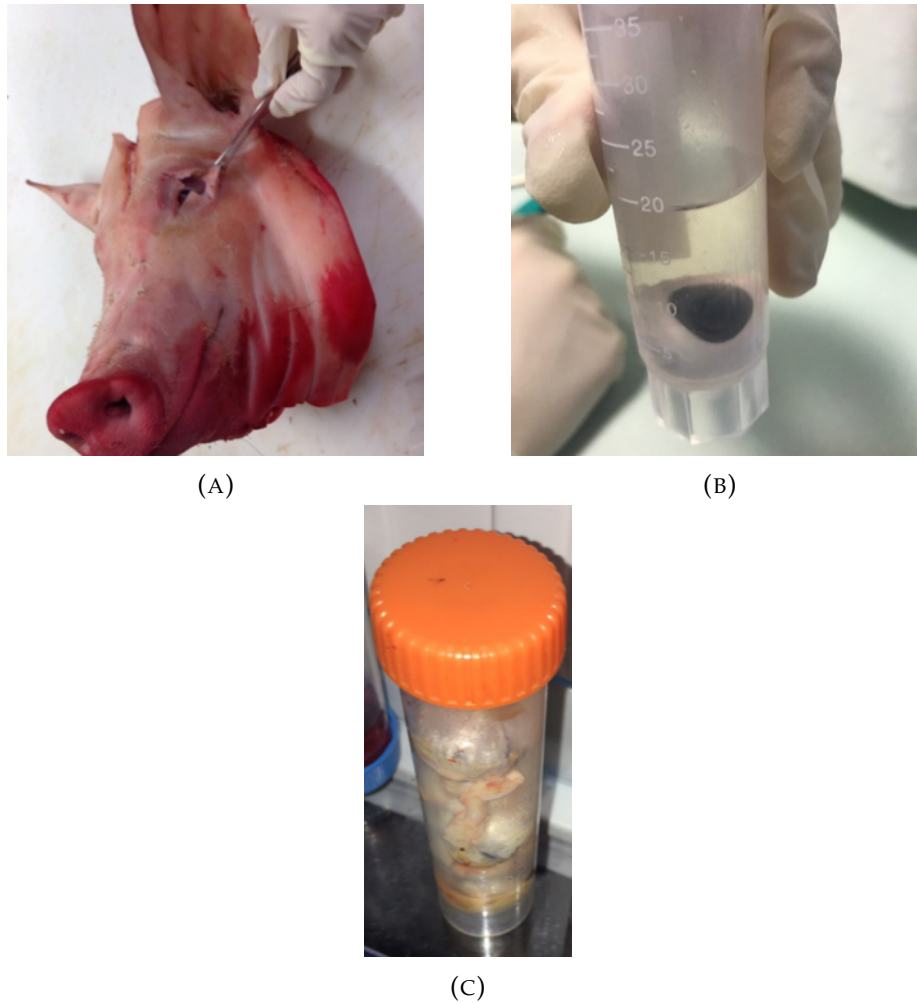


FIGURE 3.1: Enucleation of the porcine eyeball (A), and its transportation in supplemented storage solution (B) and air (C).

LLC, San Jose, US). In addition, dynamic mechanical analysis (DMA) was performed to evaluate viscoelastic properties in two corneas transported in the transport solution using a shear rate and yield stress rheometer (Bohlin CVO, Malvern Instruments LTD, Malvern, UK). All measurements were obtained within 36-hour after enucleation (Figure 3.2), and for measurements performed 24 hours and 36 hours after enucleation, eyes were stored at 4° C either in air or in the transport solution.

A crucial drawback of the spectrophotometry and DMA is that they require harvesting replicate samples at specific time points for evaluating tissue quality. Laser fluorescence spectroscopy (LFS) is currently one of the most promising methods for a non-invasive characterisation of biological tissue, especially in the oncologic field, as it allows measuring the dynamics of metabolism without the need to take biopsies (Rogatkin et al. 1998).

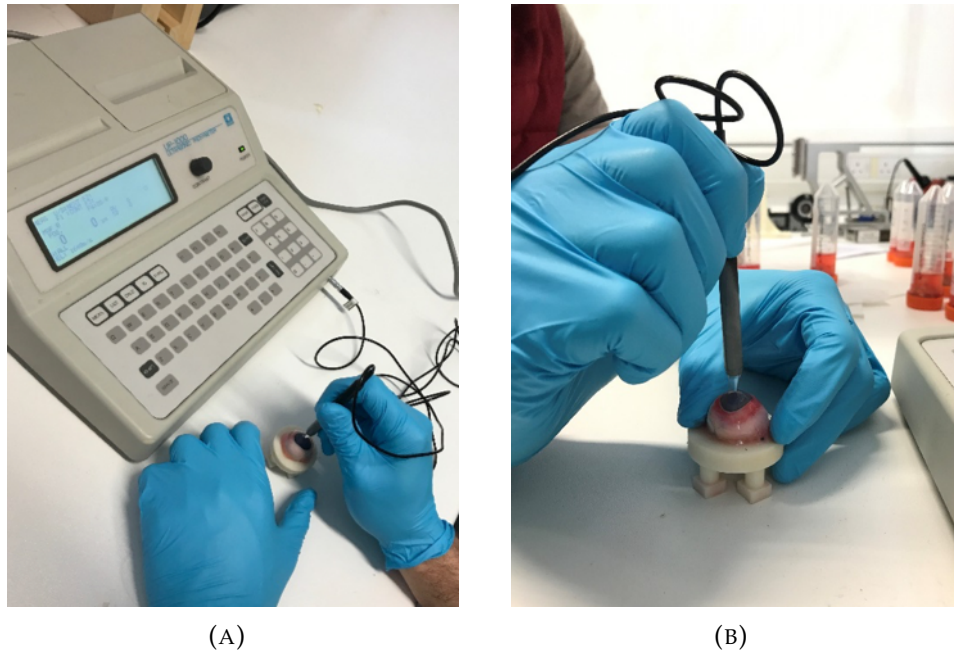


FIGURE 3.2: Exemplary pictures of ultrasonic pachymetry measurements performed on porcine eyeball.

The LAKK-M system (SPE LAZMA, Moscow, Russia) is a multifunctional non-invasive laser diagnostic instrument that, when used in its Fluorescence operation regime, evaluates tissue fluorescent biomarkers by measuring the endogenous tissue fluorescence induced by external laser irradiation (Figure 3.3). For excitation of fluorescence biomarkers, this system is equipped with fibre optic probe and uses laser sources with three wavelengths: 365 nm (UV), 532 nm (Green) and 630 nm (Red). This allows estimation of fluorescence radiation intensity for nicotinamides, flavin, lipofuscin, porphyrin and other fluorescing biomolecules (Raznitsyna et al. 2018).

Therefore, the remaining 13 porcine eyes transported in the transport solution were analysed via LAKK-M system within 6 hours after enucleation to investigate the viability of detecting corneal deterioration while avoiding tissue sacrifice (Figure 3.4).

Spectroscopic data were analysed using Matlab software (The Mathworks, Inc., Natick, MA).

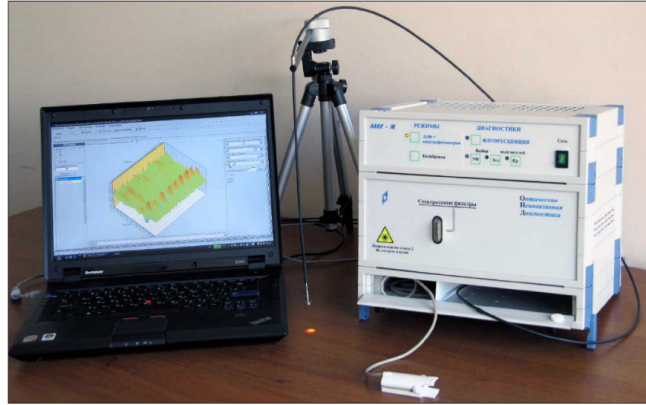


FIGURE 3.3: Exterior view of the LAKK-M system, which includes a diagnostics block for data processing, a light-guide cable, a pulse oximeter and calibrated light filters.

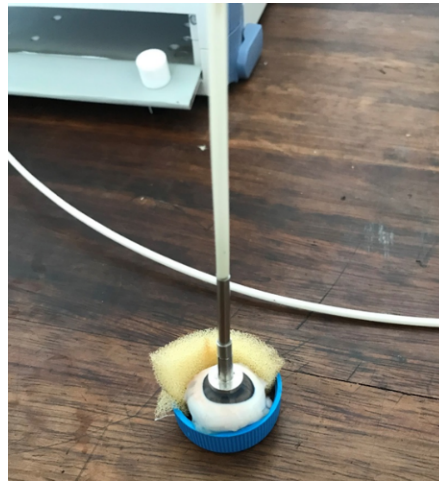


FIGURE 3.4: Experimental setup of LFS on porcine eyeballs.

3.3 Results

The corneal tissue transparency was influenced by both the freshness of the eyeball and the storage conditions ($n = 25$). The critical factor appears to be the freshness and quality of the eye at collection as any of the transport methods used was able to restore transparency in cloudy eyes (Figure 3.5). However, using supplemented DMEM without Phenol Red as transport solution reduced corneal turgidity ($n = 10$), thereby maintaining corneal thickness and transparency up to 36 hours after enucleation, and avoiding pink colouring of the cornea (Figure 3.6).

The use of spectral transmission represented a further way to assess both the corneal

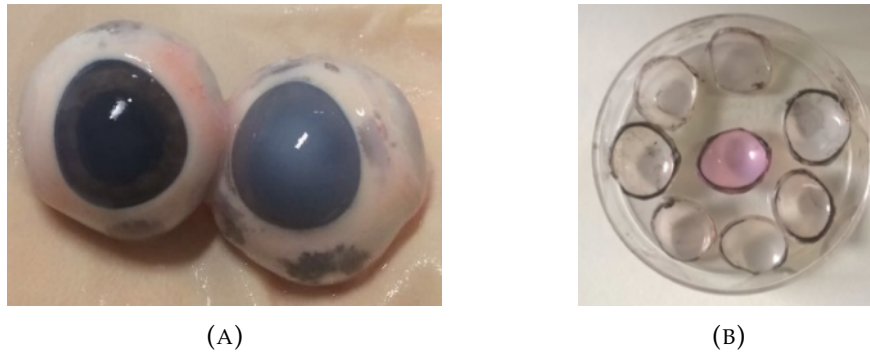


FIGURE 3.5: Exemplary pictures of porcine eyes immediately after enucleation (A), and corneas after dissection (B). Eyeballs may be already cloudy after enucleation and the use of DMEM containing Phenol Red as transport solution turned corneas pink.

and crystalline lens tissue. As shown in Figure 3.7, transparent corneas were characterised by an average percentage of light transmission 2.11x higher than cloudy corneas up to 36 hours after enucleation and independently from the storage method applied ($n = 10$). On the other hand, crystalline lenses were less influenced by the storage conditions due to the protection of the eyeball, and lenses with un-intact capsule showed a characteristic drop in transmission between 200 and 300 nm.

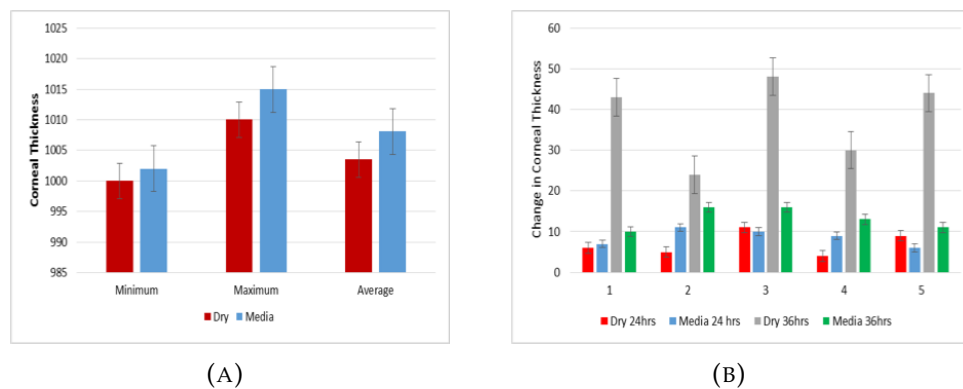
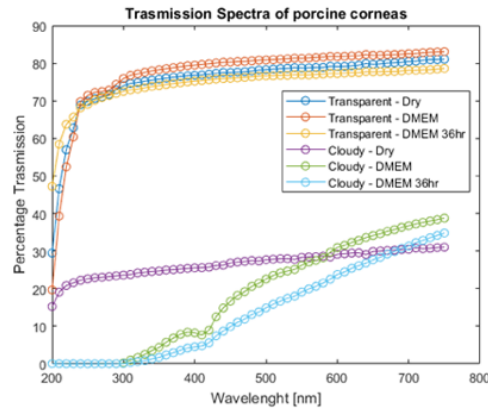
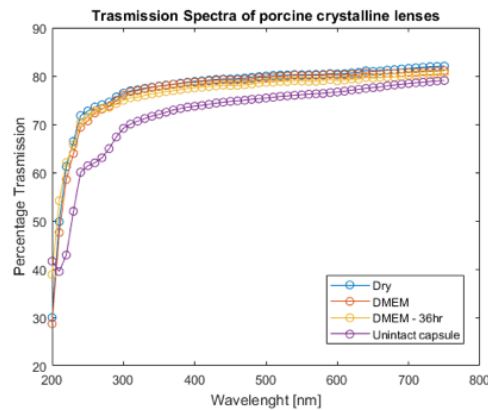


FIGURE 3.6: Effect of initial storage on corneal thickness (A), and effect of storage over time on corneal thickness (B). Storing eyes in supplemented DMEM minimised changes in corneal thickness over 36 hours. Error bars = 1 STD.

In terms of viscoelastic properties, the corneas tested using DMA retained both their dynamic elastic modulus G' and dynamic viscous modulus G'' after storage in supplemented DMEM for 36 hours (Figure 3.8), suggesting that this may be another useful tool to use for assessment of ocular tissue properties ($n = 2$).



(A)



(B)

FIGURE 3.7: Representative transmission spectra of six porcine corneas (A) and four porcine crystalline lenses (B). Transparent corneas showed higher transmission than cloudy corneas. Un-intact crystalline lenses were characterised by a change in transmission between 200 and 300 nm.

Spectroscopic data obtained via the LAKK-M system are reported in Figure 3.9. Transparent corneas were characterised by lower UV backscatter and greater fluorescence signals associated with elastin, NADH and pyridoxine than cloudy corneas ($n = 13$). In particular, the most transparent eye showed a backscattered signal 4.88x less intense than the cloudiest cornea (Figure 3.10), while being characterised by more intense fluorescent signals of elastin (+97.8%) and NADH (+94.8%), as shown in Figure 3.11.

Due to the uncertainty of the results of such measurements, which may amount up to 40% of the measured value (Rogatkin et al. 1998), the experimentally observed differences between LFS signals from transparent and cloudy corneas were significant for the backscatter, the elastin and the NADH, but not for the collagen and the pyridoxine.

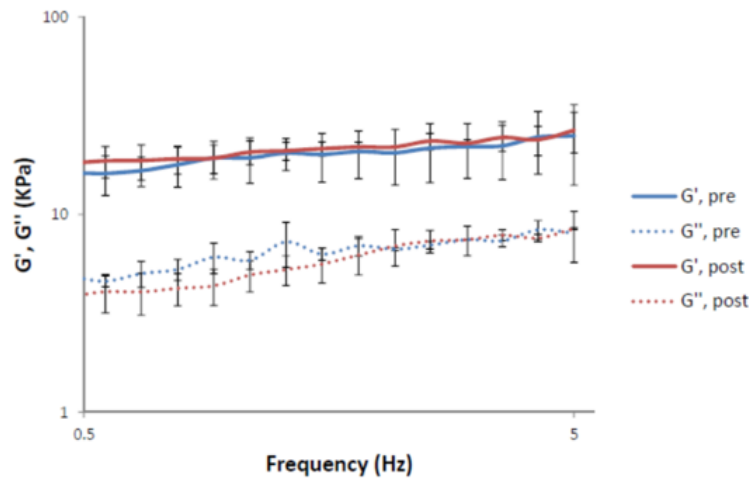


FIGURE 3.8: Dynamic mechanical traces of two porcine corneas pre and post storage in supplemented DMEM for 36 hours.

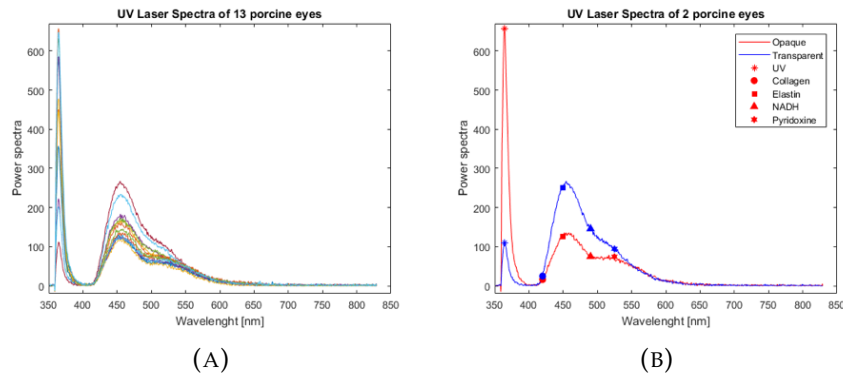


FIGURE 3.9: Spectroscopic data of 13 porcine eyes analysed using LAKK-M system (A). Spectroscopic data of the most transparent and most opaque eye, and associated biomarkers (B).

3.4 Discussion

A local abattoir could serve as a source of reliable, high quality biological tissue for *ex-vivo* anterior eye models. Pig eyes are an attractive model for research and xenotransplantation due their low costs and close correlation with human anatomy (Loewen et al. 2016). However, the reproducibility of the scientific findings derived from *ex-vivo* models based on porcine eyes is strongly dependent on the eyeball quality and storage procedure.

This chapter highlighted that the condition of the eyeball at enucleation dictates the performance of the biological tissue in experimental tests. Porcine eyeballs should be

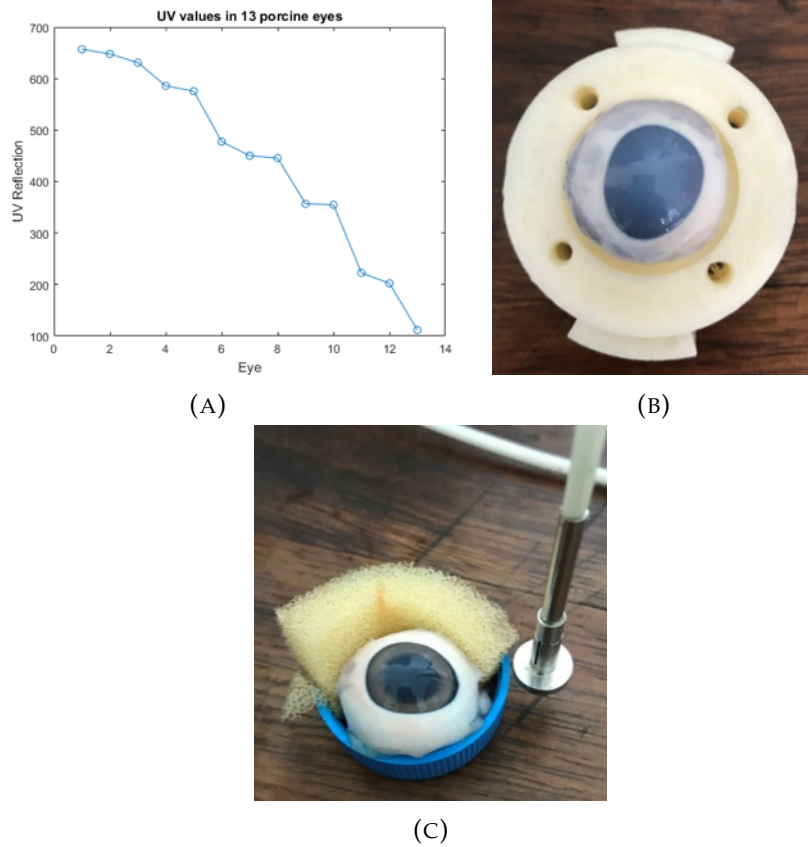


FIGURE 3.10: Peak of the backscattered signal received from the 13 porcine corneas analysed using LAKK-M system. Picture of the cloudiest (A) and most transparent (B) cornea analysed.

collected fresh and only transparent corneas should be further processed for examination up to 36 hours after enucleation. The suggested time frame of 36 hours takes also into account the viability of LECs, which has been previously shown to be of 50 hours when porcine eyeballs are simply stored at 4°C in tap water (Nibourg & Koopmans 2014, Hatami-Marbini & Rahimi 2014).

Tissue transportation should be carried out at 4°C to attenuate cellular metabolism, and using DMEM based solutions supplemented with hydrophilic macromolecules that produces colloid osmotic pressure to extract excess water accumulated in the stroma and, therefore, reduce corneal swelling (Zhao et al. 2012, Dias & Ziebarth 2015). In addition, it would be preferable to use cell medium which does not contain Phenol Red as it seems to facilitate corneas turning pink, possibly influencing study outcome depending on the type of testing. Further tests will be needed to examine if the Phenol Red itself is causing the corneas to turn pink, or it is the presence of FBS that facilitate

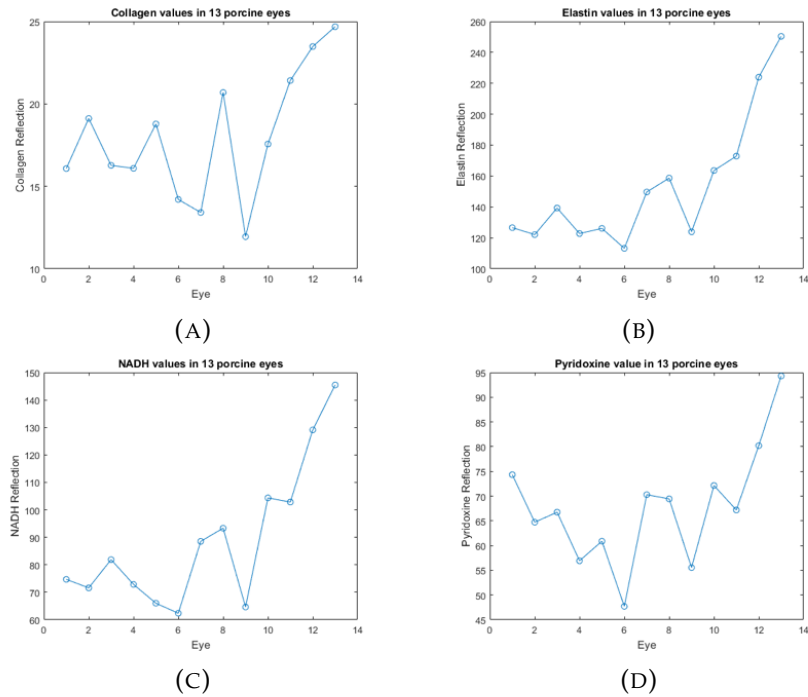


FIGURE 3.11: Fluorescent peaks of different biomarkers in 13 porcine corneas. A (Collagen), B (Elastin), C (NADH), D (Pyridoxine).

the migration of the coloured dye within the cornea.

Corneal transparency can be evaluated using spectrophotometry, however, here it has also been demonstrated the utility of using laser fluorescence spectroscopy to quantify transparency throughout the culture period avoiding tissue sacrificing. Due to the possibility of measuring porphyrins with LFS, this technique may also be used for the diagnosis of a local inflammation in corneal tissues in DED research, as one of the reason of the enhanced accumulation of porphyrins in tissues is chronic hypoxia (Rogatkin et al. 2009).

In an abattoir, all pig carcasses undergo a scalding process immediately post-mortem to remove hair and reduce skin-dwelling bacterial contamination (Bolton et al. 2003). In particular, pig carcasses are immersed in a scald tank containing water heated to $\sim 65^{\circ}\text{C}$ for removing remaining bristles from the hair follicles. During this process pig eyelids usually remain open, exposing the anterior surface of the cornea to a possible thermal injury that leads to a clear physical disruption and loss of the corneal epithelium from the underlying stroma (Chinnery et al. 2005).

During the last part of this PhD project, a business relationship was established with an abattoir, which allowed eye enucleation to be performed before the scalding procedure. Four eyes were obtained, photographed and stained with fluorescein to analyse epithelial corneal damage. Preliminary results showed that pre-scalded eyes were characterised by superior transparency and a perfectly intact corneal epithelium (Figure 3.12). Therefore, pre-scalded porcine eyes should be used when corneal integrity is a crucial aspect of the research project.

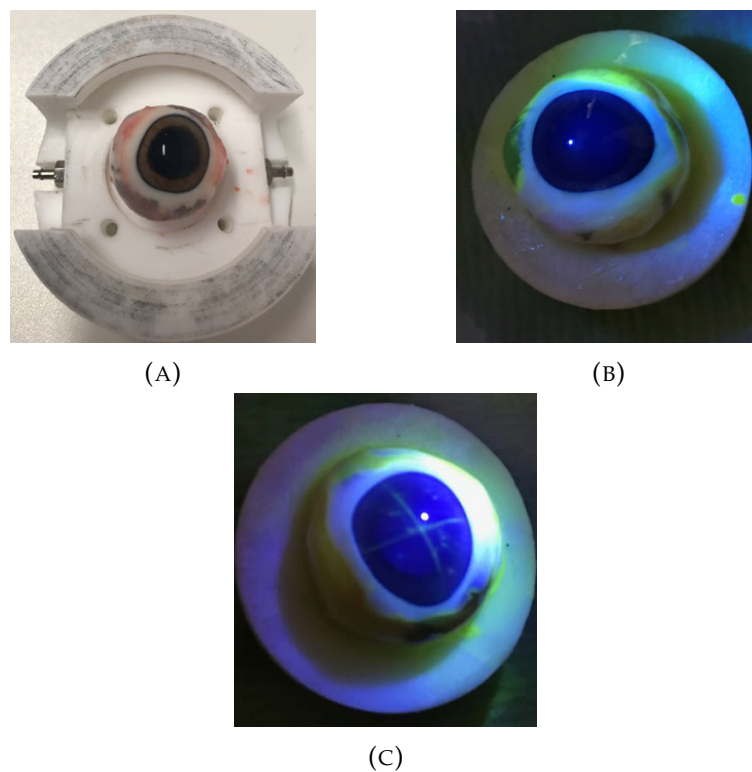


FIGURE 3.12: Pre-scalded eye (A). Fluorescein staining of an intact corneal epithelium of a pre-scalded eye (B). Corneal epithelial fluorescein staining after inducing injury (C).

In conclusion, this chapter provides initial guidelines on optimal storage of porcine tissue samples for their use in biomedical research. Using pre-scalded eyes and adopting standard handling and storing procedures would result in higher consistency and reproducibility of experimental results obtained using *ex-vivo* porcine ocular models, ultimately improving the effectiveness of those cost-effective preclinical platforms.

4

Anatomical Biometry of the Porcine Eyeball

4.1 Introduction

The use of animals in biomedical research is a longstanding practice beginning in ancient Greece, when Alcmaeon of Croton determined that the brain is the seat of intelligence and sensory integration by studying dogs (Ericsson et al. 2013). In the ophthalmic field, *in-vivo* animal models have been used for many years to evaluate how vision has evolved and to study the pathophysiologic mechanisms causing ocular diseases (Chader 2002). In DED research, many animal models have been developed to mimic the multiplicity of mechanisms underlying the pathology and to explore treatment options, however none of them seems to precisely mirror the complexity and chronicity of this disease (Barabino & Dana 2004).

While the mouse remains the most attractive *in-vivo* animal model of DED due to the extensive availability of transgenic and knockout strains and specific reagents

(Beyazyldz et al. 2012), recently the porcine eye has been extensively used as an *ex-vivo* animal model due to its proposed similar morphology and tear film to the human eye (Fyffe et al. 2005, Ruiz-Ederra et al. 2005, Wong et al. 2007, Fernandez-Bueno et al. 2008, Chan et al. 2014, Loewen et al. 2016). In particular, Choy et al. developed a system in which different levels of severity of dry eye can be mimicked manipulating blinking rate and tear volume (Choy, Cho, Benzie, Choy & To 2004). Moreover, porcine lacrimal and meibomian glands have been shown to be similar to humans (Henker et al. 2013), and the recently sequenced genome of *Sus scrofa* indicates that pigs are genetically more similar to humans than mice, further stressing the validity of this model (Groenen et al. 2012).

In 1997 Bartholomew et al. analysed 25 porcine globes using ultrasound biomicroscopy (Bartholomew et al. 1997). Since then, further studies have examined some porcine eye parameters, but, as summarised in Table 4.1 their sample size and the parameters investigated have been limited. In addition, in these studies eyes have generally been transported dry on ice prior to measurement, which may affect the structural and physiological integrity of the sample. Therefore, a source of reproducible data concerning the parameters of the porcine eye, including corneal topography and confocal microscopy, is still missing.

The aim of this chapter is to provide an extensive characterisation of the porcine eyeball, to help vision scientists to effectively use the pig eye as a biomedical model in the applied ophthalmic research such as dry eye.

4.2 Methods

Sixty pre-scalded porcine eyes were obtained from a local abattoir around 12:00 noon and transferred to the laboratory in a transport solution at 4°C. The transport solution consisted of Dulbeccos Modified Eagles Medium (DMEM; Lonza, Berkshire, UK), supplemented with 1% penicillin (10,000 units/ml) and streptomycin (10,000 mg/ml),

TABLE 4.1: Key aspects of previous studies analysing the porcine eye-ball parameters. ACD: Anterior chamber depth; HCD: Horizontal corneal diameter; VCD: Vertical corneal diameter; CCT: Central corneal thickness; CCP: Central corneal pachymetry; CD: Corneal diameter; Ks: Steepest meridian; Kf: Flattest meridian.

Author/s	Eyes No.	Measurement	Method	Results
Bartholomew et al. 1997	25	Anterior Chamber Globe Diameters Corneal Diameters	Ultrasound biomicroscopy	ACD: 2.21 mm HCD: 16.61 mm VCD: 14.00 mm
Asejczyk-Widlicka et al. 2008	12 12	Anterior Chamber Scleral thickness	OCT	CCT: 0.96 ± 0.05 mm ACD: 2.13 ± 0.22 mm
Sanchez et al. 2011	5	Keratometric power	Keratometry	Ks: 41.19 ± 1.76 D Kf: 38.83 ± 2.89 D ΔK : 2.36 ± 1.70 D
		Corneal Astigmatic power	Ultrasound Pachymetry	HCD : 14.3 ± 0.25 mm VCD : 12.00 ± 0 mm
		Corneal thickness	Corneal Topography	CCP: 877 ± 13.58 μ m
Heichel et al. 2016	5	Keratometric power	Keratometry	Ks: 39.6 ± 0.89 D Kf: 38.5 ± 0.92 D
		Corneal Astigmatic power	Corneal Topography	ΔK : 1.10 ± 0.78 D
		Corneal thickness	Ultrasound Pachymetry	CCP: 832.6 ± 40.18 μ m CD: 13.81 ± 0.83 μ m

1% v/v L-glutamine (Lonza, Berkshire, UK), 10% Foetal Bovine Serum (FBS; Sigma-Aldrich, UK) and 20% w/v Dextran ($M_w \sim 250kDa$, Sigma-Aldrich, UK) to minimise corneal swelling (Kim et al. 2014). Animals were white domestic pigs aged between 12 to 25 weeks. To avoid tissue deterioration, examinations were performed within 6 hours after enucleation.

Central corneal curvature was estimated with E300 Corneal Topographer (Medmont, Melbourne, Australia). Corneal thickness (central and at 5mm and 9mm eccentricity), anterior chamber depth and angle were measured with a Visante AS-OCT system (Carl Zeiss Meditec, Dublin, CA). Anterior chamber depth was measured from the posterior corneal surface to the anterior lens, Figure 4.1. Corneal thickness was also evaluated using an ultrasonic pachymeter (UP-1000, Nidek, Gamagori, Aichi, Japan). Eyeballs images were taken with a digital slit-lamp (CSO, Firenze, Italy) and both corneal horizontal and vertical diameter were evaluated using ImageJ software (<https://imagej.nih.gov/ij/>).

Corneal endothelial cells are highly specialised cells, which do not divide in vivo. Endothelial cell density (ECD) is, therefore, a commonly reported indicator of corneal

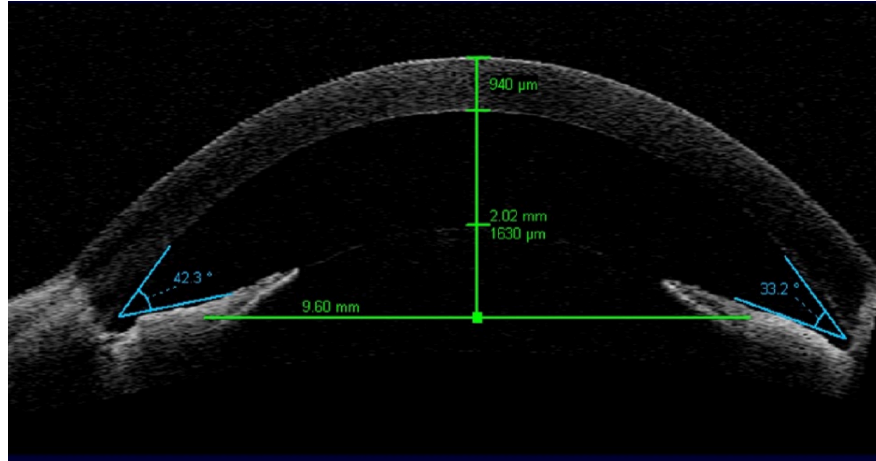


FIGURE 4.1: Representative Visante AS-OCT image of an examined porcine eyeball. Central Corneal Thickness = $940\ \mu\text{m}$, Anterior Chamber Depth = $2.02\ \text{mm}$.

health, as values below ~ 500 lead to oedema, corneal clouding and eventually vision loss in humans (Engelmann et al. 2004). A small sample of ten porcine eyes that guaranteed the best corneal transparency were used for the determination of ECD, which was obtained using a scanning slit confocal microscope (ConfoScan 3, Nidek Technologies, Padova, Italy). Different eyeball holders were specially designed to securely position samples during imaging and measurements without distorting the natural structure (Figure 4.2). To prevent dehydration, samples were irrigated with saline solution during the experimental procedure, and experiments were performed at room temperature ($\sim 20^\circ\text{C}$).

Statistical analysis was performed using Matlab software (The Mathworks, Inc., Natick, MA). Kolmogorov-Smirnov test was used to compare the data with the normal distribution. Data were found not significantly different than a normal population ($p > 0.05$).

4.3 Results

4.3.1 Corneal curvature

Corneal curvature data are illustrated in Figure 4.3 ($n = 60$). The average corneal steepest and flattest meridian were $7.85 \pm 0.32\ \text{mm}$ and $8.28 \pm 0.32\ \text{mm}$, respectively, with associated shape factor (p-value) of 0.38 ± 0.25 and 0.51 ± 0.30 (Benes et al. 2013), and

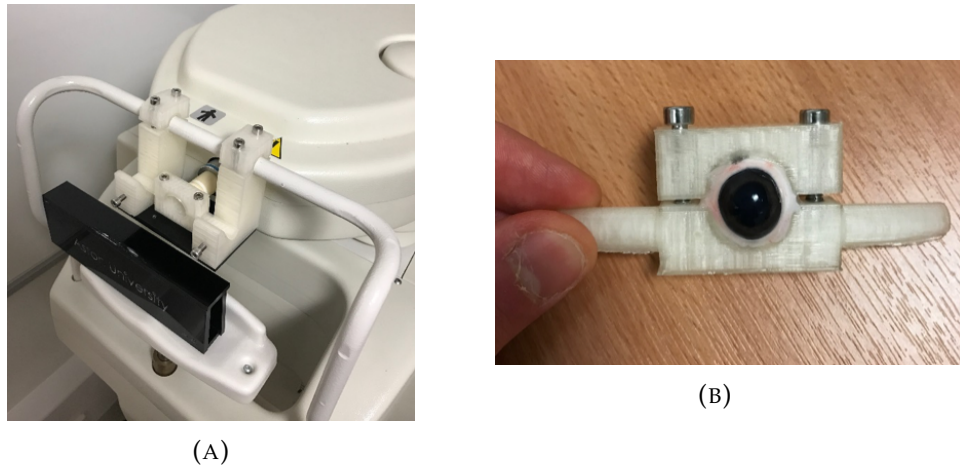


FIGURE 4.2: Setup for scanning slit confocal examination of porcine eyeballs. Overall measuring configuration (A); porcine eye secured in the holder (B). Due to the size variability of porcine eyes, the holder has been designed to fit different globe sizes by adjusting the two top screws in the right image.

a mean curvature difference (ΔK) of 0.43 ± 0.18 mm.

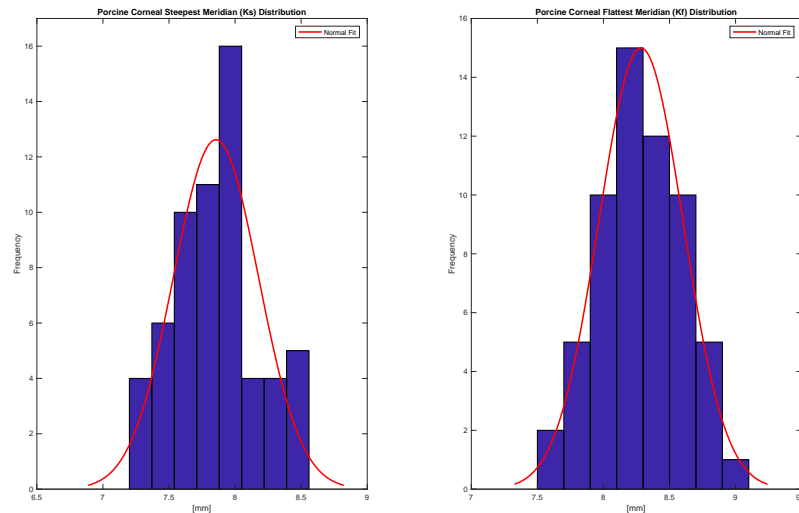


FIGURE 4.3: Steepest meridian data distribution and associated Gaussian fitting (Left); Flattest meridian data distribution and associated Gaussian fitting (Right).

4.3.2 Corneal thickness

Central corneal thickness, measured with the ultrasonic pachymeter and the Visante OCT system, were 1009 ± 1 μm and 1248 ± 144 μm , respectively ($n = 60$). OCT data

distribution is presented in Figure 4.5 (n = 60).

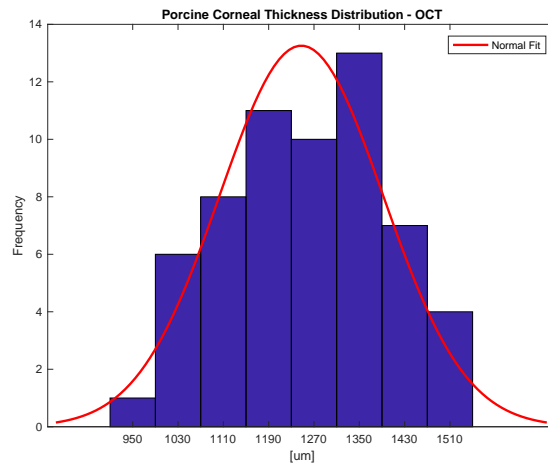


FIGURE 4.4: Central corneal thickness data distribution (Visante AS-OCT) and associated Gaussian fitting.

The porcine corneal thickness was relatively constant in the centre and slightly thickened towards the limbus. In particular, the corneal thickness was found to be 2% and 8% thicker at 5 mm and 9 mm from the centre, respectively, in a sample of twenty eyeballs that guaranteed the best alignment with the instrument, Figure 4.5.

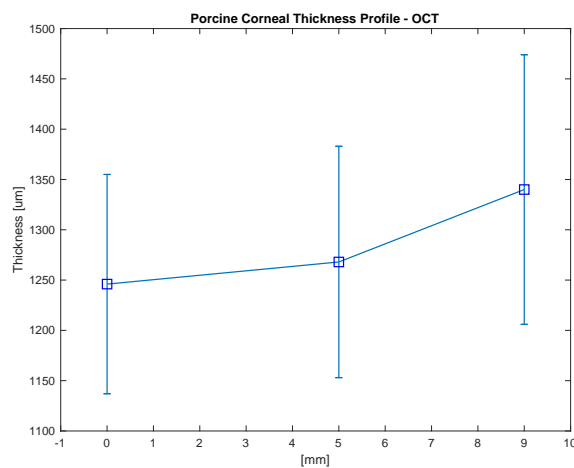


FIGURE 4.5: Porcine corneal thickness profile. The figure shows the corneal thickness at the centre, at 5 mm and 9 mm in twenty porcine eyeballs. Error bars = 1 STD.

4.3.3 Anterior chamber angle and depth

Data distributions relative to anterior chamber angle and depth are shown in Figure 4.6 ($n = 60$). The average anterior chamber angle was $28.83 \pm 4.16 \text{ deg}$, while the mean anterior chamber depth was $1.72 \pm 0.26 \text{ mm}$. It has to be noted that the OCT obtains the geometrical path measure dividing the optical path length by the refractive index value of 1.376. Taking into account that the anterior chamber is filled with aqueous humour, whose refractive index is 1.333, correcting for this discrepancy the mean anterior chamber depth was $1.77 \pm 0.27 \text{ mm}$ (Podoleanu et al. 2004).

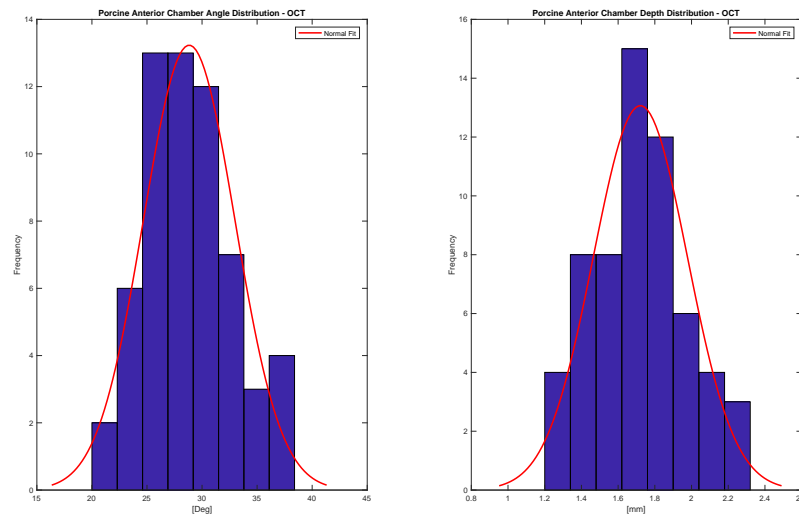


FIGURE 4.6: Anterior chamber angle data distribution and associated Gaussian fitting (Left); Anterior chamber depth data distribution and associated Gaussian fitting (Right).

4.3.4 Corneal diameters

Data for corneal diameters are reported in Figure 4.7 ($n = 60$). The average shortest corneal diameter was $12.69 \pm 0.58 \text{ mm}$, while the mean longest corneal diameter was $14.88 \pm 0.66 \text{ mm}$. Corneal diameters were measured white to white.

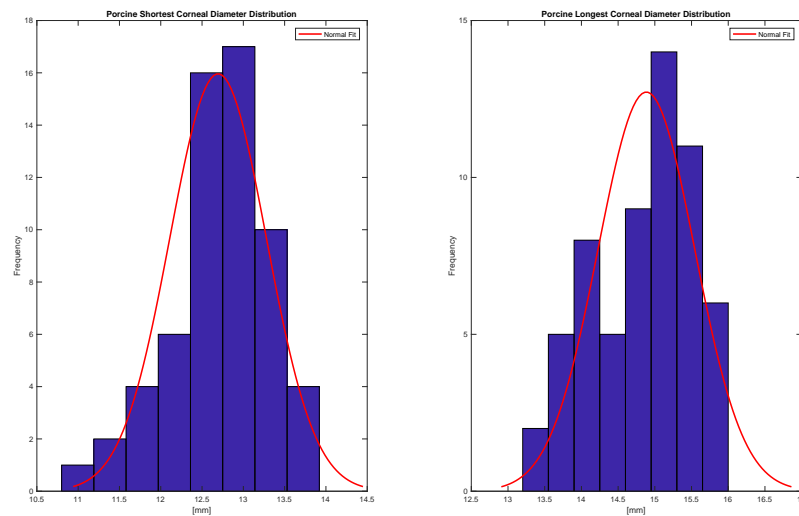


FIGURE 4.7: Shortest corneal diameter data distribution and associated Gaussian fitting (Left); Longest corneal diameter data distribution and associated Gaussian fitting (Right).

4.3.5 Endothelial cell density (ECD)

The average ECD was $3250 \pm 172 \text{ cells/mm}^2$ ($n = 10$), and an exemplary confocal image of the porcine corneal endothelial layer is shown in Figure 4.8.

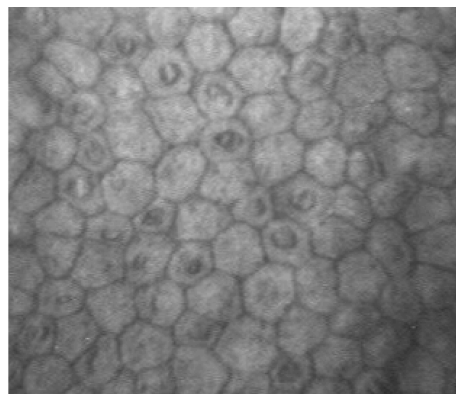


FIGURE 4.8: Representative confocal image of the endothelial cell layer of an examined porcine eyeball.

4.4 Discussion

Ex-vivo eye models provide economic and logistical advantages for animal alternatives, as they allow faster safety and risk assessment of chemicals/pharmaceuticals, with a potential greater predictive relevance for human and environmental safety compared to cumbersome animal-based approaches (Doke & Dhawale 2015). In vision

science research, the porcine eye is one of the most commonly used models, as its morphology has been widely investigated (van Vreeswijk & Pameyer 1998, Shentu et al. 2009, Menduni et al. 2018). However, experimental evaluations of the main parameters of the porcine eyeball are scarce in literature, especially with regard to corneal topography and endothelial imaging.

This chapter investigated several anatomical parameters of the porcine eye, combining optical mapping, confocal microscopy, ultrasonic pachymetry and OCT. The viability of using optical mapping systems such as the Medmont E300 Corneal Topographer was assessed in evaluating porcine corneal topography *ex-vivo*. An average corneal steepest and flattest meridian of 7.85 ± 0.32 mm and 8.28 ± 0.32 mm were respectively found, with associated eccentricity ($\epsilon = \sqrt{(1 - p)}$) of 0.79 ± 0.17 and 0.70 ± 0.20 , and with a mean ΔK of 0.43 ± 0.18 mm. These values are slightly smaller than those reported by Sanchez et al. (8.19 mm and 8.69 mm, $\Delta K = 0.50$ mm) and Heichel et al. (8.52 mm and 8.77 mm, $\Delta K = 0.25$ mm), but more closely centred in the range of human anterior corneal curvature (7.06 to 8.66 mm) (Mashige 2013, Sanchez et al. 2011, Heichel et al. 2016).

This is the first time the shape factor (or rate of flattening of the cornea from the centre to the periphery) of porcine eyes has been reported. Being greater than humans (0.41 ± 0.11), it reflects that the porcine corneal surface is flatter, but both corneal geometries are elliptical in shape (Benes et al. 2013). These interesting findings suggest that porcine eyes may also be used as a valuable tool in the research and development of new contact lens materials (Figure 4.9), bearing in mind the difference in corneal diameters that would require size modification of standard commercial contact lenses.

With regards to corneal thickness, it is worth noting that the porcine cornea is characterised by a thicker epithelium and stroma than the human, and lacks Bowmans layer (Sanchez et al. 2011). Using ultrasonic pachymetry and OCT, a mean corneal thickness of 1009 ± 1 μ m and 1248 ± 144 μ m were respectively obtained. The former value is comparable to both the one obtained *ex-vivo* by Jay et al. using laser scanning

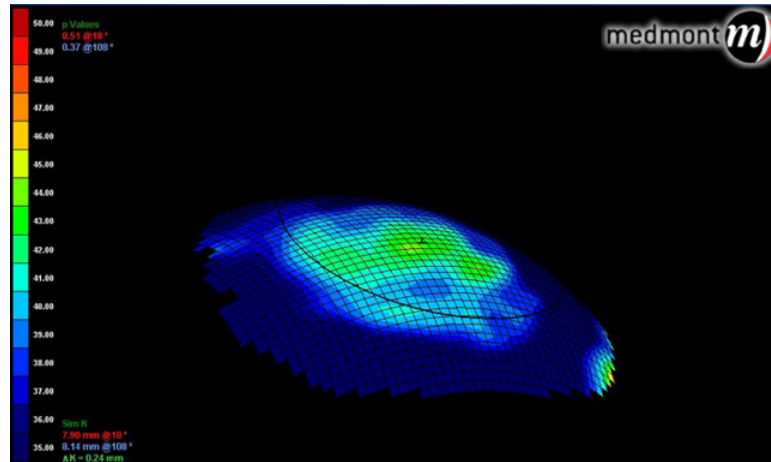


FIGURE 4.9: Exemplary 3D topography of a porcine cornea.

microscopy ($1013 \pm 10 \mu m$) (Jay et al. 2008), and the one obtained *ex-vivo* by Asejczyk-Widlicka et al. using a Visante OCT ($960 \pm 50 \mu m$) (Asejczyk-Widlicka et al. 2008). In addition, all *in-vitro/ex-vivo* study findings are considerably higher than *in-vivo* findings ($666 \mu m$) (Faber et al. 2008). This difference may be related to the different ages and types of pig used, together with potential corneal swelling occurring due to the time after enucleation *ex-vivo* measurements are taken. The corneal thickness only increased slightly in the periphery ($1.02x$ at $5mm$ eccentricity and $1.08x$ at $9mm$ eccentricity) so was more similar to the human peripheral cornea (Prospero Ponce et al. 2009).

Furthermore, anterior segment OCT was used to measure anterior chamber angle and depth, revealing an average anterior chamber angle of $28.83 \pm 4.16 \text{ deg}$, and a mean (refractive index corrected) anterior chamber depth of $1.77 \pm 0.27 \text{ mm}$. These values are smaller than the ones reported in previous studies (Bartholomew et al. 1997, Asejczyk-Widlicka et al. 2008), which may be accounted for by the mounting or transportation methods, or by the pig age.

The mean shortest and longest diameter of $12.69mm$ and $14.88mm$ found in this study are in accordance with previous findings *in vivo* ($12.4mm$ and $14.9mm$, respectively) and *ex-vivo* ($14.00mm$ and $16.61mm$, respectively) (Bartholomew et al. 1997, Faber et al. 2008). These data outline the asymmetrically oval shape of the porcine cornea, also indicating that standard diameter commercial contact lenses, which have a diameter

TABLE 4.2: Comparison of mean porcine eye parameters experimentally obtained and estimated average human eye parameters according to the scientific literature.

Parameter	Porcine eye	Human eye
Corneal steepest meridian	7.85 mm	7.65 mm
Corneal flattest meridian	8.28 mm	7.79 mm
Corneal astigmatism (ΔK)	0.43 mm	0.14 mm
Central corneal pachymetry	1009 μm	523 μm
Peripheral corneal thickness (7-9 mm)	1340 μm	564 μm
Anterior chamber depth (OCT)	1.77 mm	3.11 mm
Anterior chamber angle (OCT)	28.8 deg	38.1 deg
Shortest corneal diameter	12.69 mm	11.71 mm
Longest corneal diameter	14.88 mm	12.00 mm
Endothelial cell density (ECD)	3250 cell/mm^2	2496.9 - 4049.5 cell/mm^2

of approximately 14mm, would not fit well on a porcine eye.

Finally, a scanning slit confocal system (ConfoScan3, Nidek Technologies, Padova, Italy) was used to evaluate porcine ECD *ex-vivo*. A mean ECD of $3250 \pm 172 \text{ cell}/\text{mm}^2$ was found, which is lower than the ones reported in previous studies ($4411 \pm 280 \text{ cell}/\text{mm}^2$) (Kim et al. 2010, Schroeter et al. 2015). The discrepancy may be due to the different technique used, especially because ConfoScan3 data on porcine eyes were not found in the literature. The findings of this chapter are, however, within the human normal range ($2496.9 - 4049.5 \text{ cell}/\text{mm}^2$) assessed using scanning slit confocal systems (Bourne 2003).

The differences between the porcine eye data obtained in this chapter and corresponding human anterior segment parameters are summarised in Table 4.2, which clearly shows the really similar morphology to the human eye, a key feature that may allow researchers to conduct reproducible studies on contact lenses and solution cytotoxicity (Bourne 2003, Rufer et al. 2005, Nemeth et al. 2007, Leung et al. 2008, Prospero Ponce et al. 2009, Hashemi et al. 2010, Benes et al. 2013, Mashige 2013).

In conclusion, this chapter represents a further source of reproducible data that should be considered when using porcine eyes as *ex-vivo* model for experimental research.

The cost and availability of high quality human donor eyes are obstacles to vision science research. Porcine eyes, if properly handled and stored, represent a reliable and high quality tissue source with similar glands producing the tear film that may be combined with bioengineering and bio-photonics technologies to provide new useful tools and models in applied ophthalmic research, in particular in dry and ageing eye research (Choy et al. 2008, Loewen et al. 2016).

5

The Aston Biological Anterior Eye Model

5.1 Introduction

Developing *ex-vivo* anterior eye models is an intuitive, necessary surrogate to illuminate some of the intricate mechanisms of ocular pathologies such as Dry Eye Disease (DED) which are challenging to analyse *in-vivo* (Choy, Cho, Benzie, Choy & To 2004, Spoler et al. 2010). De facto, *ex-vivo* organ cultures are becoming increasingly important in both fundamental and applied biomedical research, as they more closely retain the natural cellular behaviour found *in-vivo* than *in-vitro* monolayer cultures (Figure 5.1). However, organ culture is extremely challenging, as environmental conditions must be controlled and optimised to maintain tissue viability and stable matrix composition (Shafaie et al. 2016).

Tissue viability is generally prolonged when pseudo physiological conditions are recreated as closely as possible and sufficient levels of supplements are retained at cellular

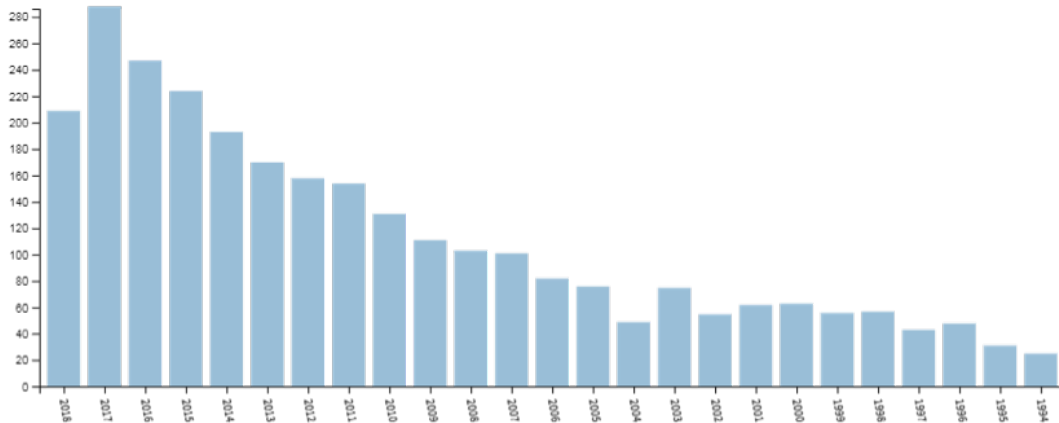


FIGURE 5.1: Number of publications per year with the keywords *ex vivo* model in the title. There has been an evident increase in the number of publications related with *ex-vivo* organ culture from 1995 to date. Search has been performed on all databases of Web of Science on September 2018.

level by periodically refreshing the culture medium that eliminates metabolic waste products from the cellular environment (Elson et al. 2015). Recently, advances in biomedical technologies have led to the development of bioreactors capable of closely controlling environmental and operating conditions, such as temperature, pressure, flow rate and nutrient supply in organotypic models of the cornea and the crystalline lens, retaining cell viability over seven days (Guindolet et al. 2017, Cleary et al. 2010, Zhao et al. 2006). As discussed in Chapter 2, these models represent cost-effective platforms for preclinical experiments, though they still leave room for improvement toward the creation of a complete anterior eye model that could elucidate the complex interaction between the different structures of the anterior eye in pathologies such as DED.

This chapter describes how biomedical technologies such as rapid prototyping and manufacturing, electronic design, optical imaging and biological assays have been combined to devise a novel *ex-vivo* complete anterior eye model that could be a meaningful alternative to animal testing for studying anterior eye physiopathology.

The chamber consisted of a **Suction module**, which was devised to satisfactory capture the porcine globe at its pre-equatorial region during the dissection procedure, and a **Perfusion module**, instead devised to securely clamp the anterior segment creating a watertight seal, and to allow media perfusion to the crystalline lens and corneal endothelium. Both modules were design to be harmoniously adopted into a Mounting protocol that could allow the operator to dissect the globe and securely mount it for perfusion in the shortest amount of time possible, minimising tissue deterioration.

Suction module

Initial design concepts were based on the biometric references reviewed in Chapter 4, and then evolved until the globe equator was easily accessible for dissection and the whole cornea was visible and irrigable (Figure 5.3). A modular suction chamber was thus designed to firmly hold the globe during dissection by creating a light vacuum using a 25ml syringe (Figure 5.4).

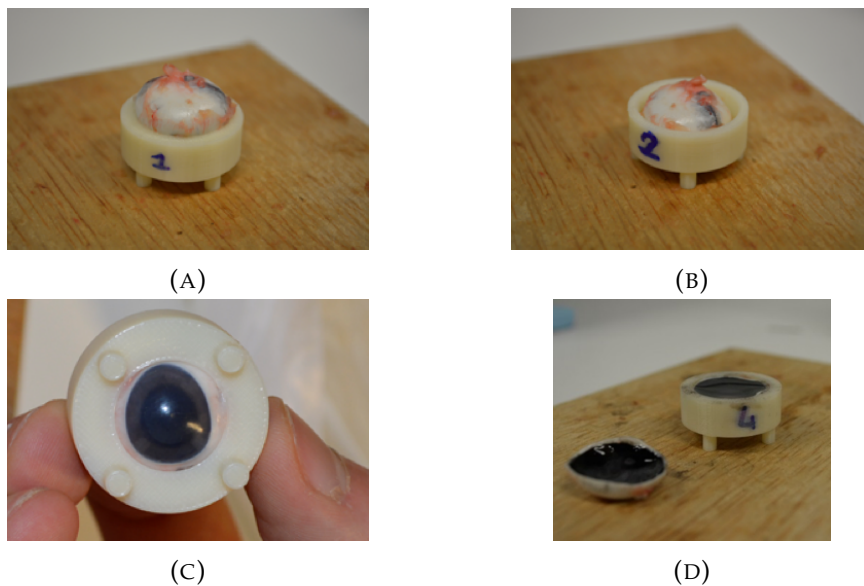


FIGURE 5.3: Evolution of the prototyping phase of the suction module. Sustainability was reinforced minimising the amount of material used via 3D printing, reducing energy consumption and using local resources.

Due to the interspecies variability of the biological tissue (see Chapter 4), the physical dimensions of the chamber needed to be optimised to ensure air-tight clamping of the sample while minimising tissue distortion, which was achieved by iteratively 3D

printing, laser cutting and trialling several chamber prototypes, prior to construction of the finalised prototype in biologically inert and autoclavable PTFE (Figure 5.4).

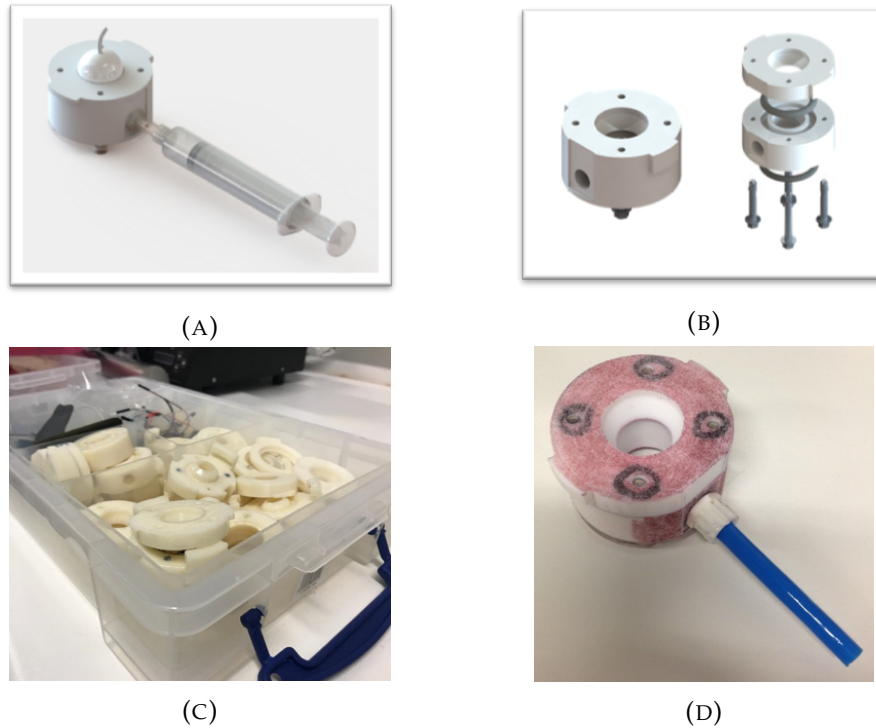


FIGURE 5.4: Suction module design and manufacturing. SOLIDWORKS renderings (A and B). 3D printed prototypes tested (C). Final suction chamber manufactured in PTFE (D).

Perfusion module

As well as for the suction chamber, initial design concepts of the perfusion module were based on the biometric references reviewed in Chapter 4, and then the physical dimensions of the chamber evolved until the porcine tissue could be perfused without significantly altering the morphological structure of the anterior segment. The final prototype was optimised by having a wall thickness sufficiently large to bear the sterilisation process without bending and was manufactured in PTFE (Figure 5.5).



FIGURE 5.5: Perfusion module design and manufacturing. SOLIDWORKS renderings (A) and final prototypes manufactured in PTFE (B).

Mounting protocol

The mounting protocol was devised to securely clamp the porcine anterior segment in the perfusion module within the shortest amount of time possible to minimise tissue handling (Figure 5.6).

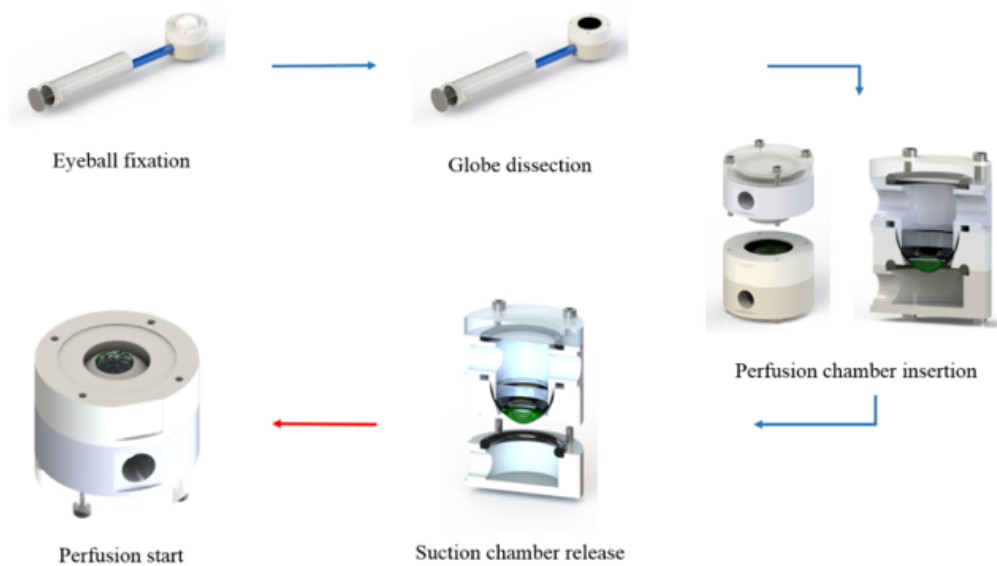


FIGURE 5.6: Schematic description of the procedure devised to mount a porcine anterior segment in the perfusion chamber.

The procedure was composed by the key steps below:

1. **Eyeball holding**: the porcine eyeball was placed epithelial side down into the suction module. A light suction was generated using a 25 ml syringe, consequently holding the tissue in place;

2. **Globe dissection:** the porcine globe was dissected at the equator using a vibrating blade (PMF 220 CE, Bosch), the posterior segment was discarded, exclusively leaving in place the anterior segment and relative vitreous;
3. **Perfusion chamber mounting:** the perfusion module was pressed on the suction module and attached to it via a rotation mechanism. Tolerances of both modules had been optimised to allow for smooth components rotation, while still guaranteeing a water-sealed clamping of the porcine anterior segment to the perfusion chamber;
4. **Endothelial perfusion:** the suction module was unscrewed, and the perfusion chamber was connected to both the peristaltic pump and the pressure sensors to initiate endothelial perfusion and stabilise IOP.
5. **Epithelial irrigation:** the perfusion chamber was mounted vertically into the automatic irrigation system and epithelial irrigation was initiated.

The whole procedure is reported in the video footage no 1, which has been supplied as supplementary data. Combining rapid prototyping with traditional mechanical manufacturing minimised prototyping time and final chambers allowed the author to successfully dissect, mount and perfuse more than 95% of the samples.

To further validate the mounting technique, morphometric data regarding anterior chamber depth (ACD) and central corneal thickness (CCT) were obtained from eight freshly enucleated pre-scalded porcine eyes using SD-OCT (Ganymede Series SD-OCT, Thorlabs) before and after dissection / mounting (Figure 5.7). Parameters of the SD-OCT system used in the study are reported in Table 5.1, while experimental results are detailed in Table 5.2 and Table 5.3.

TABLE 5.1: Parameters of the Ganymede Series SD-OCT, Thorlabs.

Central wavelength	930 nm
Axial resolution	5.8 μm (air)
Lateral resolution	8 μm
Sensitivity	101 dB (at 5.5 kHz)

TABLE 5.2: Anterior chamber depth (ACD) measured in eight porcine eyes before and after the mounting procedure using OCT.

ACD before mounting [mm]	ACD after mounting [mm]
2.23	2.27
1.63	1.11
1.78	2.06
1.44	1.84
2.06	1.63
1.99	2.08
1.71	1.96
1.57	1.82

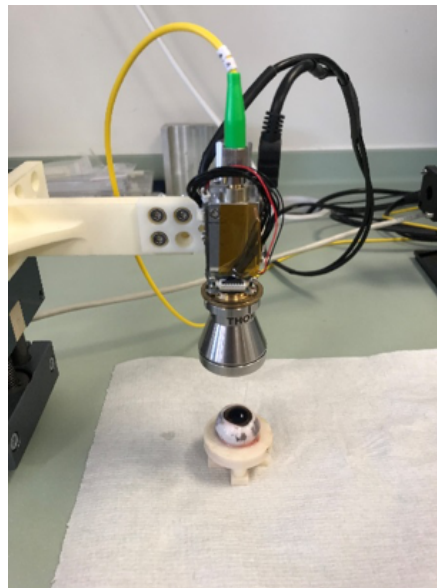


FIGURE 5.7: Exemplary image of the SD-OCT setup to image porcine eyes.

There was no significant ($p > 0.05$) difference in corneal thickness (by 0.03 ± 0.04 mm; $p = 0.163$) and anterior chamber depth (by 0.18 ± 0.33 mm; $p = 0.100$) calculated before and after the mounting procedure ($n = 8$), suggesting that the porcine eyes could be dissected and mounted without causing main structural changes to the anterior segment morphology.

TABLE 5.3: Central Corneal Thickness (CCT) measured in eight porcine eyes before and after the mounting procedure using OCT.

CCT before mounting [mm]	CCT after mounting [mm]
1.84	1.84
1.68	1.68
1.75	1.77
2.03	1.99
1.91	1.85
1.75	1.66
1.96	1.97
1.80	1.75

5.2.2 Environmental control system

The environmental control system was designed to recreate physiological IOP and flow rate in the endothelial compartment, while reproducing intermittent irrigation and air exposure to the porcine epithelium.

Endothelial perfusion

The endothelial perfusion system consisted of a microfluidic 4-channel, 12-roller, variable speed peristaltic pump (ISM597, Ismatec REGLO, Wertheim, Germany) passing temperature controlled physiological solution (Dulbeccos Modified Eagles Medium (DMEM; Lonza, Berkshire, UK), supplemented with 1% penicillin (10,000 units/ml) and streptomycin (10,000 mg/ml), 1% v/v L-glutamine (Lonza, Berkshire, UK), 10% Foetal Bovine Serum (FBS; Sigma-Aldrich, UK)) through the perfusion chamber at a monitored intraocular pressure (IOP) (Kim et al. 2014). The temperature of the biological solution was set at 37°C and controlled using a digital, PID controlled hot plate (SH-5H, MESE Ltd., Leeds, UK), while the IOP was controlled via compensated gauge pressure sensors (ADP51B63, Panasonic, Bracknell UK) and adjusted by altering the height differential of the solution to create a pressure in the anterior chamber 18-20 mmHg higher than atmospheric pressure. Flow rate was set to 1 ml/min to ensure constant delivery of culture medium into the anterior segment maintaining constant perfusion pressure. Main parameters of the endothelial perfusion system are reported in Table 5.4.

TABLE 5.4: Main parameters of the endothelial perfusion system.

Parameter	Setting
Medium temperature	37°C
Flow rate	1 ml/min
IOP	18–20 mmHg

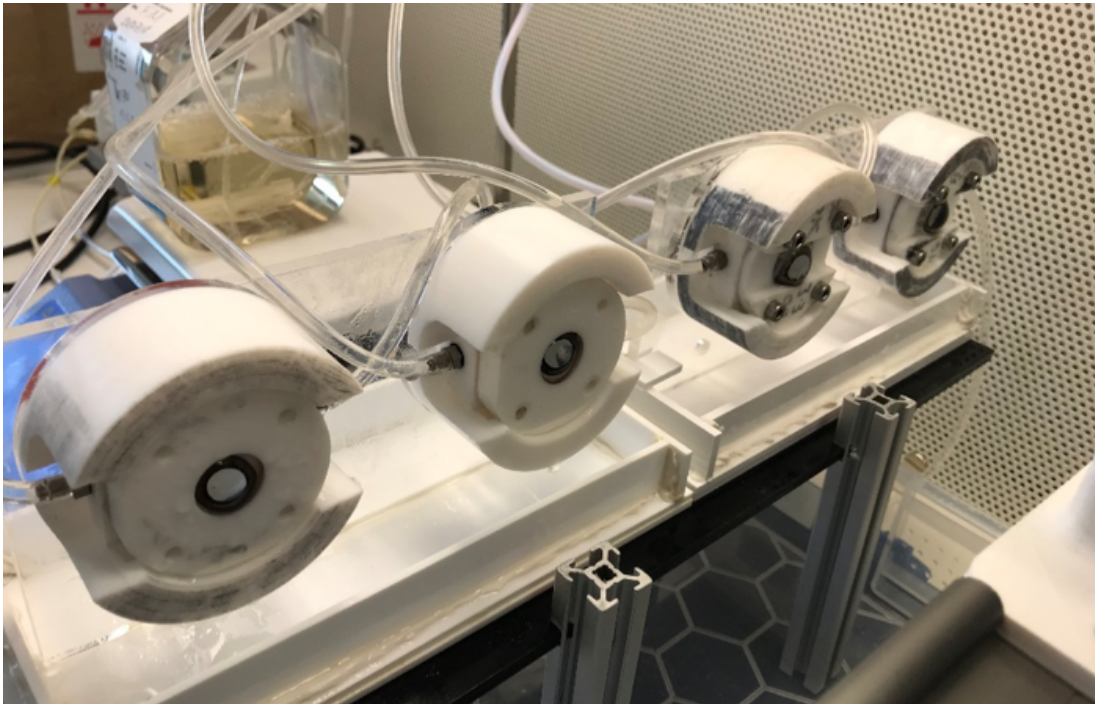


FIGURE 5.8: Experimental image of four porcine anterior segments mounted in the Aston biological anterior eye model and perfused with transparent DMEM at 37°C at 1ml/min, under 18-20 mmHg.

Figure 5.8 illustrates four porcine anterior segments mounted in the Aston biological anterior eye model and connected to the endothelial perfusion system, clearly showing that the model was capable of maintain anterior chamber patency.

Epithelial irrigation

A human eye holds approximately 30 μL of tears, and spontaneous blinking helps to spread the tear film evenly across the ocular surface (Gurung et al. 2016). Mimicking tear replenishment in the eye requires the delivery of a tear analogue to the surface of the *ex-vivo* eye model followed by a period of drying in a recurring fashion under physiological conditions. Inspired by the tear replenishment spray system proposed

by Mohammadi and colleagues in 2014, a novel tear replenishment engineering solution was developed to recurrently spray tear analogue on the corneal epithelium, sufficiently moisturising the surface of the model while maintaining the air-liquid interface (Mohammadi et al. 2014).

The system was composed of a linear actuator activated by electronically controlled relays. Once activated, the actuator pressed on the spray head mechanism of four 250 ml aluminium spray bottles, simultaneously moisturising four corneas with physiological solution (Dulbeccos Modified Eagles Medium (DMEM; Lonza, Berkshire, UK), supplemented with 1% penicillin (10,000 units/ml) and streptomycin (10,000 mg/ml), 1% v/v L-glutamine (Lonza, Berkshire, UK), 10% Foetal Bovine Serum (FBS; Sigma-Aldrich, UK). Anterior segments secured in perfusion chambers were mounted vertically to allow the excess fluid to automatically be drained, consequently avoiding the need for aspiration systems and minimising costs (Figure 5.9).



FIGURE 5.9: 3D rendering of the automated spray system.

In detail, the linear actuator was driven by a 12V DC motor requiring ~ 1 A of current

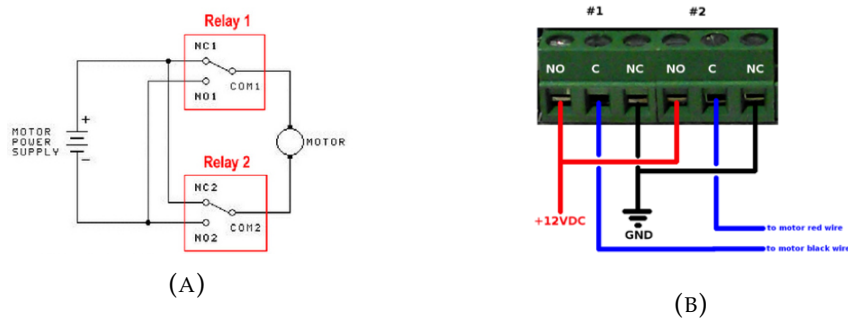


FIGURE 5.10: DC Motor Direction control scheme using two SPDT relays.

TABLE 5.5: 12V DC linear actuator specifications.

Specification	Value
Load capacity	750 N
Protection class	IP54
Input Voltage	12v DC
Speed	10 mm/s
Stroke Length	100 mm

to run (Table 5.5). Controlling the travel direction of the motor required reversing the polarity of the electricity in input to the linear actuator. To achieve so, the motor was wired in the configuration shown in Figure 5.10 to the power supply using an opto-isolated relay board composed of 2 SPDR (Single Pole Double Throw) relays.

When both relays were off, both motor terminals were connected to the same point and the motor was stopped. If one relay was activated, one motor terminal was connected to the opposite polarity and the piston would run in one direction. If the other relay was activated, the motor connected in the opposite polarity reversing piston direction. Finally, if both relays were activated the motor would stop.

To automate the system, the relay board was governed by a microcontroller (Arduino Mega, Arduino, Italy) coupled with a 4.3 colour TFT LCD Resistive Touch display (4D Systems, Minchinbury, Australia) programmed by the author to allow the user to visualise the IOP of the connected chambers and to select the desired misting frequency (Figure 5.11). Separate power sources for the motor and control were used due to the required current for the linear actuator. In these regards, the relay board

was opto-isolated to avoid any possible damage to the microcontroller due to back currents generated by the heavy current load of the motor, and the touch display was chosen to be resistive so to be easily activated when wearing laboratory gloves.

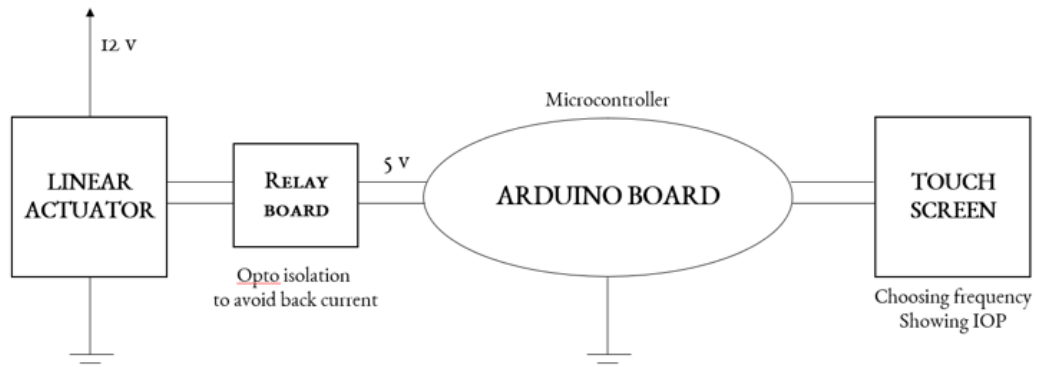


FIGURE 5.11: Electronic design scheme of the automated epithelial irrigation system.

The electronics were enclosed in a custom-made 3D-printed box, and a PCB shield was designed in KiCad (open source software suite for Electronic Design Automation) and manufactured in China (Shenzhen JLC Electronics Co. Ltd, Shenzhen, China) to stabilise electronic connections between the different electronic parts (Figure 5.12).

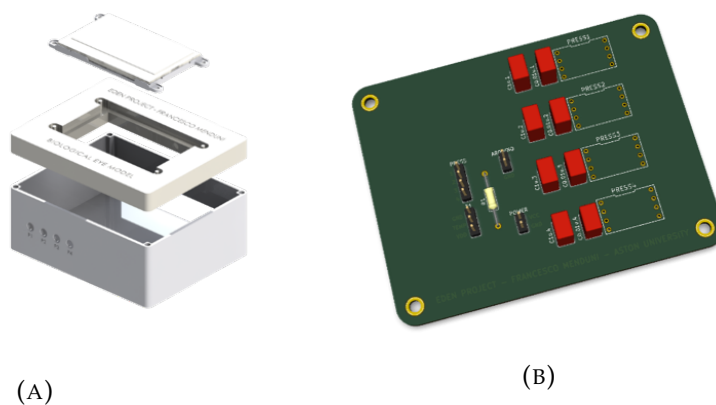


FIGURE 5.12: Electronic enclosure rendering of the Aston Biological Anterior Eye Model (A). Connecting shield PCB of the Aston Biological Anterior Eye Model (B).

To avoid biological contamination, the whole system was fitted in a laminar flow cabinet (HeraGuard ECO, ThermoFisher, Germany), to protect the biological sample and

avoid contamination. The final system, which is reported in the video footage no 2, consisted of four test cells controlled by the same touch screen to allow incremental differences to be examined simultaneously and to maximise experimental reliability (Figure 5.13).

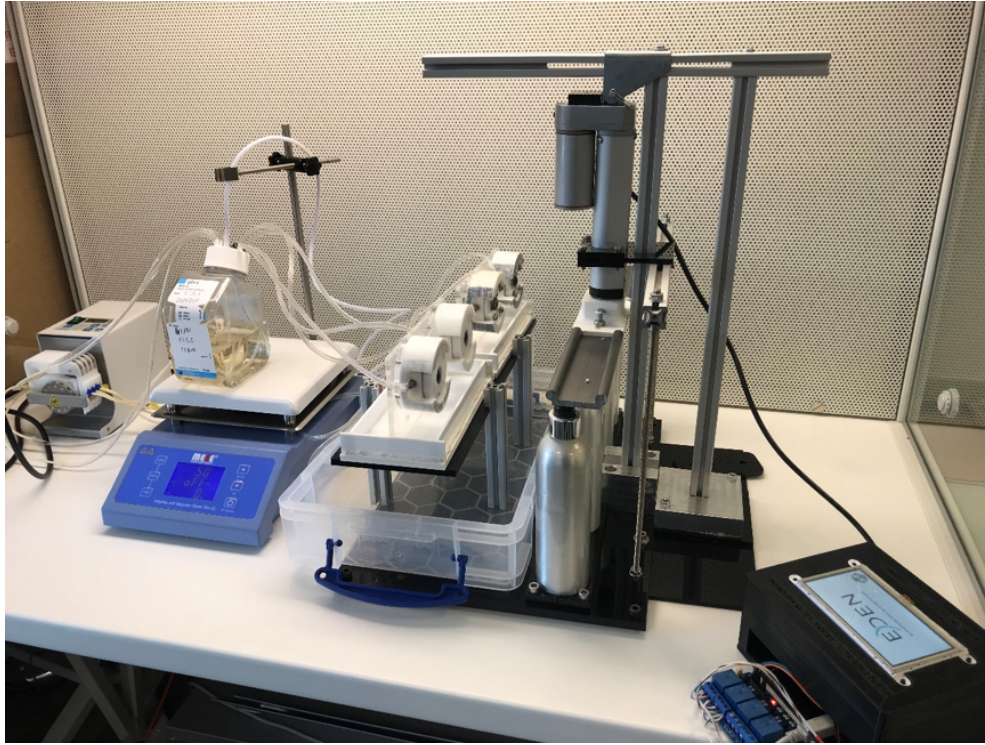


FIGURE 5.13: Experimental overview of the Aston Biological Anterior Eye Model fitted in the laminar flow cabinet. Multichannel peristaltic pump (1), PID controlled hot plate (2), porcine anterior chambers vertically mounted (3), automated epithelial irrigation system (4) and associated electronic box (4).

After the overall system was established, it was crucial to choose an appropriate epithelial irrigation frequency that could allow the external corneal surface to be hydrated in a physiological fashion. In humans, tear film stability is defined as the time interval between a complete blink and the first occurrence of a dry spot in the tear film (Lemp 1973, Norn 1969), and it is ideally clinically measured non-invasively using tear interferometry (Mengher et al. 1985, Wolffsohn et al. 2017). Therefore, the epithelial hydration layer produced by the automated irrigation system was assessed and optimised using a compact and portable tearscope (EASYTEARview+ All in One, Easytear, Italy).

Three pre-scalded porcine eyes were freshly enucleated at a local abattoir, and mounted in the Aston biological anterior eye model. After irrigation, changes in the reflection patterns were video recorded and subsequently interpreted by the author and an experienced optometrist. Representative images are presented in Figure 5.14, which clearly shows that an irrigation frequency lower than 30s was required to ensure a stable epithelial hydration layer on the porcine eye ($n = 3$).

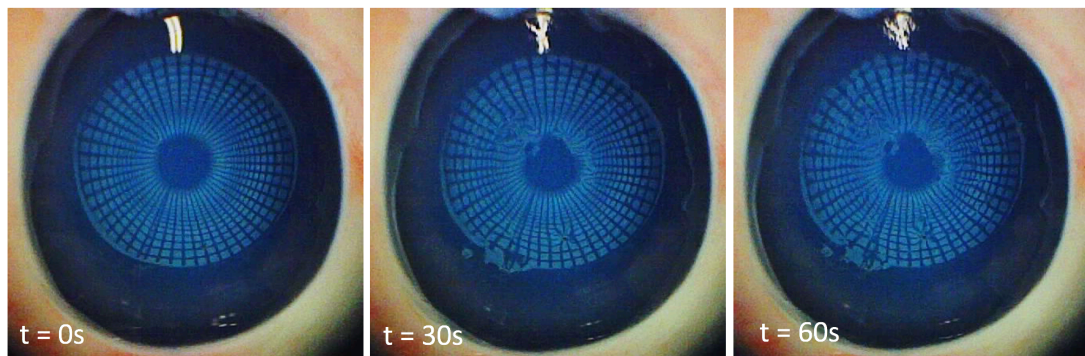


FIGURE 5.14: Representative NIBUT images on a porcine eye. The tear film becomes unstable after 30s from irrigation.

Based on these findings, a 20s interval was selected as default irrigation rate in order to replicate physiological tear dynamics, while still allowing for the 250ml aluminium bottle refilling time to be ~ 13 hr, allowing experiments to be comfortably run over night unsupervised.

5.3 Biological evaluation

Successful organ culture requires the long-term survival of cells, which can be evaluated by estimating cell viability (CV), one of the most important parameters in tissue engineering and culture studies (Johnson & Rabinovitch 2012). Staining and imaging cells with vital fluorescent dyes is a highly versatile approach widely used among cell biologists to estimate cell viability, as specific dyes are activated and retained only in intact cells, providing positive markers for cell viability (Gantenbein-Ritter et al. 2008). To image 3D biological tissues, fluorescent dyes are imaged using multiphoton confocal laser scanning microscopy (Figure 5.15), a technique which has the ability to produce optical sections through a 3D sample by moving the focal plane through the

depth of the biological specimen (Fischer et al. 2011).

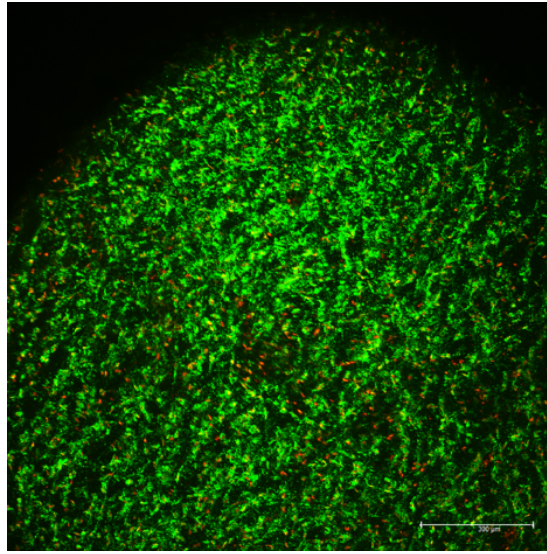


FIGURE 5.15: 3D-stack image of a porcine cornea at stromal level. Green represents live cells, while red indicates dead cells. Because optical sectioning with confocal imaging is non-invasive, the 3D distribution and relative spatial relationship of stained living cells can be observed with reasonable clarity. The z-stack has been taken from the endothelial side. Scale bar = 300 μm .

These techniques were hence adopted in this work to analyse the Aston biological anterior eye model at cellular level and assess its viable time frame. Moreover, a clinically relevant technique such as 'Conjunctival impression cytology' (CIC) was applied to test the feasibility of replicating in the model pathologies such as Dry Eye Disease.

5.3.1 Long term survival

Calcein AM with Ethidium Homodimer-1 staining, commercialised as Live/Dead (Invitrogen, Cambridge, UK) Viability/Cytotoxicity Assay Kit provides a two-colour fluorescence cell viability assay that is based on the simultaneous determination of live and dead cells with two probes that measure intracellular esterase activity and plasma membrane integrity. In particular, live cells are distinguished by the presence of ubiquitous intracellular esterase activity, determined by the enzymatic conversion of the

TABLE 5.6: Excitation and Emission peaks of Calcein AM and Ethidium Homodimer-1.

Fluorescent Dye	Excitation peak	Emission peak
Calcein AM	495 nm	515 nm
Ethidium Homodimer-1	495 nm	635 nm

virtually non-fluorescent cell-permeant Calcein AM to the intensely fluorescent calcein. The polyanionic dye calcein is well retained within live cells, producing an intense uniform green fluorescence in viable cells (Table 5.6). On the other hand, EthD-1 enters cells with damaged membranes and undergoes a 40-fold enhancement of fluorescence upon binding to nucleic acids, thereby producing a bright red fluorescence in dead cells (Figure 5.16). EthD-1 is excluded by the intact plasma membrane of live cells, and background fluorescence levels are inherently low with this assay technique because the dyes are virtually non-fluorescent before interacting with cells.

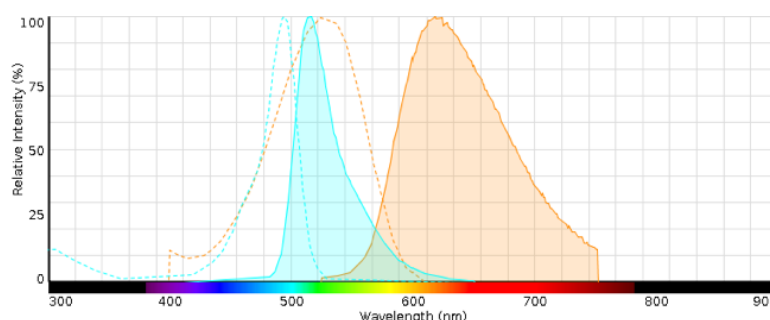


FIGURE 5.16: Excitation (- -) and Emission (-) spectra of Calcein AM (Blue) and Ethidium Homodimer-1 (Orange). The kit has been optimised so to be able to excite both dyes with a single 488 nm multiphoton laser line, while still being able to independently capture emitted signals on two different channels.

The viability of stromal fibroblasts was therefore visualised in six freshly enucleated pre-scalded porcine eyes using the Live/Dead viability kit. Following the manufacturers protocol, three porcine corneas were dissected and incubated with the recommended concentrations of calcein AM and ethidium homodimer (EthD-1) for 1 hour in the dark at day zero. The remaining corneas were firstly cultured in the Aston biological anterior eye model for seven days, and then dissected and stained as previously described. Post-incubation, tissues were carefully washed with PBS and finally imaged on a multiphoton confocal laser scanning microscope (Leica Microsystems,

Wetzlar, Germany).

Live/Dead assay results are indicated in Figure 5.17, which clearly illustrates that porcine stromal fibroblasts remained viable after seven days of organ culture in the Aston biological anterior eye model.

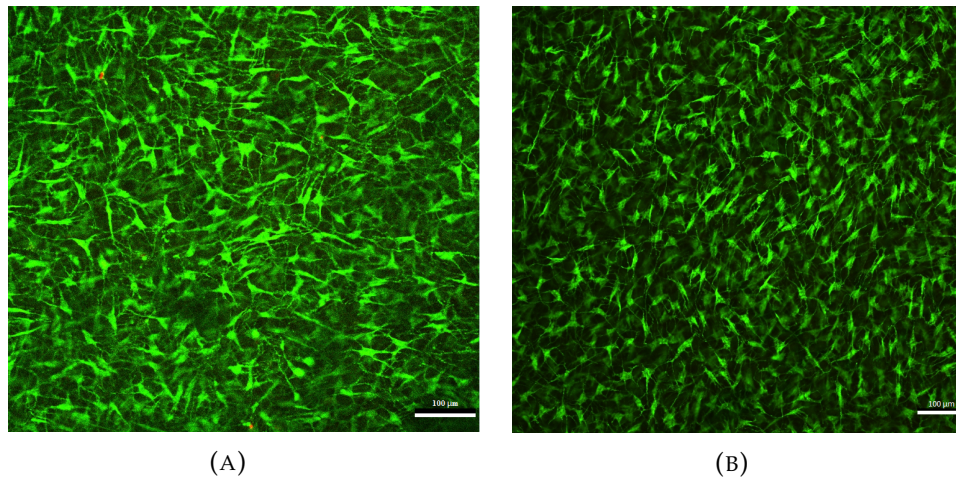


FIGURE 5.17: Live/Dead 2D images of a porcine cornea at day 0 (A) and day 7 (B). Images have been chosen as a representative of three replicates. Scale bar = 100 μm .

A representative image at higher magnification is reported in Figure 5.18, lucidly showing the fibroblastic morphology of the analysed cell, confirming the correct visualisation of the corneal stroma.

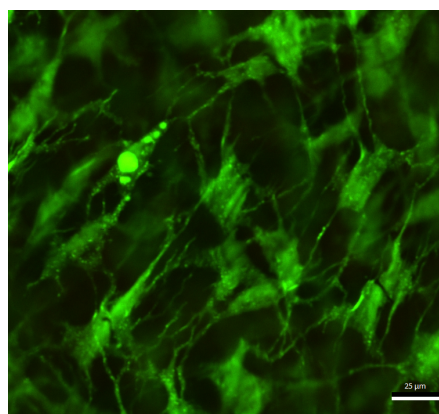


FIGURE 5.18: Higher magnification representative image of corneal fibroblasts obtained using confocal microscopy. Scale bar = 25 μm .

Finally, a porcine anterior segment after seven days of culture is shown in Figure 5.19,

which indicates that the culture system did not cause loss of transparency in the corneal and crystalline lens tissue, being able to preserve the crystalline lens in loco throughout the whole culture period.

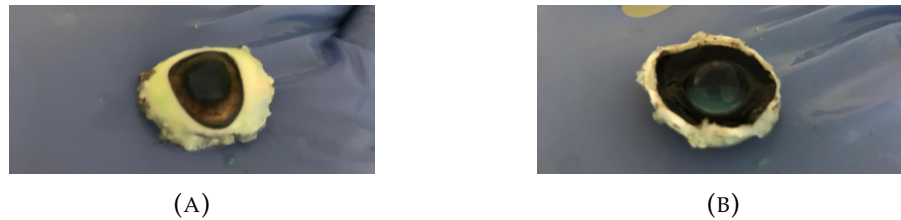


FIGURE 5.19: Transparent cornea (A) and crystalline lens (B) after 7 days of storage in the Aston biological anterior eye model.

5.3.2 Dry eye replication

The latest DEWS TFOS report defines DED as "a multifactorial disease of the ocular surface characterised by a loss of homeostasis of the tear film, and accompanied by ocular symptoms, in which tear film instability and hyperosmolarity, ocular surface inflammation and damage, and neurosensory abnormalities play etiological roles." (Craig, Nelson, Azar, Belmonte, Bron, Chauhan, de Paiva, Gomes, Hammitt, Jones, Nichols, Nichols, Novack, Stapleton, Willcox, Wolffsohn & Sullivan 2017). In this disease, the conjunctival epithelium often undergoes a pathological transition to a keratinized non-secretory corneal and conjunctival surface, characterised by epithelial cells squamous metaplasia and goblet cell depletion (Murube & Rivas 2003). Conjunctival impression cytology (CIC) represents a minimally invasive method to collect superficial epithelial layers for analysing these changes at a molecular level via the application of cellulose acetate filters over the ocular surface (Tole et al. 2001). As a result, CIC is considered a clinically useful test in the diagnosis of DED, as it has shown a promising correlation with the duration of computer use (Bhargava et al. 2014), and it has been used to evaluate the efficacy of topical cyclosporine in different grades of DED (Yuksel et al. 2010). However, CIC studies on *ex-vivo* eye models are still not present in the academic literature, leaving an open question about the possible use of this technique as a non-destructive monitoring method of the ocular surface in *ex-vivo* organ cultures. Therefore, a feasibility study was conducted to explore the *ex-vivo*

characterisation of the porcine conjunctival surface using CIC, and the potential application of this technique to assess the viability of replicating DED using the Aston biological anterior eye model.

Nine freshly enucleated pre-scalded porcine eyes underwent conjunctival impression cytology (CIC) near the limbus. Specimens were respectively collected in three eyes immediately after the mounting procedure, three eyes after 2hr of culture in the Aston biological anterior eye model with an irrigation rate of 20s, and three eyes after 2hr of culture in the Aston biological anterior eye model with an irrigation rate of 40s (Evaporative Dry Eye condition). Two 2x3 mm rectangular pieces of nitrocellulose filter paper (Pall, New York, NY, USA) were cut and placed separately on the nasal and temporal bulbar conjunctiva with filter paper dull-side down and held in place for 10 seconds under constant pressure. The filter paper was then gently lifted and fixed with 96% alcohol. Haematoxylin and periodic acid-Schiff (PAS) reagents were used to stain the cells. In particular, after a minimum of ten minutes in 96% ethanol, the filter material was hydrated with distilled water (10 min), oxidised in 1% periodic acid (10 min), rinsed in distilled water (3 min), and stained with Schiff's reagent (3 min) (Li et al. 2012). Strips that developed a pink colour were then rinsed in distilled water to provide oxidation (five minutes) for following staining. Filter materials were counter-stained with haematoxylin (20 s), rinsed in distilled water (3 min), dehydrated by two successive baths of 96% ethanol (2 minute each), two successive baths of 100% ethanol (2 minute each) and a bath in xylene (9 min). Afterward, specimens were placed on a glass slide and permanently mounted on a glass slide using Entellan (Merck KGaA, Darmstad, Germany), a rapid mounting medium for microscopy (Figure 5.20).

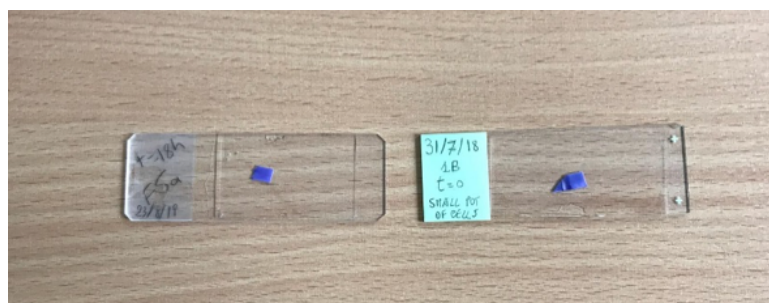


FIGURE 5.20: Examples of CIC filter papers stained and permanently fixed.

After staining, three different sections of each specimen were selected randomly for evaluation under a light microscope with a 10X and 40X objective, and digital images of representative areas were taken using a scientific CCD camera (Retiga R1, QImaging, USA) camera and evaluated using the Nelson system (Nelson et al. 1983). This grading system considers the density, morphology, cytoplasmic staining affinity and nucleus/cytoplasm ratio of conjunctival epithelial and goblet cells to grade the ocular surface in 4 stages (0-1: normal, 2-3: altered).

Representative images are reported in Figure 5.21, which successfully shows epithelial and goblet cell morphologic features on cytological impressions obtained from *ex-vivo* porcine eyes, as well reveals cytological changes associated with the longer epithelial irrigation frequency of 40s (Evaporative Dry Eye condition).

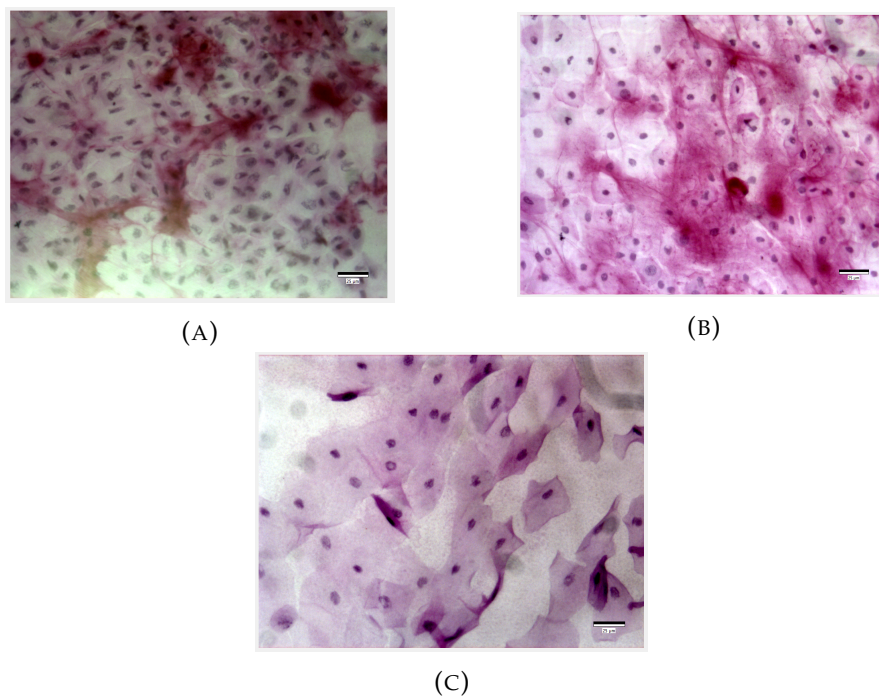


FIGURE 5.21: Ocular surface samples before the mounting procedure (A), after two hours of irrigation every 20s (B) and 40s (C). Scale bar = 25 μ m.

At time zero, conjunctival epithelial cells were healthy, small, and characterised by large, basophilic nuclei with nucleocytoplasmic ratio of 1:2 ($n = 3$). Goblet cells were present, however not oval (Figure 5.21, A). This abnormal feature may be an artefact

due to the excessive pressure of the filter paper on the porcine ocular surface, underlining the importance of trained personnel for sample taking and processing.

An epithelial irrigation rate of 20s ensured the maintenance of a healthy conjunctival epithelium ($n = 3$). Epithelial cells remained small, and with a maximum nucleocytoplasmic ratio of 1:3 (Figure 5.21, B). This is perfectly in line with our previous interferometric findings, as an epithelial irrigation rate smaller than 30s was shown to ensure a stable epithelial hydration layer on the porcine eye.

Finally, an epithelial irrigation rate of 40s caused changes typical of Dry Eye Disease (Zuazo et al. 2014) just after 2 hours of culture ($n = 3$). Epithelial cells were hence large and polygonal, with small, pyknotic, and, in some cells, completely absent nuclei. Nucleocytoplasmic ratio was greater than 1:3, and goblet cells were completely absent (Figure 5.21, C).

5.4 Discussion

Over the years, a great amount of research has been dedicated to the development of laboratory alternatives that could minimise the use of animals wherever possible (Kirk 2018). Alternatives to animal studies span from the complete to the partial replacement of live animals in biomedical research; in the ophthalmic field important contributions have been made by the development of *ex-vivo* ocular models (Shafaie et al. 2016). For example, in the early 1990s the Bovine Corneal Opacity and Permeability (BCOP) and the Isolated Chicken Eye (ICE) *ex-vivo* ocular safety methods were successfully validated by the regulators, and led to an estimated reduction in the use of live animals for eye safety testing of more than 10% (Hood 2008).

For anterior eye investigations, although several *ex-vivo* models have been developed for the corneal and crystalline lens tissue (Chapter 2), any of them allows scientists and regulators to retain the intercellular connections and interplays between these two systems. This chapter described the development of a novel and complete *ex-vivo* anterior eye model capable of sustaining the porcine cornea and crystalline lens

in a physiologically stable state in loco for up to seven days. The model has been named the Aston Biological Anterior Eye Model, and its development encompassed approximately 8,000 man hours of work across multiple engineering and biomedical disciplines.

First of all, this platform was based on porcine eyes, which are readily available slaughterhouse waste and show the closest anatomical and biochemical makeup to human eyes (Menduni et al. 2018, Groenen et al. 2012). This choice minimised not only the model developmental time and cost due to the inexpensive and high-quality nature of the porcine tissue, but also the experimental effort that would be needed to adapt the model to accommodate human anterior segments.

Secondly, the Aston biological anterior eye model overcame several of the challenges and limitations of previously published instruments by culturing both the corneal and crystalline lens tissue in loco for up to seven days. To achieve this, a bespoke anterior segment dissection and mounting procedure was designed and optimised until the biological specimen could be successfully clamped in the model within minutes. Moreover, to ensure biological viability, an environmental control system which maintained both tissues at physiologically realistic temperatures and hydration levels was developed and tested. In particular, a peristaltic pump was coupled with a PID controlled hot plate to perfuse temperature-controlled physiological solution through the anterior chamber at a pressure monitored by a sensor, which could easily be adjusted by altering the height differential of the solution. Additionally, the action of the tear film was mimicked by creating a novel tear replenishment engineering solution recurrently spraying tear analogue on the corneal epithelium, sufficiently moistening the surface of the model while maintaining the air-liquid interface. The whole system consisted of four test cells controlled by the same touch screen to maximise experimental reliability, and it was designed to be fitted in a laminar flow cabinet to avoid biological contamination. Therefore, the model enabled porcine anterior segment storage in sterile conditions, enabling optical measurements such as OCT and transparency assessment to be performed in situ, and cellular samples to be easily collected at various points in the model for biological analysis.

Further, cell viability was evaluated in the Aston biological anterior eye model using confocal microscopy and conjunctival impression cytology (CIC). Stromal fibroblasts were found to be viable after seven days of culturing, and conjunctival epithelial cells did not show any typical sign of Dry Eye when epithelial irrigation was performed every 20s, i.e. when a stable tear layer was maintained in the model. These initial findings show the potential of the Aston biological anterior eye model to maintain porcine anterior eye tissue physiologically viable for a week, and represent a promising foundation for further experimentation aimed at the full histochemical validation of the model. The high number of biological techniques required to accomplish this goal actually made it not achievable by the author within the PhD timeframe. However, fruitful academic collaboration within Aston University and with other universities have been established to reach this ambitious biological objective in the near future.

Finally, a study to assess the possibility of reproducing the damage to the ocular surface caused by DED in the Aston biological anterior eye model was also carried out in this chapter. Irrigating the corneal epithelium every 40s destabilised the artificial tear layer, causing ocular surface desiccation. Effectively, conjunctival epithelial cells showed changes typical of DED after 2hr of culturing, and conjunctival goblet cells were absent. To reinforce this findings, future studies will be carried out to test the potential of simulating different severities of DED, and to include in the Aston biological anterior eye model an immune system, potentially upgrading this platform to the only tool available worldwide for studying the multifactorial pathogenesis of this disease *ex-vivo* (Bron et al. 2017).

In conclusion, the Aston biological anterior eye model was able to preserve porcine anterior segments for one week in a near natural physiological environment. If successfully brought to market, this novel *ex-vivo* anterior eye model may play a key role in the applied ophthalmic research, potentially bridging the gap currently existing between *in-vitro* and *in-vivo* anterior eye investigations. As a result, the efficiency of clinical trials may dramatically increase, ultimately allowing governments to better redistribute healthcare funding.

6

A Novel Training Platform for Ocular Surgery

6.1 Introduction

In an era characterised by unprecedented ageing populations and decreased birth rates, societies around the world are constantly facing increasing healthcare challenges to find sustainable ways to manage the complexity of this growing population with pragmatism and respect for the patient (Nicol 2017). According to the last assessment of The World Health Organization, 20 million people worldwide are blinded due to age-related cataract formation, which remains the leading cause of avoidable blindness in poor and emerging countries (Ellwein & Kupfer 1995). The goal of the Vision 2020: The Right to Sight initiative is to make high quality eye care services accessible to all, and the treatment of cataracts has been identified as a major priority to eliminate avoidable blindness by the year 2020 (Rao et al. 2011). Modern cataract surgery is a

cost-effective intervention that restores vision. However, to achieve population wide high quality eye health, it is essential to develop adequate and appropriate resources that could enable the delivery of high quality cataract surgery with good visual outcomes and patient satisfaction (Qureshi & Khan 2014).

According to consultant ophthalmic surgeons, supervised training and practice are the cornerstones to reaching a level of expertise and experience that leads to good outcomes in cataract surgery (Benjamin 2002, Coroneo 1990). Traditionally, ophthalmic surgical training programmes were based on the Halsted apprenticeship model, in which trainees performed surgical techniques step by step on actual patients under close physician supervision (Grillo 2004). This model was characterised by high costs of training during live surgery, and, most importantly, patient safety was often compromised. For these reasons, ophthalmic surgical training programmes have been evolved during the last two decades, shifting towards a competency-based system that could ensure that only surgeons who meet the defined benchmark progress eventually will operate on living patients (M et al. 2018). Posterior capsular rupture (PCR) with or without vitreous loss is the most common intra-operative complication during cataract surgery, and is widely agreed as the key indicator to judge surgical quality. In the United Kingdom, there has been a trend for improvement from the mean benchmark rate of 4.4% in 1999 (Desai et al. 1999), to 2.68% in 2004 and 1.92% in a more recent survey of 55 567 cases (Johnston et al. 2010). However, when analysing inter-surgeon variation of this benchmark complication, PCR is found to be much lower for independent surgeons (consultants, staff grades, and associate specialists,) than for senior trainees and the most junior trainee surgeons (Figure 6.1). Therefore, a substantial ethical concern regarding trainees operating on living patients still exists, especially as at the onset of training the vast majority of first-year trainees have never performed in vivo intraocular surgery, for which the learning curve remains very steep (Oetting et al. 2006).

Time spent in practising surgical techniques in training laboratories (Wet labs) or in simulated physical environment has been shown to be an effective method to speed up

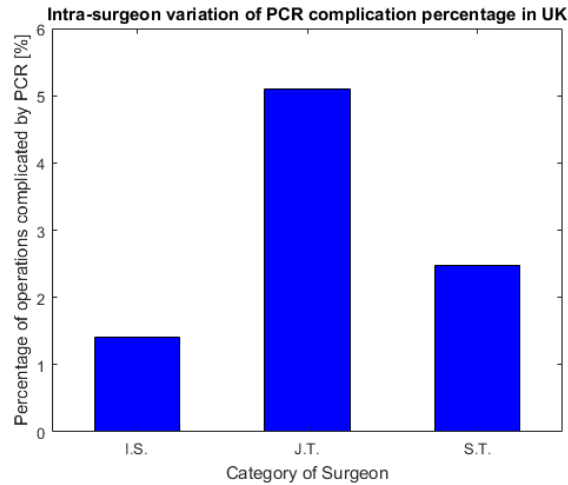


FIGURE 6.1: Percentage of cataract operations complicated by PCR for Independent Surgeons (I.S.), Junior Trainees (J.T.) and Senior Trainees (S.T.).

the learning curve and reduce potential risks for the patients used as subjects for training (Velmahos et al. 2004). Ophthalmic surgical simulator, such as Eyesi (VRmagic Holding AG, Mannheim, Germany), MicroVisTouch (ImmersiveTouch, Chicago, IL), or PhacoVision (Melerit Medical, Linkoping, Sweden) use virtual reality technology to simulate intraocular surgery (M et al. 2018, Alwadani 2018). However, the system's cost (between \$100,000 and \$200,000) still represents a barrier to the broad adoption of this technology. On the other side, hands-on experience in surgical wet labs remains the gold standard for surgical training as wet labs provide a risk-free environment where trainees can be introduced to the technical aspects of cataract surgery, and trainers can develop professional teaching and communication skills. Handing over individual technical steps of surgery to a trainee in wet labs allows the trainer to minimise operative time in the surgical theatres, and risk to the patient.

Over the years, human cadaver, porcine, or manufactured eyes have been used as *ex-vivo* models for cataract surgery (Henderson et al. 2009). Although they allow for inexpensive practice of intraocular surgery in a fairly reproducible manner, they have been designed for mainly teaching basic steps in phacoemulsification or corneal suturing (Machuk et al. 2016, Sugiura et al. 1999). However, there are many challenging scenarios or surgical complications that junior surgeon are likely to never encounter

TABLE 6.1: Challenging scenarios for cataract surgery and their prevalence estimated from scientific literature.

Challenging scenario	Estimated prevalence
Corneal opacification, Ho et al. 2018	11.9%
Intraoperative floppy iris syndrome (IFIS), Zaman et al. 2012	2.33%
Small pupil, Halkiadakis et al. 2017	1.6%
Zonular dialysis, Narendran et al. 2009	0.46%
Paediatric cataract, Sheeladevi et al. 2016	22.9/10000

during their training due to their low prevalence (Table 6.1). Practicing those complications in a wet lab environment would further reduce patient risk and, at the same time, highly increase the robustness of wet lab cataract models.

The Aston biological eye model described in the previous chapter is the only *ex-vivo* anterior eye model capable of maintaining both the porcine corneal and crystalline lens physiologically stable in loco for several days. This unique feature may allow this model to be also used as a training tool suitable for mimicking different cataract surgery scenarios, and this chapter evaluates the further engineering of this model to assess the feasibility of this assumption.

6.2 Methods

6.2.1 Wet Lab for animal tissue handling setup

A viable wet lab for animal tissue handling was established within Aston University (Figure 6.2). It consisted of an ophthalmic surgical microscope (Zeiss, Oberkochen, Germany) coupled with a Nikon D5200 digital camera, a phacoemulsification machine (Zeiss, Oberkochen, Germany), a working surface for sample handling, a sink with water supply, a storage space and a refrigerator-freezer.

Standard Operating Procedures (SOPs) were defined and risk and chemical assessments were carried out before any work with biological samples and chemicals commenced to mitigate any potential hazards (see Appendix A). In particular, personal protective items to be worn were defined, hazardous chemicals to be stored in flammable

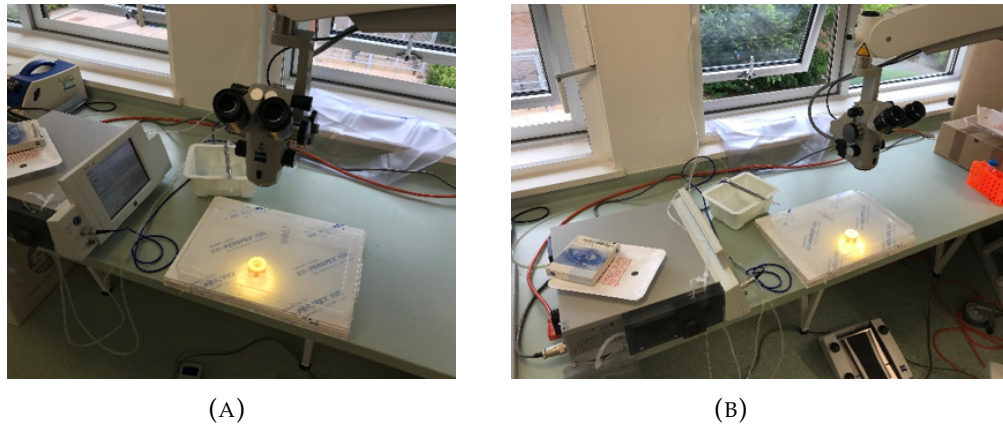


FIGURE 6.2: Exemplary pictures of the working area for ophthalmic surgery training in the Aston wet lab.

storage cabinets were identified and sterilisation and disposal procedures for the biological and non-biological waste were described.

6.2.2 Perfusion chamber re-engineering

The Aston biological eye model needed to be re-engineered to ensure feasibility of the cataract surgery procedure using the model. First of all, due to the great amount of stress and pressure created by the phacoemulsification, the porcine anterior segment had to be firmly secured to the perfusion chamber. To do so, the anterior segment was fixed to the chamber by gluing the scleral rim to the PTFE using 3MTM VetbondTM, a veterinary approved tissue adhesive (Figure 6.3). This 2-octyl cyanoacrylate adhesive polymerises in seconds without creating an exothermic reaction and releasing irritant cyanoacetate and formaldehyde, and contains a blue dye for easy-to-see drop application (Jenkins & Davis 2018). Using the tissue adhesive allowed to firmly secure the porcine tissue to the chamber throughout the whole surgical procedure, avoiding any fluid or pressure loss.

Secondly, the frontal aperture of the perfusion chamber that exposes the porcine tissue to the surgeon required design modification to fully accommodate the accurate positioning of surgical instruments during cataract surgery. In particular, during the surgical procedure the trainee needed to access the limbus from the side to create a pars-plana clear incision into the porcine cornea. Unfortunately, the original design of



FIGURE 6.3: 3MTM VetbondTM tissue adhesive (A); porcine anterior segment glued to the perfusion chamber (B).

the chamber did not allow sufficient tissue exposure, resulting in an angled incision architecture of 22.5° (Figure 6.4).

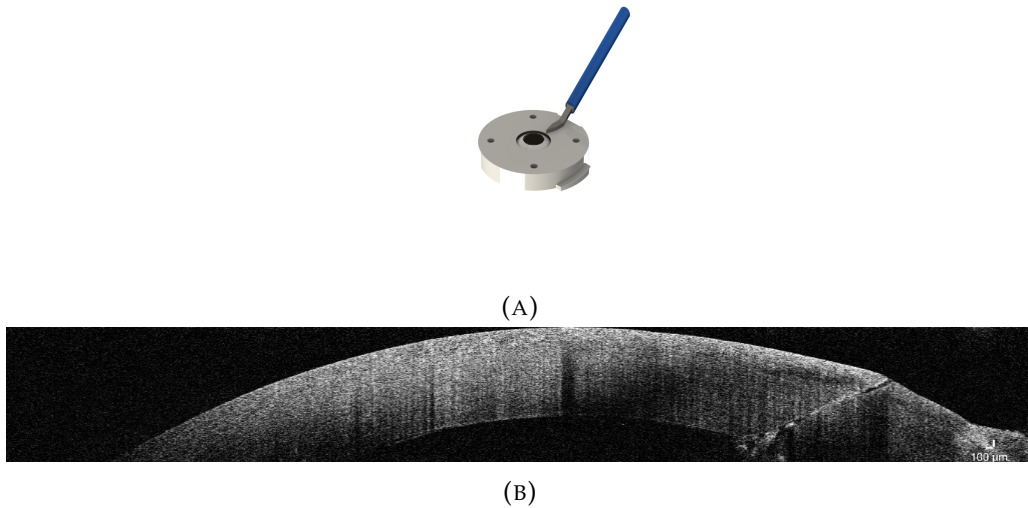


FIGURE 6.4: A non-horizontal corneal incision using the original perfusion chamber. The surgeon did not have enough space to access the cornea as in a real-life cataract surgery. The angle of the corneal incision was evaluated using ImageJ software.

After evaluating the 3D CAD designs of the perfusion chamber, the optimal engineering compromise between manufacturing time and model adaptation was established to be grooving a slot in the perfusion chamber with a width of 30 mm and a depth of 5mm (Figure 6.5). These dimensions allowed the tissue to be completely exposed to the surgeon, while still offering enough mechanical structure for tissue anchoring.



FIGURE 6.5: Modified perfusion chamber allowing greater tissue exposure to the surgeon while practicing cataract surgery. (A) represents the 3D CAD rendering, while (B) shows the 30mm groove manufactured in PTFE.

The modified aperture more closely mimicked the ordinary operating field of view, allowing the surgeon to successfully create a pars-plana corneal incision at the limbus with an angle smaller than 10° (Figure 6.6) .

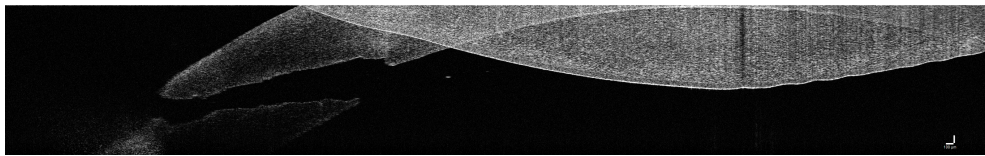


FIGURE 6.6: Horizontal corneal incision using modified perfusion chamber.

6.2.3 Cataract surgery

Five porcine eyes were freshly enucleated at a local abattoir before scalding and transferred to the laboratory in a transport solution at 4°C . The transport solution consisted of Dulbeccos Modified Eagles Medium (DMEM; Lonza, Berkshire, UK), supplemented with 1% penicillin (10,000 units/ml) and streptomycin (10,000 mg/ml), 1% v/v L-glutamine (Lonza, Berkshire, UK), 10% Foetal Bovine Serum (FBS; Sigma-Aldrich, UK) and 20% w/v Dextran ($M_w \sim 250kDa$, Sigma-Aldrich, UK) to minimise corneal swelling (Kim et al. 2014). Animals were white domestic pigs aged between 12 to 25 weeks. To avoid tissue deterioration, eyeballs were dissected and mounted in the devised chambers on arrival to the laboratory, and cataract surgery was performed on the same day. Six millimeter optic foldable acrylic and silicone intraocular lenses (IOLs), lens injectors, 1.4% high molecular weight hyaluronic acid (HA) and

ophthalmic viscosurgical devices (OVD) were obtained from Rayner Ltd. (Worthing, UK), the company that manufactured the worlds first IOL and the only manufacturer of IOLs in United Kingdom. A trainee with a log of over one hundred cataract cases was enrolled for performing the surgical procedures, and was supplied with surgical instruments, blades, irrigating solution, and irrigation/aspiration tips needed to perform the surgical procedure (Figure 6.7).

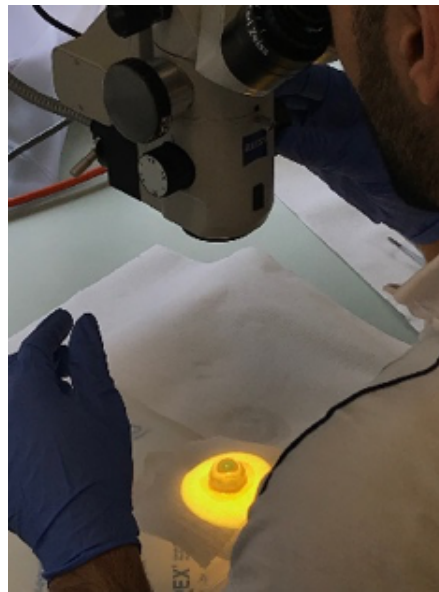


FIGURE 6.7: Trainee preparing a porcine eye for cataract surgery.

6.2.4 Inducing cataract in porcine eyes

Although pig eyes resemble human eye morphology, pigs anterior capsule is thicker, more viscous and more elastic (Sanchez et al. 2011). As a consequence, the feel of performing continuous curvilinear capsulorhexis (CCC) differs from that in human eyes and practicing nucleofractis techniques such as divide and conquer and phaco chop may be difficult (see Appendix B). To overcome this limitation, the possibility of inducing cataract in porcine lenses to simulate human cataract was investigated in this chapter.

In the literature, the most promising way to achieve this appears to be the combination of a microwave heating for at least 5 seconds and an injection of a formaldehydemethanol mixture (formaldehyde 38% and methanol 100%, 2:1 ratio) left for 15 minutes before irrigation under viscoelastic endothelial protection (Saraiva & Casanova 2003, Shentu et al. 2009). This technique was tested in three porcine eyes freshly enucleated before scalding. Globes were placed with the cornea facing upwards in the centre of a small microwave-compatible container, and heated for time intervals ranging from 5s to 10s with a set power of 700 mW. Subsequently, a 15-minute chemical injection of formaldehydemethanol mixture was performed by the trainee in each eye.

6.3 Surgical Results

6.3.1 Non cataractous eyes

Four sutureless cataract surgery procedures were successfully performed by the trainee, followed by IOL implantation ($n = 4$). Every step of surgical procedure was distinctly performed, as clearly shown by the video footages 3-6 that have been supplied as supplementary data. In particular, after having stabilised the porcine anterior segment in the perfusion chamber, the surgical procedure started with a clear corneal incision obtained using a trapezoidal blade precisely matched in width to the phaco tip to avoid conjunctival chemosis (Figure 6.8).

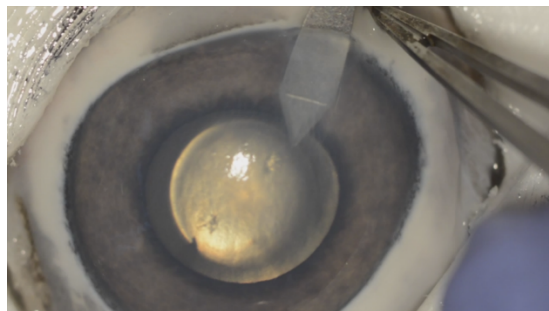


FIGURE 6.8: Cataract surgery on a porcine eye: sutureless clear corneal incision.

To ensure optimal flattening of the anterior lens capsule and to maintain anterior chamber shape, the anterior chamber was filled with OVD (Figure 6.9).

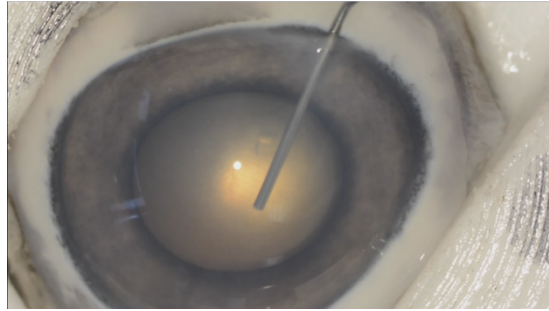


FIGURE 6.9: Cataract surgery on a porcine eye: anterior chamber filling with OVD.

Once the anterior chamber was filled with OVD, the capsule was punctured centrally with a sharp bent cystotome needle or a sharp capsule forceps and the tear was guided away from the centre to easily grasp the developing flap with the forceps (Figure 6.10).

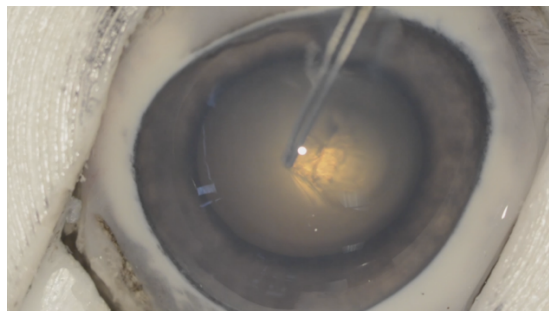


FIGURE 6.10: Cataract surgery on a porcine eye: anterior capsule tearing for continuous curvilinear capsulorrhexis (CCC).

The tear was then continued in a circumferential direction to create a flap edge. Once the flap was elevated, continuous curvilinear capsulorrhexis (CCC) was performed. The optimal diameter of the capsular opening is currently believed to be about 5 mm in uncomplicated procedures. This allows the CCC rim to cover the edge of the 6-mm IOL optic (Figure 6.11).



FIGURE 6.11: Cataract surgery on a porcine eye: capsular opening obtained by continuous curvilinear capsulorrhexis (CCC).

After continuous curvilinear capsulorrhexis, the anterior capsule was elevated and hydrodissection and hydrodelineation of the nucleus was performed to free the nucleus from its cortical attachments for disassembly and removal (Figure 6.12).

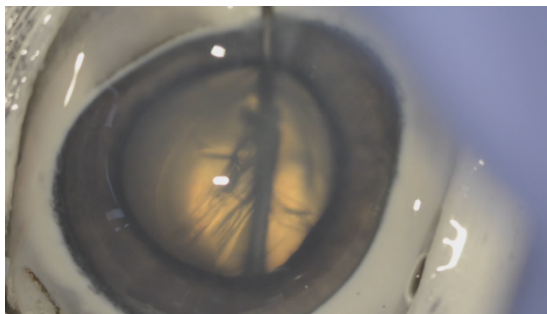


FIGURE 6.12: Cataract surgery on a porcine eye: hydrodissection and hydrodelineation of the nucleus.

Subsequently, the phaco tip of the right size was inserted and using moderate flow, low phaco power, and low vacuum, the nucleus was fractured. Due to the high elasticity of the porcine capsule and the softer nucleus of the essentially healthy porcine sample, sculpting and fracturing techniques could not be practiced as the lens was always aspirated as a whole (Figure 6.13).

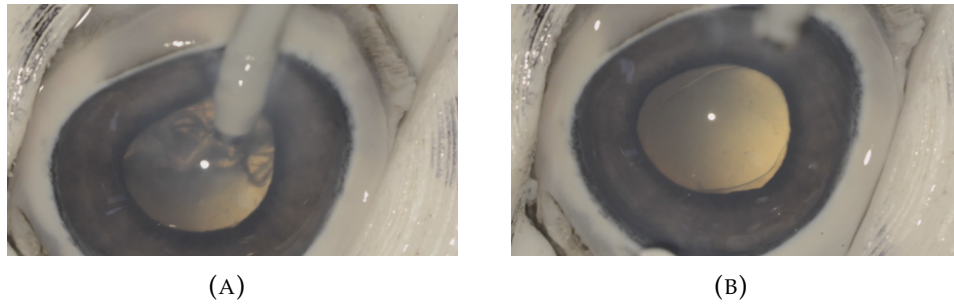


FIGURE 6.13: Cataract surgery on a porcine eye: phacoemulsification of the nucleus.

Once the nucleus and soft cortical lens matter were removed, the lens capsule bag was filled with OVD. The trainee loaded the IOL in the injector which was inserted into the eye, bevel down. The IOL was gently injected with the leading haptic pointing to the left in its proper orientation. Before the optic exited the cartridge, the leading haptic and lens optic were placed in the lens capsule bag before complete unfolding (Figure 6.14).



FIGURE 6.14: Cataract surgery on a porcine eye: : IOL insertion in the capsular bag.

The trailing haptic was then positioned into the bag and the optic centred. Residual OVD was removed utilising the irrigation/aspiration hand-piece with low aspiration settings (Figure 6.15).

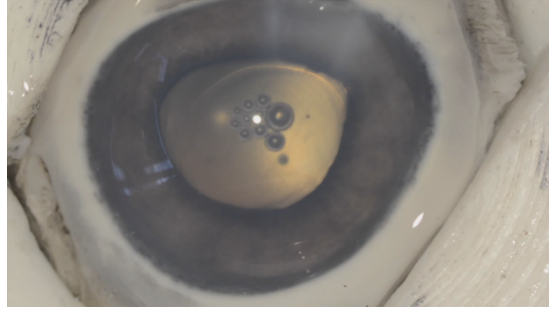


FIGURE 6.15: Cataract surgery on a porcine eye: remaining OVD is removed with the lens remaining well centred.

6.3.2 Cataractous eye

Microwave heating produced a significant posterior cataract to an extent proportional to the heating time. A minimum period of 7 seconds was required to create a homogeneous opalescent cataract in the porcine lens, however corneal clarity drastically decreased with heating (Figure 6.16).

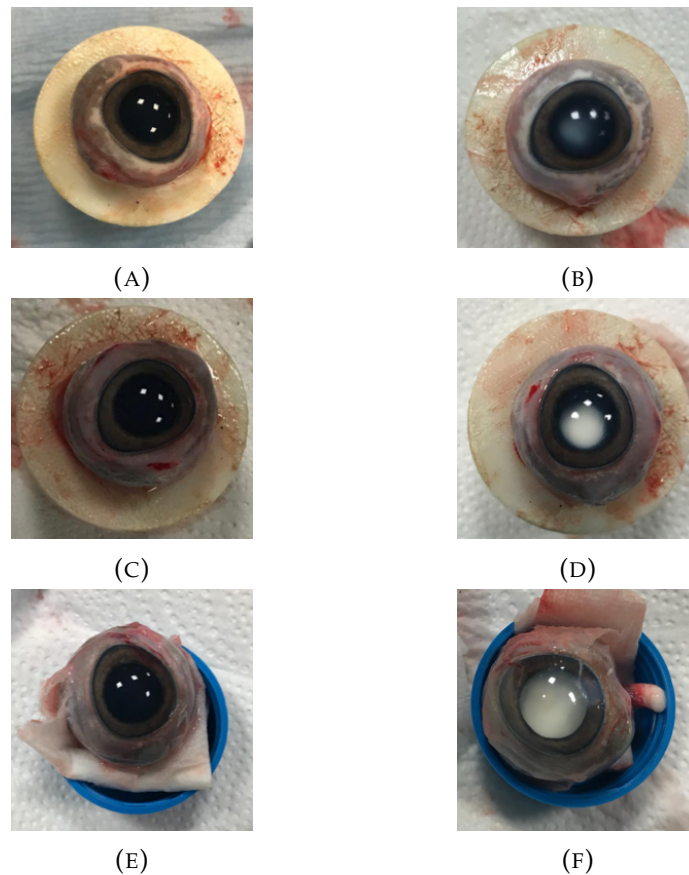


FIGURE 6.16: Pictures before and after cataract induction in porcine globes by microwave heating for 5s (A-B), 7s (C-D) and 10s (E-F).

The chemical injection did not produce any opacity improvement in the short period, and after 24hr corneal haze became excessive, causing the globe to be un-suitable for operation (Figure 16).

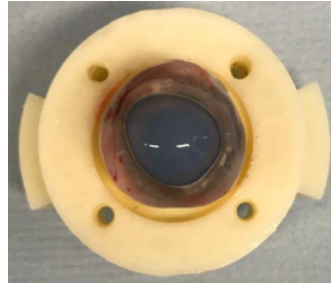


FIGURE 6.17: Porcine globe 24hr after microwave heating for 7 seconds and 15-minute chemical injection of formaldehydemethanol mixture.

A sutureless cataract surgery procedure was performed by the trainee on a cataractous porcine eye ($n = 1$), which is reported in the video footage no 7 (supplementary data).

6.3.3 Trainee feedback

Scores from the trainee feedbacks are summarised in (Table 6.2). Scores were classified from 0 = poor to 5 = excellent.

TABLE 6.2: Summary of the trainee's feedbacks on the cataract surgery performed on the Aston Biological Anterior Eye model.

Surgical step	Non cataractous model	Cataractous model
Cornea	4	2
Incision	4	4
Iris	2	2
Lens capsule	2	4
CCC	4	4
Hydro Dissection	3	2
Phacoemulsification	3	2
Soft Lens Matter Removal	1	1
Intra ocular lens insertion	5	4
Total	28	25

The trainee was highly satisfied by both the non cataractous model and the level of cataract induced. However, the corneal opacity generated by the microwaving treatment significantly reduced intraocular visibility, resulting in an overall poorer surgical model than intact porcine eyes (see Appendix C).

6.4 Discussion

During World War II, Sir Harold Ridley, an English ophthalmologist, devised the first IOL out of Perspex after observing that splinters of acrylic plastic from aircraft cockpit canopies did not trigger inflammation in Royal Air Force pilots injured eyes, provided they did not touch the iris. On 29 November 1949 at St Thomas' Hospital, Ridley achieved the first implant of an IOL, although it was not until 8 February 1950 that he left an IOL permanently in place in an eye (Jaffe, 1996). Since then, cataract surgery has developed vastly, becoming the most prevalent operation worldwide, with more than 15 million artificial IOLs implantations performed every year (Rush et al., 2015).

The delicate nature of ocular tissues and narrow margin of error necessitates surgical precision. Competent surgical performance requires hands-on-training of key surgical steps to such an extent that the American Board of Ophthalmology recommended adding surgery as a core competency required to obtain accreditation in ophthalmology (Mills and Mannis, 2004). In this regards, wet labs represent safe harbours where trainees can be introduced to the technical aspects of the surgery, and develop surgical confidence and adaptability that allows their time spent in the operating theatre to be more productive and safer (Henderson et al., 2009).

Typically, wet labs use human cadaver, porcine or manufactured eyes as a surrogate for human tissue, but none are perfect in simulating actual surgery (Machuk et al., 2016). A successful wet lab model for cataract surgery should provide realistic visuospatial and tactile feedbacks to acquire precise psychomotor skills and develop micro-surgical spatial awareness that can be applied to real-life cataract surgery. In addition, it should be reliable, accurate, cost effective and easily reproducible (Kaplowitz et al., 2018). This chapter investigated the use of the Aston biological anterior eye

model as a reliable wet lab model for cataract surgery training, potentially overcoming many of the drawbacks associated with previous wet labs eye models.

The Aston biological anterior eye model is based on porcine eyes, a readily available source of inexpensive high quality tissue. Human cadaver eye with a clear cornea and a well-developed cataract are extremely difficult to find, and artificial eyes manufactured from various materials can only simulate some steps of the surgical procedure (Sengupta et al. 2015). Here, four un-treated porcine eyes have been securely mounted in the perfusion chambers and four IOLs have been successfully implanted in them. The secure mounting procedure allowed the trainee to perform every step of the surgical procedure without any tissue torsion or IOP loss, guaranteeing accurate tactile feedback and stable intra-globe optics without the need of frequent injection of fluid or OVD. In addition, the modified chamber with a greater frontal aperture was highly rated by the trainee, as he could perform a clear horizontal entry in the cornea with a keratome, previously difficult to achieve due to the relatively poorer exposure of the tissue (see Appendix B).

Nonetheless, the essentially healthy pig lenses were not cataractous, but they were very soft. On one hand, this difference represents a model strength as it enables the porcine lens to better replicate pediatric capsulotomy, a procedure that trainees rarely encounter during their training period. In addition, as evident from the trainee feedback, this model smoothly resembles other unusual surgical scenarios such as small pupil and IFIS (see Appendix B), further emphasising the great potential of this model in reducing patient risk associated with surgical training (Messano et al. 2013). On the contrary, this appears to be a substantial model limitation as performing CCC and phacoemulsification is generally recognised by trainees as the most challenging step of the cataract surgery procedure (Mohammadpour et al. 2012). For this reason, induction of cataract was attempted in porcine lenses to simulate human cataract. Microwave heating at 700mW for a minimum of 7s produced a significant posterior cataract, which appeared though not to be enhanced by a further injection of formaldehydemethanol mixture. This finding differs from previous scientific reports, however the difference may be due the arduous learning curve required to properly treat eyes with chemical

based treatments (Machuk et al. 2016). Inducing cataract should therefore be a prerequisite of a successful porcine anterior segment model for cataract surgery training. Even if microwave heating the porcine globe for at least 7s represented a basic and rapid method to prepare the crystalline lens with minimal effort, a standardised treating protocol is still needed to preserve acceptable corneal clarity and minimise cellular damage.

Finally, it is crucial to consider that the Aston biological anterior eye model is a research platform specifically developed for maintaining corneal and crystalline lens tissue physiologically stable for a period of time of one week. This actually means that the Aston model is the only platform currently available that enables tissue culture of pseudophakic eyes over several days, paving the way for the possibility of practicing IOLs exchange, examining corneal and lenticular wound healing and fibrosis, studying posterior capsule opacification (PCO), IOLs orientation, and the effect of different IOLs coating procedures *ex-vivo* (Figure 6.18). Coupling those new clinical outcomes with the motion analysis of the surgical video recordings will allow senior educators to provide a clear set of goals to lab participants, creating an enhanced, realistic educational experience.

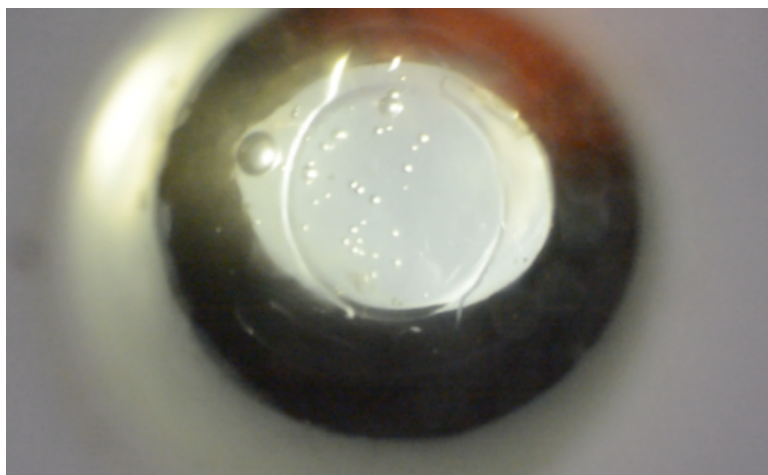


FIGURE 6.18: Back-side view of an IOL implanted in the Aston Biological Eye Model.

In conclusion, the Aston biological eye model represents a unique wet lab training model for cataract surgery, characterised by high-fidelity guiding benchmarks for

evaluating progression towards proficiency never achieved before. If successfully brought to market, this wet lab model may have the potential to reshape the future format of ophthalmic specialist training, bridging the gap between text-book surgery and real-life theatre experience, and, ultimately, maximising patient safety in an era where the cost of care is one of the strongest selective pressures driving practice patterns.

'If you find a need, fulfil the gap.'

Lailah Gifty Akita

7

Conclusions

The work detailed in this thesis adds testament to the benefits of working at the interface of biomedical engineering and optometry, by describing the development and refinement of a laboratory platform "*The Aston Biological Anterior Eye Model*", which aims to fill the existing gap between *in-vitro* and *in-vivo* anterior segment investigations in ophthalmology.

A novel and complete *ex-vivo* anterior eye model has been created, which is capable of sustaining the cornea and crystalline lens in a physiologically stable state in loco for up to 7 days. The platform is based on porcine eyes, which are not only the best high quality and reliable human tissue source substitute, but as they are slaughterhouse waste, also perfectly align the project with the 3Rs principles of replacing, refining and reducing living animal experimentation (Kirk 2018). Furthermore, the model is modular and scalable, allowing for the maximisation of experimental reliability, and the minimisation of waste and energy use. In addition, as the whole system is designed to

be fitted in a laminar flow cabinet, it avoids external biological contamination, and is easily transportable between tissue engineering laboratories, maximising accessibility.

As the first of its kind, this model may have effective applications in applied and pre-clinical research in fields involving ocular surface tissue investigations, inclusive of, but not limited to: ophthalmology, cosmetics, and pharmacological development and testing. For example, the similarity in anterior corneal curvature between porcine and human eyes, coupled with the novel tear replenishment solution engineered in this study, may be useful in the study of new contact lens materials, helping them be optimised for physiological compatibility. The efficacy of new artificial drops could also be evaluated using this model. In addition, epithelial irrigation can be easily manipulated to simulate different severities of Dry Eye Disease (DED), potentially allowing studies to elucidate the basic science behind its association with contact lens wear.

Moreover, owing to the unique *in loco* preservation of the corneal and crystalline lens tissue, this model is the only platform currently available that could allow scientists to systemically evaluate intraocular lenses (IOLs) implantation *ex-vivo*. By doing so, the enormous cost and potential safety implications of clinical trials of new IOL designs and materials, could potentially be reduced, along with associated regulatory approvals relating to ophthalmic instrumentation. Additionally, as exacerbation of ocular surface disease which may result in dry eye symptoms is a known potential corollary of intraocular surgery and is generally recognised as a major reason for patient discomfort after cataract surgery, this model could become a powerful laboratory platform to advance the understanding of its underlying mechanisms, which are currently unclear due to the complex and multifactorial pathophysiology of the disease.

Similarly, the model may have potential applications for enhancing methods of ophthalmic specialist training for intraocular surgery. The mounting of freshly enucleated, un-scalded porcine eyes to the model was shown to provide a simple, cost-effective, reliable and reproducible training platform, which offers clear corneas for the practice and perfection of new surgical techniques, in a risk-free environment, ultimately increasing patient safety.

A summary of the main findings of this thesis by chapter is detailed below:

Chapter 2 systematically reviewed existing *ex-vivo* ocular surface models, their applications, merits and limitations. This review highlighted that replication of physiological anterior segment conditions *ex-vivo* strictly requires hemispherical dissection of the globe, independent corneal endothelial and epithelial irrigation with suitable media to replicate tear film dynamics and to ensure endothelial cell viability, and high quality relevant biological tissue. Porcine eyes were found to be the best human alternative in terms of anatomical parameters and accessibility, however scarce information was found in literature regarding the optimal enucleation and storage condition of the biological specimen.

Chapter 3 hence evaluated the optimal preservation technique for porcine eyes in respect to corneal transparency and tissue deterioration combining invasive and non-invasive characterisation techniques of biological tissue, highlighting that the success and utility of experimental tests is highly dependent on the condition of the porcine eyeball at enucleation. As such, corneal transparency and epithelial integrity were identified as reliable indicators of eyeball condition. Un-scalded porcine eyes, stored at 4° C in supplemented phenol red-free DMEM, and used within 36 hours of enucleation were shown to guarantee optimum ocular tissue quality.

Chapter 4 therefore utilised this standard preservation protocol to reproducibly investigate the anatomical biometry of the porcine globe, via optical mapping, confocal microscopy, ultrasonic pachymetry and optical coherence tomography (OCT). This study is the biggest anatomical characterisation of the porcine eye which exists in the scientific literature, and successfully shows that porcine corneal curvature is similar to that of the human eye, highlighting the potential suitability of the porcine eye for studies which assess contact lens fitting. Moreover, the biometric data obtained in this study served as a reference for the mechanical design of the *Aston Biological Anterior Eye Model*.

Chapter 5 described the engineered design of the "*Aston Biological Anterior Eye Model*"

from its inception, refinement and subsequent testing and validation. To date, this platform overcomes several of the challenges and limitations of previously published models by uniquely maintaining the whole porcine anterior segment physiologically stable for up to 7 days, consequently posing the base for further studies to expand its applications. For example, a replication of the blinking mechanism could be developed to allow for frictional forces between the cornea and the bulbar conjunctiva to be studied. This upgrade will pose a real engineering challenge as it would require fine control of shear stress between soft tissues. Biologically, immunohistology could be performed to further validate the model on a cellular level. A similarly exciting future avenue to explore would be the integration of an immune system within the *ex-vivo* platform, to enable study of the prominent role of inflammation which is an already recognised factor in the development and propagation of DED. A possible way to achieve this would be the integration of Neutrophils (the most abundant type of white blood cells in most mammals) in the perfusion media, to mimic neutrophil migration into the corneal stroma following epithelial surface injury, a process which is evident *in-vivo* within a few hours of injury. Finally, the possibility of reducing or removing the FBS from the perfusing media could be explored. In fact, while the FBS is full of hormonal factors that stimulate cell growth and proliferation *in-vitro*, it may affect gene and protein expression of cells, ultimately altering cell phenotypes. Due to the minimal presence of growth factors in the aqueous humour, additional studies could be conducted to possibly removing the FBS from the perfusing media, further aligning the project to the 3R principles by helping reducing harvesting of FBS from bovine fetuses.

Chapter 6 finally explored the possibility of using the *Aston Biological Anterior Eye Model* described in the previous chapter as a wet lab training tool for cataract surgery. The model was successfully re-engineered to allow every step of the surgical procedure to be performed without any tissue torsion or IOP loss, guaranteeing accurate tactile feedback and stable intra-globe optics, and a significant posterior cataract was successfully induced in the porcine lens via a microwave treatment at 700mW for a minimum of 7s. Five cataract surgeries were successfully performed, and five IOLs were successfully implanted *ex-vivo*.

In conclusion, advancing human health nowadays requires a multidisciplinary approach, which has been adopted in this thesis to answer the research questions posed (Figure 7.1). Future aspirations of the project will focus on expanding the research into an enterprise based business model, with funding from industry and government sources, which could allow first-class scientists of different backgrounds to work together in devising the to-go-to platform for pre-clinical anterior segment investigation.

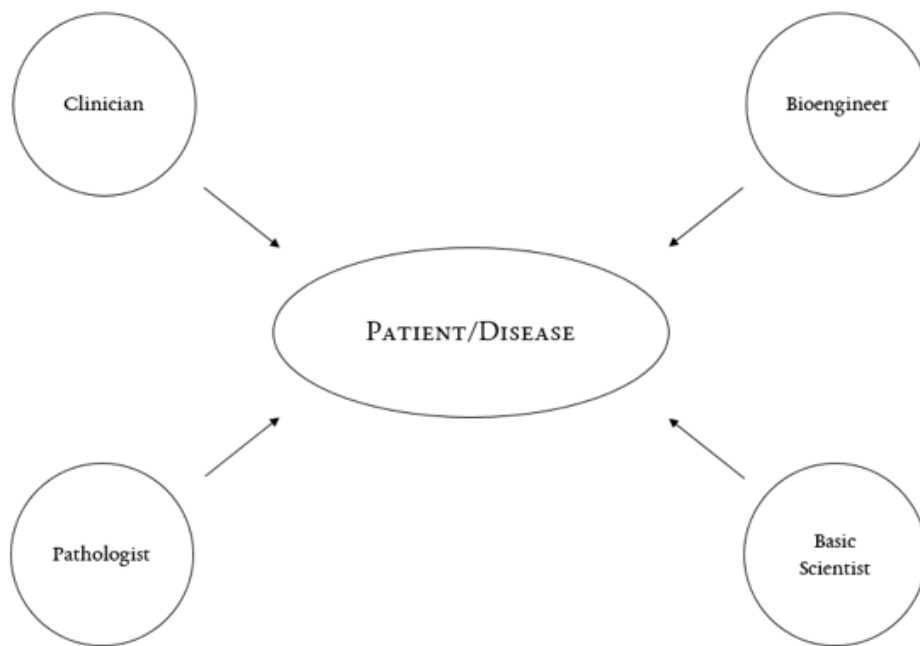


FIGURE 7.1: Advancing bioengineering for the improvement of human health and wellbeing requires multidisciplinary collaboration.

Bibliography

- Abu-Hassan, D. W., Li, X. B., Ryan, E. I., Acott, T. S. & Kelley, M. J. (2015), 'Induced pluripotent stem cells restore function in a human cell loss model of open-angle glaucoma', *Stem Cells* **33**(3), 751–761.
- Alwadani, S. (2018), 'Cataract surgery training using surgical simulators and wet-labs: Course description and literature review', *Saudi Journal of Ophthalmology* .
- Arafat, S. N., Robert, M. C., Shukla, A. N., Dohlman, C. H., Chodosh, J. & Ciolino, J. B. (2014), 'Uv cross-linking of donor corneas confers resistance to keratolysis', *Cornea* **33**(9), 955–959.
- Asejczyk-Widlicka, M., Schachar, R. A. & Pierscionek, B. K. (2008), 'Optical coherence tomography measurements of the fresh porcine eye and response of the outer coats of the eye to volume increase', *Journal of Biomedical Optics* **13**(2), 024002–024002–6.
- Azar, D. T., Jain, S., Sambursky, R. & Strauss, L. (2001), 'Microkeratome-assisted posterior keratoplasty', *Journal of cataract and refractive surgery* **27**(3), 353–6.
- Bachmann, B., Birke, M., Kook, D., Eichhorn, M. & Lutjen-Drecoll, E. (2006), 'Ultrastructural and biochemical evaluation of the porcine anterior chamber perfusion model', *Investigative ophthalmology & visual science* **47**(5), 2011–20.
- Bahar, I., Kaiserman, I., McAllum, P. & Rootman, D. (2008), 'Femtosecond laser-assisted penetrating keratoplasty: stability evaluation of different wound configurations', *Cornea* **27**(2), 209–11.

- Bahar, I., Kaiserman, I., Slomovic, A., McAllum, P. & Rootman, D. (2007), 'Fibrin glue for opposing wound edges in "top hat" penetrating keratoplasty: a laboratory study', *Cornea* **26**(10), 1235–8.
- Bahler, C. K., Fautsch, M. P., Hann, C. R. & Johnson, D. H. (2004), 'Factors influencing intraocular pressure in cultured human anterior segments', *Investigative Ophthalmology Visual Science* **45**(9), 3137–3143.
- Bahler, C. K., Hann, C. R., Fautsch, M. P. & Johnson, D. H. (2004), 'Pharmacologic disruption of schlemm's canal cells and outflow facility in anterior segments of human eyes', *Investigative Ophthalmology & Visual Science* **45**(7), 2246–2254.
- Bahler, C. K., Hann, C. R., Fjield, T., Haffner, D., Heitzmann, H. & Fautsch, M. P. (2012), 'Second-generation trabecular meshwork bypass stent (istent inject) increases outflow facility in cultured human anterior segments', *American Journal of Ophthalmology* **153**(6), 1206–1213.
- Bahler, C. K., Howell, K. G., Hann, C. R., Fautsch, M. P. & Johnson, D. H. (2008), 'Prostaglandins increase trabecular meshwork outflow facility in cultured human anterior segments', *American Journal of Ophthalmology* **145**(1), 114–119.
- Bahler, C. K., Smedley, G. T., Zhou, J. & Johnson, D. H. (2004), 'Trabecular bypass stents decrease intraocular pressure in cultured human anterior segments', *American Journal of Ophthalmology* **138**(6), 988–994.
- Ban, Y., Cooper, L. J., Fullwood, N. J., Nakamura, T., Tsuzuki, M., Koizumi, N., Dota, A., Mochida, C. & Kinoshita, S. (2003), 'Comparison of ultrastructure, tight junction-related protein expression and barrier function of human corneal epithelial cells cultivated on amniotic membrane with and without air-lifting', *Experimental Eye Research* **76**(6), 735–743.
- Barabino, S. & Dana, M. R. (2004), 'Animal models of dry eye: A critical assessment of opportunities and limitations', *Investigative Ophthalmology & Visual Science* **45**(6), 1641–1646.
- Baradia, H., Nikahd, N. & Glasser, A. (2010), 'Mouse lens stiffness measurements', *Exp Eye Res* **91**(2), 300–7.

- Barre-Sinoussi, F. & Montagutelli, X. (2015), 'Animal models are essential to biological research: issues and perspectives', *Future Sci OA* **1**(4), FSO63.
- Bartholomew, L. R., Pang, D. X., Sam, D. A. & Cavender, J. C. (1997), 'Ultrasound biomicroscopy of globes from young adult pigs', *Am J Vet Res* **58**(9), 942–8.
- Behrens, A., Dolorico, A. M. T., Kara, D. T., Novick, L. H., McDonnell, P. J., Chao, L. C., Wellik, S. R. & Chuck, R. S. (2001), 'Precision and accuracy of an artificial anterior chamber system in obtaining corneal lenticules for lamellar keratoplasty', *Journal of Cataract and Refractive Surgery* **27**(10), 1679–1687.
- Behrens, A., Ellis, K., Li, L., Sweet, P. M. & Chuck, R. S. (2003), 'Endothelial lamellar keratoplasty using an artificial anterior chamber and a microkeratome', *Archives of ophthalmology (Chicago, Ill. : 1960)* **121**(4), 503–8.
- Benes, P., Synek, S. & Petrova, S. (2013), 'Corneal shape and eccentricity in population', *Coll Antropol* **37 Suppl 1**, 117–20.
- Benjamin, L. (2002), 'Training in surgical skills', *Community Eye Health* **15**(42), 19–20.
- Beyazyldz, E., Acar, U. & Sobac, G. (2012), 'Animal models of dry eye syndrome for stem cell based therapies', *INTERNATIONAL ADVISORY BOARD* p. 49.
- Bhargava, R., Kumar, P., Kaur, A., Kumar, M. & Mishra, A. (2014), 'The diagnostic value and accuracy of conjunctival impression cytology, dry eye symptomatology, and routine tear function tests in computer users', *J Lab Physicians* **6**(2), 102–8.
- Bhattacharya, S. K., Gabelt, B. T., Ruiz, J., Picciani, R. & Kaufman, P. L. (2009), 'Cochlin expression in anterior segment organ culture models after tgf beta 2 treatment', *Investigative Ophthalmology & Visual Science* **50**(2), 551–559.
- Bhogal, M. S., Angunawela, R. I., Bilotti, E., Eames, I. & Allan, B. D. (2012), 'Theoretical, experimental, and optical coherence tomography (oct) studies of graft apposition and adhesion in descemets stripping automated endothelial keratoplasty (dsaek)', *Investigative ophthalmology & visual science* **53**(7), 3839–46.
- Bill, A. & Phillips, C. I. (1971), 'Uveoscleral drainage of aqueous humour in human eyes', *Exp Eye Res* **12**(3), 275–81.

- Birke, M. T., Birke, K., Lütjen-Drecoll, E., Schlötzer-Schrehardt, U. & Hammer, C. M. (2011), 'Cytokine-dependent elam-1 induction and concomitant intraocular pressure regulation in porcine anterior eye perfusion culture', *Investigative Ophthalmology and Visual Science* **52**(1), 468–475.
- Bolton, D. J., Pearce, R., Sheridan, J. J., McDowell, D. A. & Blair, I. S. (2003), 'Decontamination of pork carcasses during scalding and the prevention of salmonella cross-contamination', *J Appl Microbiol* **94**(6), 1036–42.
- Borras, T., Matsumoto, Y., Epstein, D. L. & Johnson, D. H. (1998), 'Gene transfer to the human trabecular meshwork by anterior segment perfusion', *Investigative Ophthalmology & Visual Science* **39**(8), 1503–1507.
- Borras, T., Rowlette, L. L., Erzurum, S. C. & Epstein, D. L. (1999), 'Adenoviral reporter gene transfer to the human trabecular meshwork does not alter aqueous humor outflow. relevance for potential gene therapy of glaucoma', *Gene Ther* **6**(4), 515–24.
- Borras, T., Rowlette, L. L., Tamm, E. R., Gottanka, J. & Epstein, D. L. (2002), 'Effects of elevated intraocular pressure on outflow facility and tigr/myoc expression in perfused human anterior segments', *Invest Ophthalmol Vis Sci* **43**(1), 33–40.
- Bourne, W. M. (2003), 'Biology of the corneal endothelium in health and disease', *Eye (Lond)* **17**(8), 912–8.
- Bower, T. & Rocha, G. (2007), 'Use of a disposable artificial anterior chamber for trans-epithelial trephination and endothelial keratoplasty', *Techniques in Ophthalmology* **5**(1), 21–26.
- Brereton, H. M., Taylor, S. D., Farrall, A., Hocking, D., Thiel, M. A., Tea, M., Coster, D. J. & Williams, K. A. (2005), 'Influence of format on in vitro penetration of antibody fragments through porcine cornea', *British Journal of Ophthalmology* **89**(9), 1205–1209.
- Bron, A. J., de Paiva, C. S., Chauhan, S. K., Bonini, S., Gabison, E. E., Jain, S., Knop, E., Markoulli, M., Ogawa, Y., Perez, V., Uchino, Y., Yokoi, N., Zoukhri, D. & Sullivan, D. A. (2017), 'Tfos dewes ii pathophysiology report', *Ocul Surf* **15**(3), 438–510.
- Brunette, I., Nelson, L. R. & Bourne, W. M. (1989), 'A system for long-term corneal perfusion', *Investigative ophthalmology & visual science* **30**(8), 1813–22.

- Bucher, F., Roters, S., Mellein, A., Hos, D., Heindl, L. M., Cursiefen, C. & Hermann, M. (2013), '“osmo-ut-dsaek” using thin-c medium', *Graefe's archive for clinical and experimental ophthalmology = Albrecht von Graefes Archiv fur klinische und experimentelle Ophthalmologie* **251**(9), 2181–5.
- Buller, C., Johnson, D. H. & Tschumper, R. C. (1990), 'Human trabecular meshwork phagocytosis. observations in an organ culture system', *Invest Ophthalmol Vis Sci* **31**(10), 2156–63.
- Buratto, L., Ferrari, M. & Rama, P. (1992), 'Excimer laser intrastromal keratomileusis', *Am J Ophthalmol* **113**(3), 291–5.
- Busin, M. (2003), 'A new lamellar wound configuration for penetrating keratoplasty surgery', *Archives of ophthalmology (Chicago, Ill. : 1960)* **121**(2), 260–5.
- Candia, O. A. & Podos, S. M. (1981), 'Inhibition of active transport of chloride and sodium by vanadate in the cornea', *Investigative ophthalmology & visual science* **20**(6), 733–7.
- Carrington, L. M., Albon, J., Anderson, I., Kamma, C. & Boulton, M. (2006), 'Differential regulation of key stages in early corneal wound healing by tgf-beta isoforms and their inhibitors', *Invest Ophthalmol Vis Sci* **47**(5), 1886–94.
- Chader, G. J. (2002), 'Animal models in research on retinal degenerations: past progress and future hope', *Vision Res* **42**(4), 393–9.
- Chan, K. Y., Cho, P. & Boost, M. (2014), 'Corneal epithelial cell viability of an ex vivo porcine eye model', *Clinical & experimental optometry* **97**(4), 337–40.
- Chinnery, H., Kezic, J., Yeung, S. & McMenamin, P. G. (2005), 'Band-like opacity in the corneas of abattoir-acquired pig eyes', *Clinical and Experimental Ophthalmology* **33**(6), 668–669.
- Chowdhury, U. R., Bahler, C. K., Hann, C. R., Chang, M. W., Resch, Z. T., Romero, M. F. & Fautsch, M. P. (2011), 'Atp-sensitive potassium (k-atp) channel activation decreases intraocular pressure in the anterior chamber of the eye', *Investigative Ophthalmology & Visual Science* **52**(9), 6435–6442.

- Chowdhury, U. R., Bahler, C. K., Holman, B. H., Dosa, P. I. & Fautsch, M. P. (2015), 'Ocular hypotensive effects of the atp-sensitive potassium channel opener cromakalim in human and murine experimental model systems', *Plos One* **10**(11), 16.
- Choy, E. P. Y., Cho, P., Benzie, I. F. F. & Choy, C. K. M. (2008), 'Dry eye and blink rate simulation with a pig eye model', *Optometry and Vision Science* **85**(2), 129–134.
- Choy, E. P. Y., Cho, P., Benzie, I. F. F., Choy, C. K. M. & To, T. S. S. (2004), 'A novel porcine dry eye model system (pdem) with simulated lacrimation/blinking system: Preliminary findings on system variability and effect of corneal drying', *Current Eye Research* **28**(5), 319–325.
- Choy, E. P. Y., Shun, T. S., Cho, P., Benzie, I. F. F. & Choy, C. K. M. (2004), 'Viability of porcine corneal epithelium ex vivo and effect of exposure to air - a pilot study for a dry eye model', *Cornea* **23**(7), 715–719.
- Clark, A. F., Steely, H. T., Dickerson, J. E., English-Wright, S., Stropki, K., McCartney, M. D., Jacobson, N., Shepard, A. R., Clark, J. I., Matsushima, H., Peskind, E. R., Leverenz, J. B., Wilkinson, C. W., Swiderski, R. E., Fingert, J. H., Sheffield, V. C. & Stone, E. M. (2001), 'Glucocorticoid induction of the glaucoma gene myoc in human and monkey trabecular meshwork cells and tissues', *Investigative Ophthalmology & Visual Science* **42**(8), 1769–1780.
- Clark, A. F., Wilson, K., de Kater, A. W., Allingham, R. R. & McCartney, M. D. (1995), 'Dexamethasone-induced ocular hypertension in perfusion-cultured human eyes', *Invest Ophthalmol Vis Sci* **36**(2), 478–89.
- Cleary, G., Spalton, D. J., Zhang, J. J. & Marshall, J. (2010), 'In vitro lens capsule model for investigation of posterior capsule opacification', *J Cataract Refract Surg* **36**(8), 1249–52.
- Collin, H. B., Anderson, J. A., Richard, N. R. & Binder, P. S. (1995), 'In vitro model for corneal wound healing; organ-cultured human corneas', *Curr Eye Res* **14**(5), 331–9.
- Coroneo, M. T. (1990), 'The bovine eye as a model for the novice cataract surgeon', *Ophthalmic Surgery* **21**(11), 772–777.

- Craig, J. P., Nelson, J. D., Azar, D. T., Belmonte, C., Bron, A. J., Chauhan, S. K., de Paiva, C. S., Gomes, J. A. P., Hammitt, K. M., Jones, L., Nichols, J. J., Nichols, K. K., Novack, G. D., Stapleton, F. J., Willcox, M. D. P., Wolffsohn, J. S. & Sullivan, D. A. (2017), 'Tfos dewes ii report executive summary', *Ocular Surface* **15**(4), 802–812.
- Craig, J. P., Nichols, K. K., Akpek, E. K., Caffery, B., Dua, H. S., Joo, C. K., Liu, Z., Nelson, J. D., Nichols, J. J., Tsubota, K. & Stapleton, F. (2017), 'Tfos dewes ii definition and classification report', *Ocul Surf* **15**(3), 276–283.
- Crawford, A. Z., Patel, D. V. & McGhee, C. (2013), 'A brief history of corneal transplantation: From ancient to modern', *Oman J Ophthalmol* **6**(Suppl 1), S12–7.
- Curcio, C. A. & Research Tissue Acquisition Working, G. (2006), 'Declining availability of human eye tissues for research', *Invest Ophthalmol Vis Sci* **47**(7), 2747–9.
- Dawson, D. G., Schmack, I., Holley, G. P., Waring, G. O., Grossniklaus, H. E. & Edelhauser, H. F. (2007), 'Interface fluid syndrome in human eye bank corneas after lasik - causes and pathogenesis', *Ophthalmology* **114**(10), 1848–1859.
- Desai, P., Minassian, D. C. & Reidy, A. (1999), 'National cataract surgery survey 1997-8: a report of the results of the clinical outcomes', *Br J Ophthalmol* **83**(12), 1336–40.
- Deshpande, P., Ortega, I., Sefat, F., Sangwan, V. S., Green, N., Claeysens, F. & MacNeil, S. (2015), 'Rocking media over ex vivo corneas improves this model and allows the study of the effect of proinflammatory cytokines on wound healing', *Investigative Ophthalmology & Visual Science* **56**(3), 1553–1561.
- Dias, J. & Ziebarth, N. M. (2015), 'Impact of hydration media on ex vivo corneal elasticity measurements', *Eye Contact Lens* **41**(5), 281–6.
- Dikstein, S. & Maurice, D. M. (1972), 'The metabolic basis to the fluid pump in the cornea', *J Physiol* **221**(1), 29–41.
- Doke, S. K. & Dhawale, S. C. (2015), 'Alternatives to animal testing: A review', *Saudi Pharmaceutical Journal* **23**(3), 223–229.

- Donn, A., Maurice, D. M. & Mills, N. L. (1959), 'Studies on the living cornea in vitro. i. method and physiologic measurements', *Archives of ophthalmology (Chicago, Ill. : 1960)* **62**, 741–7.
- Doughty, M. J. (1992), 'Quantitative evaluation of the effects of a bicarbonate and glucose-free balanced salt solution on rabbit corneal endothelium in vitro', *Optometry and vision science : official publication of the American Academy of Optometry* **69**(11), 846–57.
- Doughty, M. J. & Bergmanson, J. P. G. (2008), 'Use of a corneal stroma perfusion technique and transmission electron microscopy to assess ultrastructural changes associated with exposure to slightly acidic ph 5.75 solutions', *Current Eye Research* **33**(1), 45–57.
- Dua, H. S. & Forrester, J. V. (1987), 'Clinical-patterns of corneal epithelial wound-healing', *American Journal of Ophthalmology* **104**(5), 481–489.
- Ehrmann, K., Ho, A. & Parel, J. M. (2008), 'Biomechanical analysis of the accommodative apparatus in primates', *Clin Exp Optom* **91**(3), 302–12.
- Elgebaly, S. A., Forouhar, F., Gillies, C., Williams, S., O'Rourke, J. & Kreutzer, D. L. (1984), 'Leukocyte-mediated injury to corneal endothelial cells. a model of tissue injury', *American Journal of Pathology* **116**(3), 407–416.
- Elgebaly, S. A., Herkert, N., O'Rourke, J. & Kreutzer, D. L. (1987), 'Characterization of neutrophil and monocyte specific chemotactic factors derived from the cornea in response to hydrogen peroxide injury', *The American journal of pathology* **126**(1), 40–50.
- Ellwein, L. B. & Kupfer, C. (1995), 'Strategic issues in preventing cataract blindness in developing countries', *Bulletin of the World Health Organization* **73**(5), 681–690.
- Elson, K. M., Fox, N., Tipper, J. L., Kirkham, J., Hall, R. M., Fisher, J. & Ingham, E. (2015), 'Non-destructive monitoring of viability in an ex vivo organ culture model of osteochondral tissue', *Eur Cell Mater* **29**, 356–69; discussion 369.
- Engelmann, K., Bednarz, J. & Valtink, M. (2004), 'Prospects for endothelial transplantation', *Exp Eye Res* **78**(3), 573–8.

- Eppig, T., Gillner, M., Zoric, K., Jager, J., Loffler, A. & Langenbucher, A. (2013), 'Biomechanical eye model and measurement setup for investigating accommodating intraocular lenses', *Zeitschrift Fur Medizinische Physik* **23**(2), 144–152.
- Epstein, D. L., Jedziniak, J. A. & Grant, W. M. (1978), 'Obstruction of aqueous outflow by lens particles and by heavy-molecular-weight soluble lens proteins', *Investigative ophthalmology & visual science* **17**(3), 272–7.
- Epstein, D. L., Patterson, M. M., Rivers, S. C. & Anderson, P. J. (1982), 'N-ethylmaleimide increases the facility of aqueous outflow of excised monkey and calf eyes', *Investigative ophthalmology & visual science* **22**(6), 752–6.
- Epstein, D. L., Roberts, B. C. & Skinner, L. L. (1997), 'Nonsulfhydryl-reactive phenoxy-acetic acids increase aqueous humor outflow facility', *Investigative Ophthalmology & Visual Science* **38**(8), 1526–1534.
- Epstein, D. L., Rowlette, L. L. & Roberts, B. C. (1999), 'Acto-myosin drug effects and aqueous outflow function', *Investigative Ophthalmology & Visual Science* **40**(1), 74–81.
- Erb, M. H., Taban, M., Barsam, C. A., Sweet, P. M. & Chuck, R. S. (2004), 'Mechanical stability of microkeratome-assisted intracorneal keratoprosthesis implantation', *Archives of ophthalmology (Chicago, Ill. : 1960)* **122**(12), 1839–43.
- Ericksonlamy, K., Rohen, J. W. & Grant, W. M. (1988), 'Outflow facility studies in the perfused bovine aqueous outflow pathways', *Current Eye Research* **7**(8), 799–807.
- Ericsson, A. C., Crim, M. J. & Franklin, C. L. (2013), 'A brief history of animal modeling', *Mo Med* **110**(3), 201–5.
- Espana, E. M., Huang, B., Fratkin, J. & Henegar, J. (2011), 'An enzymatic technique to facilitate air separation of the stroma-descemet's membrane junction', *Investigative ophthalmology & visual science* **52**(13), 9327–32.
- Faber, C., Scherfig, E., Prause, J. U. & Sorensen, K. E. (2008), 'Corneal thickness in pigs measured by ultrasound pachymetry in vivo', *Scandinavian Journal of Laboratory Animal Science* **35**(1), 39–43.

- Fautsch, M. P., Bahler, C. K., Jewison, D. J. & Johnson, D. H. (2000), 'Recombinant tigr/myoc increases outflow resistance in the human anterior segment', *Investigative Ophthalmology & Visual Science* **41**(13), 4163–4168.
- Fautsch, M. P., Bahler, C. K., Vrabel, A. M., Howell, K. G., Loewen, N., Teo, W. L., Poeschla, E. M. & Johnson, D. H. (2006), 'Perfusion of his-tagged eukaryotic myocilin increases outflow resistance in human anterior segments in the presence of aqueous humor', *Investigative Ophthalmology & Visual Science* **47**(1), 213–221.
- Fautsch, M. P., Howell, K. G., Vrabel, A. M., Charlesworth, M. C., Muddiman, D. C. & Johnson, D. H. (2005), 'Primary trabecular meshwork cells incubated in human aqueous humor differ from cells incubated in serum supplements', *Investigative Ophthalmology and Visual Science* **46**(8), 2848–2856.
- Fautsch, M. P., Vrabel, A. M., Bahler, C. K. & Johnson, D. H. (2003), 'How do protein expression profiles from the human anterior segment culture model compare to the in vivo state?', *Investigative Ophthalmology & Visual Science* **44**, U131–U131.
- Fernandez-Bueno, I., Pastor, J. C., Gayoso, M. J., Alcalde, I. & Garcia, M. T. (2008), 'Muller and macrophage-like cell interactions in an organotypic culture of porcine neuroretina', *Mol Vis* **14**, 2148–56.
- Fischer, F., Voigt, G., Liegl, O. & Wiederholt, M. (1974), 'Effect of ph on potential difference and short circuit current in the isolated human cornea', *Pflügers Archiv European Journal of Physiology* **349**(2), 119–131.
- Fischer, R. S., Wu, Y., Kanchanawong, P., Shroff, H. & Waterman, C. M. (2011), 'Microscopy in 3d: a biologists toolbox', *Trends in cell biology* **21**(12), 682–691.
- Fisher, R. F. (1971), 'The elastic constants of the human lens', *J Physiol* **212**(1), 147–80.
- Fisher, R. F. (1977), 'The force of contraction of the human ciliary muscle during accommodation', *J Physiol* **270**(1), 51–74.
- Fleenor, D. L., Shepard, A. R., Hellberg, P. E., Jacobson, N., Pang, I. H. & Clark, A. F. (2006), 'Tgf beta 2-induced changes in human trabecular meshwork: Implications for intraocular pressure', *Investigative Ophthalmology & Visual Science* **47**(1), 226–234.

- Foreman, D. M., Pancholi, S., JarvisEvans, J., McLeod, D. & Boulton, M. E. (1996), 'A simple organ culture model for assessing the effects of growth factors on corneal re-epithelialization', *Experimental Eye Research* **62**(5), 555–563.
- Freudenthaler, N., Neuf, H., Kadner, G. & Schlote, T. (2003), 'Characteristics of spontaneous eyeblink activity during video display terminal use in healthy volunteers', *Graefes Arch Clin Exp Ophthalmol* **241**(11), 914–20.
- Frick, K. D., Joy, S. M., Wilson, D. A., Naidoo, K. S. & Holden, B. A. (2015), 'The global burden of potential productivity loss from uncorrected presbyopia', *Ophthalmology* **122**(8), 1706–1710.
- Fujimoto, T., Inoue, T., Kameda, T., Kasaoka, N., Inoue-Mochita, M., Tsuboi, N. & Tanihara, H. (2012), 'Involvement of rhoa/ rho-associated kinase signal transduction pathway in dexamethasone-induced alterations in aqueous outflow', *Investigative Ophthalmology & Visual Science* **53**(11), 7097–7108.
- Fyffe, J. G., Neal, T. A., Butler, W. P. & Johnson, T. E. (2005), 'The ex vivo pig eye as a replacement model for laser safety testing', *Comparative Medicine* **55**(6), 503–509.
- Gantenbein-Ritter, B., Potier, E., Zeiter, S., van der Werf, M., Sprecher, C. M. & Ito, K. (2008), 'Accuracy of three techniques to determine cell viability in 3d tissues or scaffolds', *Tissue Eng Part C Methods* **14**(4), 353–8.
- Gatell, J. (2012), 'Internal view of the effects of the big-bubble technique during experimental deep anterior lamellar keratoplasty', *Cornea* **31**(12), 1489–92.
- Giovingo, M., Nolan, M., McCarty, R., Pang, I. H., Clark, A. F., Beverley, R. M., Schwartz, S., Stamer, W. D., Walker, L., Grybauskas, A., Skuran, K., Kuprys, P. V., Yue, B. & Knepper, P. A. (2013), 'scd44 overexpression increases intraocular pressure and aqueous outflow resistance', *Molecular Vision* **19**, 2151–2164.
- Gipson, I. K. (2007), 'The ocular surface: The challenge to enable and protect vision: The friedenwald lecture', *Investigative Ophthalmology & Visual Science* **48**(10), 4391–4398.

- Goldwich, A., Ethier, C. R., Chan, D. W. H. & Tamm, E. R. (2003), 'Perfusion with the olfactomedin domain of myocilin does not affect outflow facility', *Investigative Ophthalmology & Visual Science* **44**(5), 1953–1961.
- Gonzalez, P., Caballero, M., Liton, P. B., Stamer, W. D. & Epstein, D. L. (2004), 'Expression analysis of the matrix gla protein and vf-cadherin gene promoters in the outflow pathway', *Investigative Ophthalmology & Visual Science* **45**(5), 1389–1395.
- Gottanka, J., Chan, D., Eichhorn, M., Hutjen-Drecoll, E. & Ethier, C. R. (2004), 'Effects of tgf-beta 2 in perfused human eyes', *Investigative Ophthalmology & Visual Science* **45**(1), 153–158.
- Grant, W. (1963), 'Experimental aqueous perfusion in enucleated human eyes', *Archives of Ophthalmology* **69**(6), 783–801.
- Graves, C. N., Sanders, S. S., Shoemaker, R. L. & Rehm, W. S. (1976), 'An intact globe technique for electrophysiological studies on cornea', *Journal of applied physiology* **40**(3), 447–50.
- Green, K. (1965), 'Ion transport in isolated cornea of the rabbit', *The American journal of physiology* **209**(6), 1311–6.
- Grillo, H. C. (2004), 'Edward d. churchill and the rectangular surgical residency', *Surgery* **136**(5), 947–52.
- Groenen, M. A., Archibald, A. L., Uenishi, H., Tuggle, C. K., Takeuchi, Y., Rothschild, M. F., Rogel-Gaillard, C., Park, C., Milan, D., Megens, H. J., Li, S., Larkin, D. M., Kim, H., Frantz, L. A., Caccamo, M., Ahn, H., Aken, B. L., Anselmo, A., Anthon, C., Auvil, L., Badaoui, B., Beattie, C. W., Bendixen, C., Berman, D., Blecha, F., Blomberg, J., Bolund, L., Bosse, M., Botti, S., Bujie, Z., Bystrom, M., Capitanu, B., Carvalho-Silva, D., Chardon, P., Chen, C., Cheng, R., Choi, S. H., Chow, W., Clark, R. C., Clee, C., Crooijmans, R. P., Dawson, H. D., Dehais, P., De Sapio, F., Dibbits, B., Drou, N., Du, Z. Q., Eversole, K., Fadista, J., Fairley, S., Faraut, T., Faulkner, G. J., Fowler, K. E., Fredholm, M., Fritz, E., Gilbert, J. G., Giuffra, E., Gorodkin, J., Griffin, D. K., Harrow, J. L., Hayward, A., Howe, K., Hu, Z. L., Humphray, S. J., Hunt, T., Hornshoj, H., Jeon, J. T., Jern, P., Jones, M., Jurka, J., Kanamori, H., Kapetanovic, R.,

- Kim, J., Kim, J. H., Kim, K. W., Kim, T. H., Larson, G., Lee, K., Lee, K. T., Leggett, R., Lewin, H. A., Li, Y., Liu, W., Loveland, J. E., Lu, Y., Lunney, J. K., Ma, J., Madsen, O., Mann, K., Matthews, L., McLaren, S., Morozumi, T., Murtaugh, M. P., Narayan, J., Nguyen, D. T., Ni, P., Oh, S. J., Onteru, S., Panitz, F., Park, E. W. et al. (2012), 'Analyses of pig genomes provide insight into porcine demography and evolution', *Nature* **491**(7424), 393–8.
- Guindolet, D., Crouzet, E., He, Z. G., Herbepin, P., Jumelle, C., Perrache, C., Dumolard, J. M., Forest, F., Peoc'h, M., Gain, P., Gabison, E. & Thuret, G. (2017), 'Storage of porcine cornea in an innovative bioreactor', *Investigative Ophthalmology & Visual Science* **58**(13), 5899–5909.
- Gurung, D. B., Gokul, K. C. & Adhikary, P. R. (2016), 'Mathematical model of thermal effects of blinking in human eye', *International Journal of Biomathematics* **9**(1).
- Halkiadakis, I., Chatziralli, I., Drakos, E., Katzakis, M., Skouriotis, S., Patsea, E., Mitropoulos, P. & Kandarakis, A. (2017), 'Causes and management of small pupil in patients with cataract', *Oman J Ophthalmol* **10**(3), 220–224.
- Hamaoui, M., Tahi, H., Chapon, P., Duchesne, B., Fantes, F., Feuer, W. & Parel, J. M. (2001), 'Corneal preparation of eye bank eyes for experimental surgery', *Cornea* **20**(3), 317–20.
- Hashemi, H., KhabazKhoob, M., Yazdani, K., Mehravaran, S., Mohammad, K. & Fotouhi, A. (2010), 'White-to-white corneal diameter in the tehran eye study', *Cornea* **29**(1), 9–12.
- Hatami-Marbini, H. & Rahimi, A. (2014), 'Effects of bathing solution on tensile properties of the cornea', *Exp Eye Res* **120**, 103–8.
- Heichel, J., Wilhelm, F., Kunert, K. S. & Hammer, T. (2016), 'Topographic findings of the porcine cornea', *Med Hypothesis Discov Innov Ophthalmol* **5**(4), 125–131.
- Henderson, B. A., Grimes, K. J., Fintelmann, R. E. & Oetting, T. A. (2009), 'Stepwise approach to establishing an ophthalmology wet laboratory', *J Cataract Refract Surg* **35**(6), 1121–8.

- Henker, R., Scholz, M., Gaffling, S., Asano, N., Hampel, U., Garreis, F., Hornegger, J. & Paulsen, F. (2013), 'Morphological features of the porcine lacrimal gland and its compatibility for human lacrimal gland xenografting', *PLoS One* **8**(9), e74046.
- Higgins, J. P. & Green, S. (2011), *Cochrane handbook for systematic reviews of interventions*, Vol. 4, John Wiley & Sons.
- Ho, Y. J., Sun, C. C. & Chen, H. C. (2018), 'Cataract surgery in patients with corneal opacities', *BMC Ophthalmol* **18**(1), 106.
- Holley, G. P., Alam, A., Kiri, A. & Edelhauser, H. F. (2002), 'Effect of indocyanine green intraocular stain on human and rabbit corneal endothelial structure and viability. an in vitro study', *Journal of cataract and refractive surgery* **28**(6), 1027–33.
- Hong, C. W., Sinha-Roy, A., Schoenfield, L., McMahon, J. T. & Dupps Jr, W. J. (2012), 'Collagenase-mediated tissue modeling of corneal ectasia and collagen cross-linking treatments', *Investigative Ophthalmology and Visual Science* **53**(4), 2321–2327.
- Hood, E. (2008), 'Alternative test models: ocular safety assays accepted', *Environ Health Perspect* **116**(9), A381.
- Hu, Y., Gabelt, B. T. & Kaufman, P. L. (2006), 'Monkey organ-cultured anterior segments: technique and response to h-7', *Experimental eye research* **82**(6), 1100–8.
- Hull, D. S., Csukas, S. & Green, K. (1982), 'Chlorpromazine-induced corneal endothelial phototoxicity', *Investigative ophthalmology & visual science* **22**(4), 502–8.
- Hull, D. S., Green, K. & Hampstead, D. (1985), 'Effect of hematoporphyrin derivative on rabbit corneal endothelial cell function and ultrastructure', *Investigative ophthalmology & visual science* **26**(11), 1465–74.
- Hunter, K. S., Fjield, T., Heitzmann, H., Shandas, R. & Kahook, M. Y. (2014), Characterization of micro-invasive trabecular bypass stents by ex vivo perfusion and computational flow modeling, in 'Clinical Ophthalmology', Vol. 8, Dove Medical Press, pp. 499–506.

- Hwang, H. & Kim, M. (2009), 'Endothelial damage of a donor cornea depending on the donor insertion method during descemet-stripping automated endothelial keratoplasty in porcine eyes', *Japanese journal of ophthalmology* **53**(5), 523–30.
- Ignacio, T. S., Nguyen, T. B., Chuck, R. S., Kurtz, R. M. & Sarayba, M. A. (2006), 'Top hat wound configuration for penetrating keratoplasty using the femtosecond laser: a laboratory model', *Cornea* **25**(3), 336–40.
- Ignacio, T. S., Nguyen, T. T. B., Sarayba, M. A., Sweet, P. M., Piovanetti, O., Chuck, R. S. & Behrens, A. (2005), 'A technique to harvest descemet's membrane with viable endothelial cells for selective transplantation', *American journal of ophthalmology* **139**(2), 325–30.
- Janin-Manificat, H., Rovere, M.-R., Galiacy, S. D., Malecaze, F., Hulmes, D. J. S., Moali, C. & Damour, O. (2012), 'Development of ex vivo organ culture models to mimic human corneal scarring', *Molecular Vision* **18**(294-97), 2896–2908.
- Jay, L., Brocas, A., Singh, K., Kieffer, J. C., Brunette, I. & Ozaki, T. (2008), 'Determination of porcine corneal layers with high spatial resolution by simultaneous second and third harmonic generation microscopy', *Opt Express* **16**(21), 16284–93.
- Jenkins, L. E. & Davis, L. S. (2018), 'Comprehensive review of tissue adhesives', *Dermatol Surg*.
- Johannesson, G., Linden, C., Eklund, A., Behndig, A. & Hallberg, P. (2014), 'Can we trust intraocular pressure measurements in eyes with intracameral air?', *Graves Archive for Clinical and Experimental Ophthalmology* **252**(10), 1607–1610.
- Johnson, D. H. (1996), 'Human trabecular meshwork cell survival is dependent on perfusion rate', *Investigative Ophthalmology & Visual Science* **37**(6), 1204–1208.
- Johnson, D. H. (1997), 'The effect of cytochalasin d on outflow facility and the trabecular meshwork of the human eye in perfusion organ culture', *Investigative Ophthalmology & Visual Science* **38**(13), 2790–2799.
- Johnson, D. H., Bradley, J. M. & Acott, T. S. (1990), 'The effect of dexamethasone on glycosaminoglycans of human trabecular meshwork in perfusion organ culture', *Investigative ophthalmology & visual science* **31**(12), 2568–71.

- Johnson, D. H. & Tschumper, R. C. (1987), 'Human trabecular meshwork organ culture. a new method', *Invest Ophthalmol Vis Sci* **28**(6), 945–53.
- Johnson, D. H. & Tschumper, R. C. (1989), 'The effect of organ culture on human trabecular meshwork', *Experimental eye research* **49**(1), 113–27.
- Johnson, M., Caro, N. & Huang, J. D. (2010), 'Adequacy of exchanging the content of the anterior chamber', *Experimental Eye Research* **91**(6), 876–880.
- Johnson, M., Gong, H., Freddo, T. F., Ritter, N. & Kamm, R. (1993), 'Serum proteins and aqueous outflow resistance in bovine eyes', *Investigative ophthalmology & visual science* **34**(13), 3549–57.
- Johnson, S. & Rabinovitch, P. (2012), 'Ex vivo imaging of excised tissue using vital dyes and confocal microscopy', *Curr Protoc Cytom* **Chapter 9**, Unit 9.39.
- Johnston, R. L., Taylor, H., Smith, R. & Sparrow, J. M. (2010), 'The cataract national dataset electronic multi-centre audit of 55 567 operations: variation in posterior capsule rupture rates between surgeons', *Eye* **24**(5), 888–893.
- Johnstone, M. A. & Grant, W. M. (1973), 'Pressure-dependent changes in structures of the aqueous outflow system of human and monkey eyes', *American Journal of Ophthalmology* **75**(3), 365–383.
- Kaiserman, I., Bahar, I. & Rootman, D. S. (2007), 'Optical coherence tomography of descemet membrane separation by the big bubble technique', *Cornea* **26**(9), 1115–7.
- Kammel, R., Ackermann, R., Mai, T., Damm, C. & Nolte, S. (2012), 'Pig lenses in a lens stretcher: implications for presbyopia treatment', *Optom Vis Sci* **89**(6), 908–15.
- Keller, K. E., Vranka, J. A., Haddadin, R. I., Kang, M.-H., Oh, D.-J., Rhee, D. J., Yang, Y.-f., Sun, Y. Y., Kelley, M. J. & Acott, T. S. (2013), 'The effects of tenascin c knockdown on trabecular meshwork outflow resistance', *Investigative Ophthalmology & Visual Science* **54**(8), 5613–5623.
- Kim, D. H., Kim, J., Jeong, H. J., Lee, H. J., Kim, M. K. & Wee, W. R. (2016), 'Biophysico-functional compatibility of seoul national university (snu) miniature pig cornea as

- xenocorneal graft for the use of human clinical trial', *Xenotransplantation* **23**(3), 202–210.
- Kim, M. K., Choi, H. J., Kwon, I., Pierson, R. N., Cooper, D. K. C., Soullillou, J.-P., O'Connell, P. J., Vabres, B., Maeda, N., Hara, H., Scobie, L., Gianello, P., Takeuchi, Y., Yamada, K., Hwang, E.-S., Kim, S. J. & Park, C.-G. (2014), 'The international xenotransplantation association consensus statement on conditions for undertaking clinical trials of xenocorneal transplantation', *Xenotransplantation* **21**(5), 420–430.
- Kim, S. Y., Yang, J. & Lee, Y. C. (2010), 'Safety of moxifloxacin and voriconazole in corneal storage media on porcine corneal endothelial cells', *J Ocul Pharmacol Ther* **26**(4), 315–8.
- Kirk, R. G. W. (2018), 'Recovering the principles of humane experimental technique: The 3rs and the human essence of animal research', *Sci Technol Human Values* **43**(4), 622–648.
- Klyce, S. D. (1972), 'Electrical profiles in the corneal epithelium', *The Journal of physiology* **226**(2), 407–29.
- Klyce, S. D. (1977), 'Enhancing fluid secretion by the corneal epithelium', *Investigative Ophthalmology and Visual Science* **16**(10), 968–973.
- Klyce, S. D., Neufeld, A. H. & Zadunaisky, J. A. (1973), 'The activation of chloride transport by epinephrine and db cyclic-amp in the cornea of the rabbit', *Invest Ophthalmol* **12**(2), 127–39.
- Kompella, U. B., Sundaram, S., Raghava, S. & Escobar, E. R. (2006), 'Luteinizing hormone-releasing hormone agonist and transferrin functionalizations enhance nanoparticle delivery in a novel bovine ex vivo eye model', *Molecular Vision* **12**(134–35), 1185–1198.
- Krabcova, I., Studeny, P. & Jirsova, K. (2011), 'Endothelial cell density before and after the preparation of corneal lamellae for descemet membrane endothelial keratoplasty with a stromal rim', *Cornea* **30**(12), 1436–41.

- Kray, O., Lenz, M., Spoler, F., Kray, S. & Kurz, H. (2011), *Pathogenesis of the dry eye syndrome observed by optical coherence tomography in vitro*, Vol. 8091 of *Proceedings of SPIE*, Spie-Int Soc Optical Engineering, Bellingham.
- Kumar, A., Qiao, Z. H., Kumar, P. & Song, Z. H. (2012), 'Effects of palmitoylethanolamide on aqueous humor outflow', *Investigative Ophthalmology & Visual Science* **53**(8), 4416–4425.
- Kupfer, C. & Ross, K. (1971), 'The development of outflow facility in human eyes', *Investigative ophthalmology* **10**(7), 513–517.
- Kwok, L. S. & Klyce, S. D. (1992), 'Physiological effects of tert-butyl hydroperoxide on the rabbit corneal epithelium', *CLAO Journal* **18**(2), 97–100.
- Le Sage, N., Verreault, R. & Rochette, L. (2001), 'Efficacy of eye patching for traumatic corneal abrasions: A controlled clinical trial', *Annals of Emergency Medicine* **38**(2), 129–134.
- Lee, E. S., Gabelt, B. T., Faralli, J. A., Peters, D. M., Brandt, C. R., Kaufman, P. L. & Bhattacharya, S. K. (2010), 'Coch transgene expression in cultured human trabecular meshwork cells and its effect on outflow facility in monkey organ cultured anterior segments', *Investigative Ophthalmology & Visual Science* **51**(4), 2060–2066.
- Lemp, M. A. (1973), 'Breakup of the tear film', *Int Ophthalmol Clin* **13**(1), 97–102.
- Leung, C. K., Li, H., Weinreb, R. N., Liu, J., Cheung, C. Y., Lai, R. Y., Pang, C. P. & Lam, D. S. (2008), 'Anterior chamber angle measurement with anterior segment optical coherence tomography: a comparison between slit lamp oct and visante oct', *Invest Ophthalmol Vis Sci* **49**(8), 3469–74.
- Li, C., Song, Y., Luan, S., Wan, P., Li, N., Tang, J., Han, Y., Xiong, C. & Wang, Z. (2012), 'Research on the stability of a rabbit dry eye model induced by topical application of the preservative benzalkonium chloride', *PLoS ONE* **7**(3), e33688.
- Li, L., Behrens, A., Sweet, P. M., Osann, K. E. & Chuck, R. S. (2002), 'Corneal lenticule harvest using a microkeratome and an artificial anterior chamber system at high intrachamber pressure', *Journal of cataract and refractive surgery* **28**(5), 860–5.

- Li, L., Ellis, K. R., Behrens, A., Sweet, P. M. & Chuck, R. S. (2002), 'A laboratory model for microkeratome-assisted posterior lamellar keratoplasty utilizing a running graft suture and a sutureless hinged flap', *Cornea* **21**(2), 192–5.
- Liton, P. B., Liu, X., Challa, P., Epstein, D. L. & Gonzalez, P. (2005), 'Induction of $\text{tgf-}\beta$ 1 in the trabecular meshwork under cyclic mechanical stress', *Journal of Cellular Physiology* **205**(3), 364–371.
- Liton, P. B., Luna, C., Challa, P., Gonzalez, P. & Epstein, D. L. (2005), 'Characterization of free-floating spheres from human trabecular meshwork (htm) cell culture in vitro', *Investigative Ophthalmology & Visual Science* **46**, 1.
- Liu, X. Y., Hu, Y. J., Filla, M. S., Gabelt, B. T., Peters, D. M., Brandt, C. R. & Kaufman, P. L. (2005), 'The effect of c3 transgene expression on actin and cellular adhesions in cultured human trabecular meshwork cells and on outflow facility in organ cultured monkey eyes', *Molecular Vision* **11**(128-29), 1112–1121.
- Ljubimov, A. V. & Saghizadeh, M. (2015), 'Progress in corneal wound healing', *Prog Retin Eye Res* **49**, 17–45.
- Loewen, N., Bahler, C., Teo, W. L., Whitwam, T., Peretz, M., Xu, R. F., Fautsch, M. R., Johnson, D. H. & Poeschla, E. M. (2002), 'Preservation of aqueous outflow facility after second-generation fiv vector-mediated expression of marker genes in anterior segments of human eyes', *Investigative Ophthalmology & Visual Science* **43**(12), 3686–3690.
- Loewen, R. T., Roy, P., Park, D. B., Jensen, A., Scott, G., Cohen-Karni, D., Fautsch, M. P., Schuman, J. S. & Loewen, N. A. (2016), 'A porcine anterior segment perfusion and transduction model with direct visualization of the trabecular meshwork', *Investigative Ophthalmology & Visual Science* **57**(3), 1338–1344.
- Lu, Z., Overby, D. R., Scott, P. A., Freddo, T. F. & Gong, H. (2008), 'The mechanism of increasing outflow facility by rho-kinase inhibition with y-27632 in bovine eyes', *Experimental Eye Research* **86**(2), 271–281.
- M, R., M, A. & D, S. (2018), 'A guide to eyes: ophthalmic simulators', *The Bulletin of the Royal College of Surgeons of England* **100**(4), 169–171.

- Machuk, R. W. A., Arora, S., Kutzner, M. & Damji, K. F. (2016), 'Porcine cataract creation using formalin or microwave treatment for an ophthalmology wet lab', *Can J Ophthalmol* **51**(4), 244–248.
- Madhu, C., Rix, P., Nguyen, T., Chien, D. S., Woodward, D. F. & Tang-Liu, D. D. S. (1998), 'Penetration of natural prostaglandins and their ester prodrugs and analogs across human ocular tissues in vitro', *Journal of Ocular Pharmacology and Therapeutics* **14**(5), 389–399.
- Maguen, E., Villasenor, R. A., Ward, D. E. & Nesburn, A. B. (1980), 'A modified artificial anterior chamber for use in refractive keratoplasty', *American journal of ophthalmology* **89**(5), 742–4.
- Maier, P., Böhringer, D., Birnbaum, F. & Reinhard, T. (2012), 'Improved wound stability of top-hat profiled femtosecond laser-assisted penetrating keratoplasty in vitro', *Cornea* **31**(8), 963–966.
- Manns, F., Parel, J. M., Denham, D., Billotte, C., Ziebarth, N., Borja, D., Fernandez, V., Aly, M., Arrieta, E., Ho, A. & Holden, B. (2007), 'Optomechanical response of human and monkey lenses in a lens stretcher', *Invest Ophthalmol Vis Sci* **48**(7), 3260–8.
- Mao, W., Tovar-Vidales, T., Yorio, T., Wordinger, R. J. & Clark, A. F. (2011), 'Perfusion-cultured bovine anterior segments as an ex vivo model for studying glucocorticoid-induced ocular hypertension and glaucoma', *Investigative Ophthalmology & Visual Science* **52**(11), 8068–8075.
- Mark, D. & Maurice, D. (1977), 'Sensory recording from the isolated cornea', *Investigative ophthalmology & visual science* **16**(6), 541–5.
- Mashige, K. (2013), 'A review of corneal diameter, curvature and thickness values and influencing factors', *The South African Optometrist* **72**(4).
- Maurice, D. M. (1968), 'Cellular membrane activity in the corneal endothelium of the intact eye', *Experientia* **24**(11), 1094–1095.
- McCarey, B. E., Edelhauser, H. F. & Van Horn, D. L. (1973), 'Functional and structural changes in the corneal endothelium during in vitro perfusion', *Investigative Ophthalmology* **12**(6), 410–417.

- McCarey, B. E., Polack, F. M. & Marshall, W. (1976), 'The phacoemulsification procedure. i. the effect of intraocular irrigating solutions on the corneal endothelium', *Investigative ophthalmology* **15**(6), 449–57.
- McCauley, M. B., Price Jr, F. W. & Price, M. O. (2009), 'Descemet membrane automated endothelial keratoplasty. hybrid technique combining dsaek stability withădmek visual results', *Journal of Cataract and Refractive Surgery* **35**(10), 1659–1664.
- McDonnell, P. J., Taban, M., Sarayba, M., Rao, B., Zhang, J., Schiffman, R. & Chen, Z. P. (2003), 'Dynamic morphology of clear corneal cataract incisions', *Ophthalmology* **110**(12), 2342–2348.
- McLaren, J. W., Herman, D. C., Brubaker, R. F., Nau, C. B., Wayman, L. L., Ciarniello, M. G., Rosignoli, M. T. & Dionisio, P. (2003), 'Effect of ibopamine on aqueous humor production in normotensive humans', *Investigative Ophthalmology & Visual Science* **44**(11), 4853–4858.
- McMenamin, P. G. & Steptoe, R. J. (1991), 'Normal anatomy of the aqueous humour outflow system in the domestic pig eye', *J Anat* **178**, 65–77.
- Mehta, J. S., Parthasarthy, A., Por, Y. M., Cajucom-Uy, H., Beuerman, R. W. & Tan, D. (2008), 'Femtosecond laser-assisted endothelial keratoplasty: A laboratory model', *Cornea* **27**(6), 706–712.
- Menduni, F., Davies, L. N., Madrid-Costa, D., Fratini, A. & Wolffsohn, J. S. (2018), 'Characterisation of the porcine eyeball as an in-vitro model for dry eye', *Contact lens & anterior eye : the journal of the British Contact Lens Association* **41**(1), 13–17.
- Mengher, L. S., Bron, A. J., Tonge, S. R. & Gilbert, D. J. (1985), 'A non-invasive instrument for clinical assessment of the pre-corneal tear film stability', *Curr Eye Res* **4**(1), 1–7.
- Messano, G. A., Spaziani, E., Turchetta, F., Ceci, F., Corelli, S., Casciaro, G., Martellucci, A., Costantino, A., Napoleoni, A., Cipriani, B., Nicodemi, S., Di Grazia, C., Mosillo, R., Avallone, M., Orsini, S., Tudisco, A., Aiuti, F. & Stagnitti, F. (2013), 'Risk management in surgery', *G Chir* **34**(7-8), 231–7.

- Mishima, S. & Kudo, T. (1967), 'In vitro incubation of rabbit cornea', *Invest Ophthalmol* **6**, 329–339.
- Mohammadi, S., Postnikoff, C., Wright, A. M. & Gorbet, M. (2014), 'Design and development of an in vitro tear replenishment system', *Annals of Biomedical Engineering* **42**(9), 1923–1931.
- Mohammadpour, M., Erfanian, R. & Karimi, N. (2012), 'Capsulorhexis: Pearls and pitfalls', *Saudi J Ophthalmol* **26**(1), 33–40.
- Moher, D., Liberati, A., Tetzlaff, J., Altman, D. G. & Group, P. (2009), 'Preferred reporting items for systematic reviews and meta-analyses: the prisma statement', *PLoS med* **6**(7).
- Moses, R. A., Etheridge, E. L. & Grodzki, W. J., J. (1982), 'The effect of lens depression on the components of outflow resistance', *Investigative ophthalmology & visual science* **22**(1), 37–44.
- Moshirfar, M., Meyer, J. J. & Kang, P. C. (2009), 'A comparison of three methods for trephining donor corneal buttons: endothelial cell loss and microscopic ultrastructural evaluation', *Current eye research* **34**(11), 939–44.
- Muraine, M., Gueudry, J., He, Z. G., Piselli, S., Lefevre, S. & Toubreau, D. (2013), 'Novel technique for the preparation of corneal grafts for descemet membrane endothelial keratoplasty', *American Journal of Ophthalmology* **156**(5), 851–859.
- Murube, J. & Rivas, L. (2003), 'Impression cytology on conjunctiva and cornea in dry eye patients establishes a correlation between squamous metaplasia and dry eye clinical severity', *European Journal of Ophthalmology* **13**(2), 115–127.
- Narendran, N., Jaycock, P., Johnston, R. L., Taylor, H., Adams, M., Tole, D. M., Asaria, R. H., Galloway, P. & Sparrow, J. M. (2009), 'The cataract national dataset electronic multicentre audit of 55 567 operations: risk stratification for posterior capsule rupture and vitreous loss', *Eye* **23**(1), 31–37.
- Nash, E. A. & Margo, C. E. (1998), 'Patterns of emergency department visits for disorders of the eye and ocular adnexa', *Archives of Ophthalmology* **116**(9), 1222–1226.

- Nelson, J., Havener, V. R. & Cameron, J. (1983), 'Cellulose acetate impressions of the ocular surface: Dry eye states', *Archives of Ophthalmology* **101**(12), 1869–1872.
- Nemeth, G., Vajas, A., Tsorbatzoglou, A., Kolozsvari, B., Modis, L., J. & Berta, A. (2007), 'Assessment and reproducibility of anterior chamber depth measurement with anterior segment optical coherence tomography compared with immersion ultrasonography', *J Cataract Refract Surg* **33**(3), 443–7.
- Neuburger, M., Maier, P., Bohringer, D., Reinhard, T. & Jordan, J. F. (2013), 'The impact of corneal edema on intraocular pressure measurements using goldmann applana-tion tonometry, tono-pen xl, icare, and ora: An in vitro model', *Journal of Glaucoma* **22**(7), 584–590.
- Nguyen, K. P., Chung, M. L., Anderson, P. J., Johnson, M. & Epstein, D. L. (1988), 'Hydrogen peroxide removal by the calf aqueous outflow pathway', *Investigative ophthalmology & visual science* **29**(6), 976–81.
- Nibourg, L. M. & Koopmans, S. A. (2014), 'Preservation of enucleated porcine eyes for use in a wet laboratory', *Journal of Cataract & Refractive Surgery* **40**(4), 644–651.
- Nicol, E. (2017), 'The ageing population in healthcare: a challenge to, and in, the work-force', *Clin Med (Lond)* **17**(4), 291–292.
- Njie, Y. F., Qiao, Z., Xiao, Z., Wang, W. & Song, Z.-H. (2008), 'N-arachidonylethanolamide-induced increase in aqueous humor outflow facility', *Investigative Ophthalmology & Visual Science* **49**(10), 4528–4534.
- Norn, M. S. (1969), 'Desiccation of the precorneal film. i. corneal wetting-time', *Acta Ophthalmol (Copenh)* **47**(4), 865–80.
- Nyberg, M. A., Peyman, G. A. & McEnerney, J. K. (1977), 'Evaluation of donor corneal endothelial viability with the vital stains rose bengal and evans blue', *Albrecht von Graefes Archiv für Klinische und Experimentelle Ophthalmologie* **204**(3), 153–159.
- O'Brien, W. J. & Edelhauser, H. F. (1977), 'The corneal penetration of trifluorothymidine, adenine arabinoside, and idoxuridine: a comparative study', *Investigative ophthalmology & visual science* **16**(12), 1093–1103.

- Oetting, T. A., Lee, A. G., Beaver, H. A., Johnson, A. T., Boldt, H. C., Olson, R. & Carter, K. (2006), 'Teaching and assessing surgical competency in ophthalmology training programs', *Ophthalmic Surgery Lasers & Imaging* **37**(5), 384–393.
- Oh, D. J., Kang, M. H., Ooi, Y. H., Choi, K. R., Sage, E. H. & Rhee, D. J. (2013), 'Overexpression of sparc in human trabecular meshwork increases intraocular pressure and alters extracellular matrix', *Investigative Ophthalmology & Visual Science* **54**(5), 3309–3319.
- Overby, D., Gong, H. Y., Qiu, G. T., Freddo, T. F. & Johnson, M. (2002), 'The mechanism of increasing outflow facility during washout in the bovine eye', *Investigative Ophthalmology & Visual Science* **43**(11), 3455–3464.
- Pai, V. C. & Glasgow, B. J. (2010), 'Muc16 as a sensitive and specific marker for epithelial downgrowth', *Arch Ophthalmol* **128**(11), 1407–12.
- Pallikaris, I. G., Papatzanaki, M. E., Stathi, E. Z., Frenschok, O. & Georgiadis, A. (1990), 'Laser in situ keratomileusis', *Lasers Surg Med* **10**(5), 463–8.
- Pang, I. H., Moll, H., McLaughlin, M. A., Knepper, P. A., De Santis, L., Epstein, D. L. & Clark, A. F. (2001), 'Ocular hypotensive and aqueous outflow-enhancing effects of al-3037a (sodium ferri ethylenediaminetetraacetate)', *Experimental Eye Research* **73**(6), 815–825.
- Patel, S. V., Bachman, L. A., Hann, C. R., Bahler, C. K. & Fautsch, M. P. (2009), 'Human corneal endothelial cell transplantation in a human ex vivo model', *Investigative ophthalmology & visual science* **50**(5), 2123–31.
- Perruccio, E. M., Rowlette, L. L. S., Balko, N. A., Becerra, S. P. & Borrás, T. (2003), 'Dexamethasone increases expression of pigment epithelium derived factor (pedf) in perfused human anterior segments from post-mortem donor eyes', *Investigative Ophthalmology & Visual Science* **44**, U305–U305.
- Perruccio, E. M., Rowlette, L. L. S., Comes, N., Locatelli-Hoops, S., Notari, L., Becerra, S. P. & Borrás, T. (2008), 'Dexamethasone increases pigment epithelium-derived factor in perfused human eyes', *Current Eye Research* **33**(5-6), 507–515.

- Pervan, C. L., Lautz, J. D., Blitzer, A. L., Langert, K. A. & Stubbs, E. B., J. (2016), 'Rho gtpase signaling promotes constitutive expression and release of tgfbeta2 by human trabecular meshwork cells', *Experimental Eye Research* **146**, 95–102.
- Pezzullo, L., Streatfeild, J., Simkiss, P. & Shickle, D. (2018), 'The economic impact of sight loss and blindness in the uk adult population', *Bmc Health Services Research* **18**.
- Pierscioneck, B. K. (1993), 'In vitro alteration of human lens curvatures by radial stretching', *Exp Eye Res* **57**(5), 629–35.
- Pierscioneck, B. K. (1995), 'Age-related response of human lenses to stretching forces', *Exp Eye Res* **60**(3), 325–32.
- Pinheiro, R., Panfil, C., Schrage, N. & Dutescu, R. M. (2015), 'Comparison of the lubricant eyedrops optive, vismed multi, and cationorm on the corneal healing process in an ex vivo model', *European journal of ophthalmology* **25**(5), 379–84.
- Pirouzmanesh, A., Herretes, S., Reyes, J. M. G., Suwan-apichon, O., Chuck, R. S., Wang, D. A., Elisseeff, J. H., Stark, W. J. & Behrens, A. (2006), 'Modified microkeratome-assisted posterior lamellar keratoplasty using a tissue adhesive', *Archives of Ophthalmology* **124**(2), 210–214.
- Plath, D. W. & Hogben, C. A. (1967), 'Ion transport by the isolated frog cornea', *Investigative Ophthalmology & Visual Science* **6**(4), 340–347.
- Podoleanu, A., Charalambous, I., Plesea, L., Dogariu, A. & Rosen, R. (2004), 'Correction of distortions in optical coherence tomography imaging of the eye', *Phys Med Biol* **49**(7), 1277–94.
- Prospero Ponce, C. M., Rocha, K. M., Smith, S. D. & Krueger, R. R. (2009), 'Central and peripheral corneal thickness measured with optical coherence tomography, scheimpflug imaging, and ultrasound pachymetry in normal, keratoconus-suspect, and post-laser in situ keratomileusis eyes', *J Cataract Refract Surg* **35**(6), 1055–62.
- Qiao, Z. H., Kumar, A., Kumar, P. & Song, Z. H. (2012), 'Involvement of a non-cb1/cb2 cannabinoid receptor in the aqueous humor outflow-enhancing effects of abnormal-cannabidiol', *Experimental Eye Research* **100**, 59–64.

- Qureshi, M. B. & Khan, M. D. (2014), 'Training a cataract surgeon', *Community Eye Health* **27**(85), 12–3.
- Rae, S. T. & Huff, J. W. (1991), 'Studies on initiation of silicone elastomer lens adhesion in vitro: binding before the indentation ring', *The CLAO journal : official publication of the Contact Lens Association of Ophthalmologists, Inc* **17**(3), 181–6.
- Rajan, M. S., Watters, W., Patmore, A. & Marshall, J. (2005), 'In vitro human corneal model to investigate stromal epithelial interactions following refractive surgery', *J Cataract Refract Surg* **31**(9), 1789–801.
- Ramos, R. F. & Stamer, W. D. (2008), 'Effects of cyclic intraocular pressure on conventional outflow', *Investigative Ophthalmology & Visual Science* **49**(1), 275–281.
- Rao, G. N., Khanna, R. & Payal, A. (2011), 'The global burden of cataract', *Current Opinion in Ophthalmology* **22**(1), 4–9.
- Rao, P. V., Deng, P. F., Sasaki, Y. & Epstein, D. L. (2005), 'Regulation of myosin light chain phosphorylation in the trabecular meshwork: role in aqueous humour outflow facility', *Experimental Eye Research* **80**(2), 197–206.
- Rao, P. V., Peterson, Y. K., Inoue, T. & Casey, P. J. (2008), 'Effects of pharmacologic inhibition of protein geranylgeranyltransferase type i on aqueous humor outflow through the trabecular meshwork', *Investigative ophthalmology & visual science* **49**(6), 2464–71.
- Raznitsyna, I., Kulikova, P., Rogatkin, D., Kulikov, D., Bychenkov, O., Chursinova, Y., Bobrov, M. & Glazkov, A. (2018), 'Fluorescence of radiation-induced tissue damage', *Int J Radiat Biol* **94**(2), 166–173.
- Reilly, M. A., Hamilton, P. D., Perry, G. & Ravi, N. (2009), 'Comparison of the behavior of natural and refilled porcine lenses in a robotic lens stretcher', *Exp Eye Res* **88**(3), 483–94.
- Reilly, M. A., Hamilton, P. D. & Ravi, N. (2008), 'Dynamic multi-arm radial lens stretcher: a robotic analog of the ciliary body', *Exp Eye Res* **86**(1), 157–64.

- Rice, A., Spokes, D. M., Anand, S. & Ball, J. L. (2011), 'Endothelial cell survival and graft profile analysis in descemet stripping endothelial keratoplasty', *Cornea* **30**(8), 865–871.
- Richard, N. R., Anderson, J. A., Weiss, J. L. & Binder, P. S. (1991), 'Air/liquid corneal organ culture: a light microscopic study', *Curr Eye Res* **10**(8), 739–49.
- Richman, J. B. & Tang-Liu, D. D. (1990), 'A corneal perfusion device for estimating ocular bioavailability in vitro', *Journal of pharmaceutical sciences* **79**(2), 153–7.
- Riley, M. V., Winkler, B. S., Starnes, C. A., Peters, M. I. & Dang, L. (1998), 'Regulation of corneal endothelial barrier function by adenosine, cyclic amp, and protein kinases', *Investigative Ophthalmology & Visual Science* **39**(11), 2076–2084.
- Rocha, G., Butler, M., Butler, A. & Hackett, J. M. (2011), 'Femtosecond-uva-riboflavin (fur) cross-linking approach to penetrating keratoplasty and anterior lamellar keratoplasty', *Saudi journal of ophthalmology : official journal of the Saudi Ophthalmological Society* **25**(3), 261–7.
- Rogatkin, D. A., Bychenkov, O. A. & Lapaeva, L. G. (2009), 'The accuracy, reliability, and interpretation of the results of in vivo laser fluorescence diagnosis in the spectral range of the fluorescence of endogenous porphyrins', *Journal of Optical Technology* **76**(11), 708–713.
- Rogatkin, D. A., Prisnyakova, O. A., Moiseeva, L. G. & Cherkasov, A. S. (1998), 'Analysis of the accuracy of clinical laser fluorescence diagnosis', *Measurement Techniques* **41**(7), 670–674.
- Rojanasakul, Y. & Robinson, J. R. (1990), 'Electrophysiological and ultrastructural characterization of the cornea during in vitro perfusion', *International Journal of Pharmaceutics* **63**(1), 1–16.
- Romano, V., Steger, B., Chen, J. Y., Hassaan, S., Batterbury, M., Willoughby, C. E., Ahmad, S., Elsheikh, A. & Kaye, S. B. (2015), 'Reliability of the effect of artificial anterior chamber pressure and corneal drying on corneal graft thickness', *Cornea* **34**(8), 866–9.

- Romppainen, T., Bachmann, L. M., Kaufmann, C., Kniestedt, C., Mrochen, M. & Thiel, M. A. (2007), 'Effect of riboflavin-uva-induced collagen crosslinking on intraocular pressure measurement', *Investigative Ophthalmology & Visual Science* **48**(12), 5494–5498.
- Rufer, F., Schroder, A. & Erb, C. (2005), 'White-to-white corneal diameter: normal values in healthy humans obtained with the orbscan ii topography system', *Cornea* **24**(3), 259–61.
- Ruiz-Ederra, J., Garcia, M., Hernandez, M., Urcola, H., Hernandez-Barbachana, E., Araiz, J. & Vecino, E. (2005), 'The pig eye as a novel model of glaucoma', *Experimental Eye Research* **81**(5), 561–569.
- Sanchez, I., Martin, R., Ussa, F. & Fernandez-Bueno, I. (2011), 'The parameters of the porcine eyeball', *Graefes Arch Clin Exp Ophthalmol* **249**(4), 475–82.
- Santas, A. J., Bahler, C., Peterson, J. A., Filla, M. S., Kaufman, P. L., Tamm, E. R., Johnson, D. H. & Peters, D. M. P. (2003), 'Effect of heparin ii domain of fibronectin on aqueous outflow in cultured anterior segments of human eyes', *Investigative Ophthalmology & Visual Science* **44**(11), 4796–4804.
- Saraiva, V. S. & Casanova, F. H. C. (2003), 'Cataract induction in pig eyes using viscoelastic endothelial protection and a formaldehydemethanol mixture', *Journal of Cataract & Refractive Surgery* **29**(8), 1479–1481.
- Sarayba, M. A., Kurtz, R. M., Nguyen, T. T. B., Ignacio, T., Mansoori, M., Sweet, P. M. & Chuck, R. S. (2005), 'Femtosecond laser-assisted intracorneal keratoprosthesis implantation: A laboratory model', *Cornea* **24**(8), 1010–1014.
- Schroeter, J., Ruggeri, A., Thieme, H. & Meltendorf, C. (2015), 'Impact of temporary hyperthermia on corneal endothelial cell survival during organ culture preservation', *Graefes Archive for Clinical and Experimental Ophthalmology* **253**(5), 753–758.
- Schumacher, S., Oberheide, U., Fromm, M., Ripken, T., Ertmer, W., Gerten, G., Wegener, A. & Lubatschowski, H. (2009), 'Femtosecond laser induced flexibility change of human donor lenses', *Vision Res* **49**(14), 1853–9.

- Scott, P. A., Lu, Z. Z., Liu, Y. & Gong, H. Y. (2009), 'Relationships between increased aqueous outflow facility during washout with the changes in hydrodynamic pattern and morphology in bovine aqueous outflow pathways', *Experimental Eye Research* **89**(6), 942–949.
- Sengupta, S., Dhanapal, P., Nath, M., Haripriya, A. & Venkatesh, R. (2015), 'Goat's eye integrated with a human cataractous lens: A training model for phacoemulsification', *Indian Journal of Ophthalmology* **63**(3), 275–277.
- Shafaie, S., Hutter, V., Cook, M. T., Brown, M. B. & Chau, D. Y. (2016), 'In vitro cell models for ophthalmic drug development applications', *Biores Open Access* **5**(1), 94–108.
- Sharma, N., Arora, T., Kaur, M., Titiyal, J. S. & Agarwal, T. (2016), 'Surrogate scleral rim with fibrin glue: a novel technique to expand the pool of donor tissues for descemet stripping automated endothelial keratoplasty', *The British journal of ophthalmology* **100**(2), 156–8.
- Sharma, P. K., Busscher, H. J., Terwee, T., Koopmans, S. A. & van Kooten, T. G. (2011), 'A comparative study on the viscoelastic properties of human and animal lenses', *Exp Eye Res* **93**(5), 681–8.
- Sheeladevi, S., Lawrenson, J. G., Fielder, A. R. & Suttle, C. M. (2016), 'Global prevalence of childhood cataract: a systematic review', *Eye (Lond)* **30**(9), 1160–9.
- Shentu, X., Tang, X., Ye, P. & Yao, K. (2009), 'Combined microwave energy and fixative agent for cataract induction in pig eyes', *J Cataract Refract Surg* **35**(7), 1150–5.
- Sideroudi, T., Pharmakakis, N., Tyrovolas, A., Papatheodorou, G., Chryssikos, G. D. & Voyiatzis, G. A. (2007), 'Non-contact detection of ciprofloxacin in a model anterior chamber using raman spectroscopy', *Journal of biomedical optics* **12**(3), 034005.
- Sikder, S., Ward, D. & Jun, A. S. (2011), 'A surgical technique for donor tissue harvesting for descemet membrane endothelial keratoplasty', *Cornea* **30**(1), 91–4.
- Slauson, S. R., Peters, D. M., Schwinn, M. K., Kaufman, P. L., Gabelt, B. T. & Brandt, C. R. (2015), 'Viral vector effects on exoenzyme c3 transferase-mediated

- actin disruption and on outflow facility', *Investigative Ophthalmology & Visual Science* **56**(4), 2431–2438.
- Sommer, A., Tielsch, J. M., Katz, J., Quigley, H. A., Gottsch, J. D., Javitt, J. & Singh, K. (1991), 'Relationship between intraocular-pressure and primary open angle glaucoma among white and black-americans - the baltimore eye survey', *Archives of Ophthalmology* **109**(8), 1090–1095.
- Spiga, M.-G. & Borrás, T. (2010), 'Development of a gene therapy virus with a glucocorticoid-inducible mmp1 for the treatment of steroid glaucoma', *Investigative Ophthalmology & Visual Science* **51**(6), 3029–3041.
- Spinowitz, B. S. & Zadunaisky, J. A. (1979), 'Action of adenosine on chloride active transport of isolated frog cornea', *Am J Physiol* **237**(2), F121–7.
- Spoler, F., Frentz, M. & Schrage, N. F. (2010), 'Towards a new in vitro model of dry eye: the ex vivo eye irritation test', *Dev Ophthalmol* **45**, 93–107.
- Springs, C. L., Joseph, M. A., Odom, J. V. & Wiley, L. A. (2002), 'Predictability of donor lamellar graft diameter and thickness in an artificial anterior chamber system', *Cornea* **21**(7), 696–699.
- Srinivas, S. P. & Maurice, D. M. (1992), 'A microfluorometer for measuring diffusion of fluorophores across the cornea', *IEEE transactions on bio-medical engineering* **39**(12), 1283–91.
- Stamer, W. D., Chan, D. W. H., Conley, S. M., Coons, S. & Ethier, C. R. (2008), 'Aquaporin-1 expression and conventional aqueous outflow in human eyes', *Experimental Eye Research* **87**(4), 349–355.
- Stamer, W. D., Chan, D. W. H. & Ethier, C. R. (2007), 'Targeted gene transfer to schlemm's canal by retroperfusion', *Experimental Eye Research* **84**(5), 843–849.
- Stanworth, A. & Naylor, E. J. (1950), 'The polarization optics of the isolated cornea', *The British journal of ophthalmology* **34**(4), 201–11.

- Stern, M. E., Edelhauser, H. F., Pederson, H. J. & Staats, W. D. (1981), 'Effects of ionophores x537a and a23187 and calcium-free medium on corneal endothelial morphology', *Investigative ophthalmology & visual science* **20**(4), 497–508.
- Sugiura, T., Kurosaka, D., Uezuki, Y., Eguchi, S., Obata, H. & Takahashi, T. (1999), 'Creating cataract in a pig eye', *J Cataract Refract Surg* **25**(5), 615–21.
- Syriani, E., Cuesto, G., Abad, E., Pelaez, T., Gual, A., Pintor, J., Morales, M. & Gasull, X. (2009), 'Effects of platelet-derived growth factor on aqueous humor dynamics', *Investigative ophthalmology & visual science* **50**(8), 3833–9.
- Tanelian, D. L. & Bisla, K. (1992), 'A new in vitro corneal preparation to study epithelial wound-healing', *Investigative Ophthalmology & Visual Science* **33**(11), 3024–3028.
- Tang, M. L., Ward, D., Ramos, J. L. B., Li, Y., Schor, P. & Huang, D. (2012), 'Measurements of microkeratome cuts in donor corneas with ultrasound and optical coherence tomography', *Cornea* **31**(2), 145–149.
- Thiel, M. A., Coster, D. J., Standfield, S. D., Brereton, H. M., Mavrangelos, C., Zola, H., Taylor, S., Yusim, A. & Williams, K. A. (2002), 'Penetration of engineered antibody fragments into the eye', *Clinical and Experimental Immunology* **128**(1), 67–74.
- Thiel, M. A., Morlet, N., Schulz, D., Edelhauser, H. F., Dart, J. K., Coster, D. J. & Williams, K. A. (2001), 'A simple corneal perfusion chamber for drug penetration and toxicity studies', *British Journal of Ophthalmology* **85**(4), 450–453.
- Tole, D. M., McKelvie, P. A. & Daniell, M. (2001), 'Reliability of impression cytology for the diagnosis of ocular surface squamous neoplasia employing the biopore membrane', *British Journal of Ophthalmology* **85**(2), 154.
- Tsatsos, M. (2014), 'Presoaking with bss used for thin manually dissected dsek (tmd-sek): a viable option for thin dsek', *Eye (London, England)* **28**(6), 701–704.
- Tschumper, R. C., Johnson, D. H., Bradley, J. M. & Acott, T. S. (1990), 'Glycosaminoglycans of human trabecular meshwork in perfusion organ culture', *Current eye research* **9**(4), 363–9.

- Ussing, H. H. & Zerahn, K. (1951), 'Active transport of sodium as the source of electric current in the short-circuited isolated frog skin', *Acta physiologica Scandinavica* **23**(2-3), 110–27.
- Vaajanen, A., Vapaatalo, H. & Oksala, O. (2007), 'A modified in vitro method for aqueous humor outflow studies in enucleated porcine eyes', *Journal of Ocular Pharmacology and Therapeutics* **23**(2), 124–131.
- Vaddavalli, P. K., Diakonis, V. F., Canto, A. P., Kankariya, V. P., Pappuru, R. R., Ruggeri, M., Banitt, M. R., Kymionis, G. D. & Yoo, S. H. (2014), 'Factors affecting dsaek graft lenticle adhesion: an in vitro experimental study', *Cornea* **33**(6), 551–4.
- Valls, R., Garcia, M. L., Egea, M. A. & Valls, O. (2008), 'Validation of a device for transcorneal drug permeation measure', *Journal of Pharmaceutical and Biomedical Analysis* **48**(3), 657–663.
- Van Horn, D. L., Edelhauser, H. F., Prodanovich, G., Eiferman, R. & Pederson, H. F. (1977), 'Effect of the ophthalmic preservative thimerosal on rabbit and human corneal endothelium', *Investigative ophthalmology & visual science* **16**(4), 273–80.
- van Vreeswijk, H. & Pameyer, J. H. (1998), 'Inducing cataract in postmortem pig eyes for cataract surgery training purposes', *J Cataract Refract Surg* **24**(1), 17–8.
- Vanhorn, D. L., Doughman, D. J., Harris, J. E., Miller, G. E., Lindstrom, R. & Good, R. A. (1975), 'Ultrastructure of human organ-cultured cornea .2. stroma and epithelium', *Archives of Ophthalmology* **93**(4), 275–277.
- Velmahos, G. C., Toutouzas, K. G., Sillin, L. F., Chan, L., Clark, R. E., Theodorou, D. & Maupin, F. (2004), 'Cognitive task analysis for teaching technical skills in an inanimate surgical skills laboratory', *Am J Surg* **187**(1), 114–9.
- Vetter, J. M., Holtz, C., Vossmerbaeumer, U. & Pfeiffer, N. (2012), 'Irregularity of the posterior corneal surface during applanation using a curved femtosecond laser interface and microkeratome cutting head', *Journal of refractive surgery (Thorofare, N.J. : 1995)* **28**(3), 209–14.

- Villarrubia, A. & Cano-Ortiz, A. (2015), 'Development of a nomogram to achieve ultrathin donor corneal disks for descemet-stripping automated endothelial keratoplasty', *Journal of cataract and refractive surgery* **41**(1), 146–51.
- Vittitow, J. L. & Borrás, T. (2002), 'Expression of optineurin, a glaucoma-linked gene, is influenced by elevated intraocular pressure', *Biochemical and Biophysical Research Communications* **298**(1), 67–74.
- Vittitow, J. L., Garg, R., Rowlette, L. L. S., Epstein, D. L., O'Brien, E. T. & Borrás, T. (2002), 'Gene transfer of dominant-negative rhoa increases outflow facility in perfused human anterior segment cultures', *Molecular Vision* **8**(5), 32–44.
- Vranka, J. A., Bradley, J. M., Yang, Y.-F., Keller, K. E. & Acott, T. S. (2015), 'Mapping molecular differences and extracellular matrix gene expression in segmental outflow pathways of the human ocular trabecular meshwork', *Plos One* **10**(3).
- Waite, A., Davidson, R. & Taravella, M. J. (2013), 'Descemet-stripping automated endothelial keratoplasty donor tissue preparation using the double-pass microkeratome technique', *Journal of cataract and refractive surgery* **39**(3), 446–50.
- Wan, Z., Woodward, D. F., Cornell, C. L., Fliri, H. G., Martos, J. L., Pettit, S. N., Wang, J. W., Kharlamb, A. B., Wheeler, L. A., Garst, M. E., Landsverk, K. J., Struble, C. S. & Stamer, W. D. (2007), 'Bimatoprost, prostamide activity, and conventional drainage', *Investigative Ophthalmology & Visual Science* **48**(9), 4107–4115.
- Wang, B., Kagemann, L., Schuman, J. S., Ishikawa, H., Bilonick, R. A., Ling, Y., Sigal, I. A., Nadler, Z., Francis, A., Sandrian, M. G. & Wollstein, G. (2014), 'Gold nanorods as a contrast agent for doppler optical coherence tomography', *PloS one* **9**(3), e90690.
- Ward, D. E. & Nesburn, A. B. (1976), 'An artificial anterior chamber', *American Journal of Ophthalmology* **82**(5), 796–798.
- Watsky, M. A., McCartney, M. D., McLaughlin, B. J. & Edelhauser, H. F. (1990), 'Corneal endothelial junctions and the effect of ouabain', *Investigative ophthalmology & visual science* **31**(5), 933–41.

- Webb, J. G., Husain, S., Yates, P. W. & Crosson, C. E. (2006), 'Kinin modulation of conventional outflow facility in the bovine eye', *Journal of Ocular Pharmacology and Therapeutics* **22**(5), 310–316.
- Whikehart, D. R. & Edelhauser, H. F. (1978), 'Glutathione in rabbit corneal endothelia: the effects of selected perfusion fluids', *Investigative ophthalmology & visual science* **17**(5), 455–64.
- Wiley, L. A., Joseph, M. A. & Springs, C. L. (2002), 'Tectonic lamellar keratoplasty utilizing a microkeratome and an artificial anterior chamber system', *Cornea* **21**(7), 661–3.
- Wilson, G. S. & Chalmers, R. L. (1990), 'Effect of h₂o₂ concentration and exposure time on stromal swelling: an epithelial perfusion model', *Optometry and vision science : official publication of the American Academy of Optometry* **67**(4), 252–5.
- Wolffsohn, J. S., Arita, R., Chalmers, R., Djalilian, A., Dogru, M., Dumbleton, K., Gupta, P. K., Karpecki, P., Lazreg, S., Pult, H., Sullivan, B. D., Tomlinson, A., Tong, L., Villani, E., Yoon, K. C., Jones, L. & Craig, J. (2017), 'TFOS DEWS II Diagnostic Methodology report', *Ocul Surf* **15**(3), 539–574.
- Wong, K. H., Koopmans, S. A., Terwee, T. & Kooijman, A. C. (2007), 'Changes in spherical aberration after lens refilling with a silicone oil', *Investigative Ophthalmology & Visual Science* **48**(3), 1261–1267.
- Wordinger, R. J., Fleenor, D. L., Hellberg, P. E., Pang, I. H., Tovar, T. O., Zode, G. S., Fuller, J. A. & Clark, A. F. (2007), 'Effects of tgf-chi 2, bmp-4, and gremlin in the trabecular meshwork: Implications for glaucoma', *Investigative Ophthalmology & Visual Science* **48**(3), 1191–1200.
- Wormstone, I. M. & Eldred, J. A. (2016), 'Experimental models for posterior capsule opacification research', *Experimental Eye Research* **142**, 2–12.
- Wormstone, I. M., Wang, L. & Liu, C. S. (2009), 'Posterior capsule opacification', *Exp Eye Res* **88**(2), 257–69.

- Wu, Q. F. & Yeh, A. T. (2008), 'Rabbit cornea microstructure response to changes intraocular pressure visualized by using nonlinear optical microscopy', *Cornea* **27**(2), 202–208.
- Yagoubi, M. I., Armitage, W. J., Diamond, J. & Easty, D. L. (1994), 'Effects of irrigation solutions on corneal endothelial function', *The British journal of ophthalmology* **78**(4), 302–6.
- Yuksel, B., Bozdog, B., Acar, M. & Topaloglu, E. (2010), 'Evaluation of the effect of topical cyclosporine a with impression cytology in dry eye patients', *Eur J Ophthalmol* **20**(4), 675–9.
- Zagon, I. S., Sassani, J. W., Ruth, T. B. & McLaughlin, P. J. (2001), 'Epithelial adhesion complexes and organ culture of the human cornea', *Brain Research* **900**(2), 205–213.
- Zaman, F., Bach, C., Junaid, I., Papatsoris, A. G., Pati, J., Masood, J. & Buchholz, N. (2012), 'The floppy iris syndrome - what urologists and ophthalmologists need to know', *Curr Urol* **6**(1), 1–7.
- Zhang, M., Maddala, R. & Rao, P. V. (2008), 'Novel molecular insights into rhoa gtpase-induced resistance to aqueous humor outflow through the trabecular meshwork', *American journal of physiology. Cell physiology* **295**(5), C1057–70.
- Zhao, B., Cooper, L. J., Brahma, A., MacNeil, S., Rimmer, S. & Fullwood, N. J. (2006), 'Development of a three-dimensional organ culture model for corneal wound healing and corneal transplantation', *Invest Ophthalmol Vis Sci* **47**(7), 2840–6.
- Zhao, B., Ma, A., Martin, F. L. & Fullwood, N. J. (2009), 'An investigation into corneal alkali burns using an organ culture model', *Cornea* **28**(5), 541–546.
- Zhao, M., Campolmi, N., Thuret, G., Piselli, S., Acquart, S., Peoc'h, M. & Gain, P. (2012), 'Poloxamines for deswelling of organ-cultured corneas', *Ophthalmic Res* **48**(3), 124–33.
- Zhou, L., Higginbotham, E. J. & Yue, B. Y. (1998), 'Effects of ascorbic acid on levels of fibronectin, laminin and collagen type 1 in bovine trabecular meshwork in organ culture', *Curr Eye Res* **17**(2), 211–7.

- Zhu, J. Y., Ye, W., Wang, T. & Gong, H. Y. (2013), 'Reversible changes in aqueous out-flow facility, hydrodynamics, and morphology following acute intraocular pressure variation in bovine eyes', *Chinese Medical Journal* **126**(8), 1451–1457.
- Zhu, Z., Rife, L., Yiu, S., Trousdale, M. D., Wasilewski, D., Siqueira, A. & Smith, R. E. (2006), 'Technique for preparation of the corneal endothelium-descemet membrane complex for transplantation', *Cornea* **25**(6), 705–8.
- Zuazo, F., Lopez-Ponce, D., Salinas-Toro, D., Valenzuela, F., Sans-Puroja, J., Srur, M., Lopez-Solis, R. O. & Traipe-Castro, L. (2014), 'Conjunctival impression cytology in patients with normal and impaired osdi scores', *Arch Soc Esp Oftalmol* **89**(10), 391–6.



Risk and COHSS assessments

RISK ASSESSMENT OF WORK WITH BIOLOGICAL MATERIALS

This form is for work with Biological Materials. Risk assessment is mandatory under Health & safety regulations and Biological material comes under the COSHH regulations:

<http://www.hse.gov.uk/pubns/books/l5.htm>

Aston University only has facilities for Category 2 Biological work. Work must be approved by the Biological safety Sub-Committee.

This form is not for Genetically Modified work please complete a GM risk assessment for that work.

Date submitted:	20.03.17	Date approved:	
-----------------	----------	----------------	--

Part A: Please provide the following general information:

School/Department:	Life and Health Sciences
--------------------	--------------------------

Principal	Francesco Menduni	Position:	Phd Student
E-mail address:		Phone	+

Please give a brief and descriptive title for this risk assessment

Title:	Risk Assessment for ex-vivo porcine eye model
--------	---

Aims and objectives of investigation:
The aim of the investigation is to develop a novel porcine anterior eye model that could maintain both the corneal and the crystalline lens tissue physiologically stable for at least 10 days, to allow the rapid, but safe, development of innovative sight enhancing ophthalmic devices.

Workers involved in work:	Post/experience/training:
Tugce Ipek	PhD Student working in the same European Dry Eye Network (EDEN). She is experienced in cell culture.
Training and Assessment of Competence <i>Specify arrangements for provision for existing and future personnel</i>	
Training for COSHH assessments	

Part B: Please indicate the type of Biological material that you will be using:

Section 1: *Micro-organisms (viruses, bacteria, fungi, parasites)*

Section 2: *cell cultures*

Section 3: *human tissues and body fluids*

Section 4: *plants and plant material*

Section 5: *animals and animal tissues*

Section 1: Micro-organisms

Nature of organism

Name and Strain	ACDP cat.*	Source	Antibiotic susceptibility/resistance	Virulence properties
Has any strain been genetically modified in any way? Yes / No (Delete, as appropriate)				
* http://www.hse.gov.uk/pubns/misc208.pdf				
If yes, complete GM risk assessment form				

Quantity of organisms to be used

volumes to be worked with	concentrations of organisms to be used

Section 2: Cell cultures

Nature of cells

Name	Anatomical and species origin
Are the cells derived from a person who currently has access to the laboratory where the work will be performed? Yes / No	
NB Persons MUST NOT work on their own cells	
If yes, what precautions are to be taken to prevent that person being exposed to the cells?	
Have they been modified in any way (e.g., by transfection, transformation etc.)? Yes / No	
If yes, complete GM risk assessment form	

Section 3. Human tissues and body fluids

Nature of tissues and body fluids

Site of tissue, nature of body fluid(s):
Details of human subjects from which tissue/body fluid is obtained (including likely presence of infective agents):
<p>Human Tissue Act: If using Human Material you must use the Universities HTA Quality Manual and inform the HTA Designated Individual (DI) what you are using.</p> <p>The basis of compliance with the act in using Human material is informed consent and ethical approval.</p>

Section 4. Plants and plant tissue or material

Nature of plant or plant tissue

Name:	
Is it infected with a pathogen?	Yes / No (Delete as appropriate)
If yes, also complete section 1	
Is it transgenic?	Yes / No (Delete as appropriate)
If yes, complete GM risk assessment form	

Section 5. Animals and animal tissues

Nature of animal or tissue:

Species	Sex	Anatomical site	Origin or geographical source
Porcine	Female, Male	Eyes	United Kingdom

Is the animal or tissue/body fluid to be worked with infected or to be infected?	Yes / No
If Yes, also complete section 1 of this form	
Is a carcinogen, drug, or other substance to be administered to the animal(s) or present in the tissue?	Yes / No
If Yes complete appropriate Chemical COSHH assessment.	
Have the investigators that will be performing work on animals obtained the appropriate Home Office Licence?	Yes / No
If No consult the Manager of the Bio-Medical Unit.	
Have Standard Operating Procedures (SOPs) for the proposed work been sent to, and approved by, the Manager of the Biomedical Unit?	Yes / No
If No, send SOPs to the Manager of the Bio-Medical Unit. If Yes attach signed approval	

Part C: Risk Assessment. Please provide the following information:

Within this section include control measures put in place to mitigate any risk from the work, please attach any other relevant documentation e.g. Methods (Standard Operating Procedures), other linked risk assessments.

Risk to Humans

Likelihood of hazardous risks to laboratory workers (including infection, allergy, toxicity etc.):
Should pose no risk to health as long as good laboratory practice is observed.
Humans at increased risk (e.g. Pregnancy, Immunocompromised)

Interim Containment

ACDP level:	
-------------	--

Are any of the work procedures likely to generate aerosols? If so, should the work be undertaken in a safety cabinet?

No.

Does your laboratory avoid the use of sharps?

No.

Protective equipment and clothing to be used (state the type/grade or make to indicate control)

Gloves (type II), lab coats, safety cabinets (class I and class II), safety goggles, safety masks.
--

Transport and storage arrangements:

Are materials to be moved outside lab/suite? (e.g., between labs, between buildings, on public roads, posted) Indicate control measures, procedures and policies used.
Porcine eyeballs will be transported from abattoir to campus in sealed plastic containers. On campus, eyes may be moved from Optegra Wetlab to Main Building in sealed plastic containers.

Disinfection

Specify dilutions of disinfectants. Specify disinfection regime (What, Where When). Have these disinfectants been validated for use with recipient micro-organisms, include reference if applicable.

Use of 70% Industrial Methylated Spirit (IMS) and 70% Ethanol for spraying surfaces to maintain aseptic technique.

Sterilisation and Disposal procedures

Autoclave will be used for material and solution required to be sterile.

Sharp material will be collected in the sharps bin. Once full, the sharps bin is sealed shut and taken away for external incineration.

All waste will be autoclaved before being taken away for incineration.

Porcine eyeballs will be frozen down and collected in the freezer using plastic bags. Mr Wayne Fleary (Aston University) will collect them for final disposal.

Environmental impact:

Outline any impact that could occur if released into the environment and controls in place to mitigate any risk

Environmental impact is less likely to happen in this study.

Emergency procedures:

To be followed in event of spills or accidental exposure to tissues or body fluids, e.g., needle stick accidents

Splashes should be immediately cleaned with water. The incident should be reported to the manager.

Occupational Health issues

Any requirements for immunization, health monitoring etc.

Additional containment

e.g. Any special requirements for other legislation such as counter terrorism

No.

Part D: Authorisation and Notification:

The work proposed can be discussed with the LHS School Technical Manager or the Schools Biological Safety Advisors or the University Biological Safety Officer for clarification etc. Consultation with other laboratory users should also take place. Completed assessments should be sent to the University Biological Safety Officer to be ratified by the University Biological Safety Sub-Committee.

Signature of
proposer



Date20.03.17.....

Please print name

Francesco Menduni

.....

Signature of
Biological Safety
Officer or authorised
Deputy

.....

Date

Please print name

.....


Signature of the
Manager of the Bio-
Medical Unit (where
appropriate)



.....

Date














IMS - Storage and Use WETLAB_MB334_MB524

Description of the work area and/or process activity	Persons Affected
The use of IMS for cleaning and maintaining aseptic technique. The use of 70% IMS in MB334 and wet lab	Cleaners x 2 Postgraduate Student x 4 Staff x 4 Students x 3
Company	Aston University
Site	Life and Health Sciences
Branch	Biology

Substance Name	Emergency Tel No.	Usage Information	MSDS Date	Cat
 Industrial Methylated Spirit Substance Form: Liquid	[REDACTED]	Method of use: Substance is used at 70% dilution with water and is sprayed onto surfaces and objects to clean them. Duration 1 Minute(s) Frequency Often During Day/Shift	25/08/2010	C

Hazard Labelling
<div style="display: flex; gap: 10px;"> <div style="text-align: center;">  <p>toxic</p> </div> <div style="text-align: center;">  <p>highly flammable</p> </div> </div>

Can a less hazardous substance(s) be used to do the same job	NO
Control Measures	
Handle in accordance with good industrial hygiene and safety practice. Wash hands before breaks and at the end of workday. Only authorised and trained personnel to use this substance. Use only in well ventilated areas.	

Personal Protective Equipment		First Aid Measures	
	Eye Protection Face shield and safety glasses Use equipment for eye protection tested and approved under appropriate government standards such as NIOSH (US) or EN 166(EU).		Eye Contact Rinse thoroughly with plenty of water for at least 15 minutes and consult a physician.
	Hand Protection Handle with gloves. Gloves must be inspected prior to use. Use proper glove removal technique (without touching glove's outer surface) to avoid skin contact with this product. Dispose of contaminated gloves after use in accordance with applicable laws and good laboratory practices. Wash and dry hands.		Ingestion Do NOT induce vomiting. Never give anything by mouth to an unconscious person. Rinse mouth with water. Consult a physician.
	Clothing Wear laboratory coat buttoned up.		Skin Contact Wash off with soap and plenty of water. Take victim immediately to hospital. Consult a physician.
	Mask / Respirator Where risk assessment shows air-purifying respirators are appropriate use a full-face respirator with multi-purpose combination (US) or type ABEK (EN 14387) respirator cartridges as a backup to engineering controls. If the respirator is the sole means of protection, use a full-face supplied air respirator. Use respirators and components tested and approved under appropriate government standards such as NIOSH (US) or CEN (EU).		Inhalation If breathed in, move person into fresh air. If not breathing, give artificial respiration. Consult a physician.
			Injection Not Specified
How the substances associated with this process should be stored			
	Store in cool place. Keep container tightly closed in a dry and well-ventilated place. Containers which are opened must be carefully resealed and kept upright to prevent leakage.		
Have persons undertaking this process been provided with information or training?			YES
Could the release of vapour/gas/dust produce an explosive atmosphere		Not Specified	
Is the flashpoint below 32°C for any of the substances identified		Not Specified	
What to do in the event of a fire			
	For small (incipient) fires, use media such as "alcohol" foam, dry chemical, or carbon dioxide. For large fires, apply water from as far as possible. Use very large quantities (flooding) of water applied as a mist or spray; solid streams of water may be ineffective. Cool all affected containers with flooding quantities of water. Wear self contained breathing apparatus for fire fighting if necessary. Use water spray to cool unopened containers.		
Other substance that this substance(s) must not come into contact with			
Conditions to avoid: Heat, flames and sparks. Extremes of temperature and direct sunlight.			
Materials to avoid: acids, Acid chlorides, Acid anhydrides, Oxidizing agents, Alkali metals, Ammonia, Peroxides.			
What to do in the event of a spillage			
	Personal precautions: Use personal protective equipment. Avoid breathing vapors, mist or gas. Ensure adequate ventilation. Remove all sources of ignition. Evacuate personnel to safe areas. Beware of vapours accumulating to form explosive concentrations. Vapours can accumulate in low areas.		
	Environmental precautions: Prevent further leakage or spillage if safe to do so. Do not let product enter drains. Discharge into the environment must be avoided.		
	Methods and materials for containment and cleaning up: Contain spillage, and then collect with an electrically protected vacuum cleaner or by wet-brushing and place in container for disposal according to local regulations.		
How dispose of substances associated with this process			
	Toxic to aquatic life.		
	Product: Burn in a chemical incinerator equipped with an afterburner and scrubber but exert extra care in igniting as this material is highly flammable. Offer surplus and non-recyclable solutions to a licensed disposal company. Contact a licensed professional waste disposal service to dispose of this material.		
	Contaminated packaging: Dispose of as unused product.		

Health / Medical Surveillance to be undertaken when using these substances



Not Specified

Are hazards to health adequately controlled with all the above control measures in place?

Yes

Additional Notes / Summary

Current Risk

Should pose no risk to health as long as good chemical practice is employed and these instructions are followed.

LOW RISK


Overall Residual Risk

LOW RISK



Photo Gallery

NOTICE

There are currently no photographs associated with the assessment.



Record Notes / History



NOTICE

There are currently no notes associated with the assessment.

Trypan Blue WETLAB_MB334_MB524













Description of the work area and/or process activity		Persons Affected
<p>Trypan blue is a carcinogen. If not stored and handled properly, this can pose a serious threat to the health and safety of laboratory personnel, emergency responders and chemical waste handlers. Hence, it is important to follow safety protocols to handle this chemical.</p> <p>Trypan Blue is a vital stain used to selectively color dead tissues or cells blue. Live cells or tissues with intact cell membranes are not colored. Cells are very selective in the compounds that pass through the membrane. In a viable cell, trypan blue is not absorbed. However, it traverses the membrane in a dead cell. Hence, dead cells are shown as a distinctive blue color under a microscope.</p>		<p>Cleaners x 2 Postgraduate Student x 4 Staff x 4 Students x 3</p>
Company	Aston University	
Site	Life and Health Sciences	
Branch	Medical School	

Substance Name	Emergency Tel No.	Usage Information	MSDS Date	Cat
 <p>Trypan Blue solution Substance Form: Liquid</p>		<p>Method of use: Not Specified</p> <p>Duration Not Specified Frequency</p>	07/07/2010	E

Hazard Labelling	
 <p>toxic</p>	 <p>serious health haz</p>

Can a less hazardous substance(s) be used to do the same job	NO
--	----

Control Measures
<p>Contains no substances with occupational exposure limit values. Personal, workplace atmosphere or biological monitoring may be required to determine the effectiveness of the ventilation or other control measures and/or the necessity to use respiratory protective equipment.</p> <p>Use only with adequate ventilation. Use process enclosures, local exhaust ventilation or other engineering controls to keep worker exposure to airborne contaminants below any recommended or statutory limits.</p> <p>Wash hands, forearms and face thoroughly after handling chemical products, before eating, smoking and using the lavatory and at the end of the working period. Appropriate techniques should be used to remove potentially contaminated clothing. Wash contaminated clothing before reusing. Ensure that eyewash stations and safety showers are close to the workstation location.</p> <p>Emissions from ventilation or work process equipment should be checked to ensure they comply with the requirements of environmental protection legislation. In some cases, fume scrubbers, filters or engineering modifications to the process equipment will be necessary to reduce emissions to acceptable levels.</p>

Personal Protective Equipment		First Aid Measures	
	Eye Protection Safety eyewear complying with an approved standard should be used when a risk assessment indicates this is necessary to avoid exposure to liquid splashes, mists, gases or dusts.		Eye Contact Rinse thoroughly with plenty of water for at least 15 minutes and consult a physician.
	Hand Protection Chemical-resistant, impervious gloves complying with an approved standard should be worn at all times when handling chemical products if a risk assessment indicates this is necessary.		Ingestion Do NOT induce vomiting. Never give anything by mouth to an unconscious person. Rinse mouth with water. Consult a physician.
	Clothing Personal protective equipment for the body should be selected based on the task being performed and the risks involved and should be approved by a specialist before handling this product. Appropriate footwear and any additional skin protection measures should be selected based on the task being performed and the risks involved and should be approved by a specialist before handling this product.		Skin Contact Take off contaminated clothing and shoes immediately. Wash off with soap and plenty of water. Take victim immediately to hospital. Consult a physician.
	Mask / Respirator Use a properly fitted, air-purifying or air-fed respirator complying with an approved standard if a risk assessment indicates this is necessary. Respirator selection must be based on known or anticipated exposure levels, the hazards of the product and the safe working limits of the selected respirator.		Inhalation If breathed in, move person into fresh air. If not breathing, give artificial respiration. Consult a physician. The exposed person may need to be kept under medical surveillance for 48 hours.
			Injection Not Specified
How the substances associated with this process should be stored			
	Storage class (TRGS 510): Non-combustible, acute toxic Cat.3 / toxic hazardous materials or hazardous materials causing chronic effects Store in original container protected from direct sunlight in a dry, cool and well-ventilated area, away from incompatible materials. Keep container tightly closed and sealed until ready for use. Containers that have been opened must be carefully resealed and kept upright to prevent leakage. Do not store in unlabeled containers. Use appropriate containment to avoid environmental contamination. Eating, drinking and smoking should be prohibited in areas where this material is handled, stored and processed. Workers should wash hands and face before eating, drinking and smoking. Remove contaminated clothing and protective equipment before entering eating areas. Take measures to prevent the build up of electrostatic charge.		
Have persons undertaking this process been provided with information or training?			YES
Could the release of vapour/gas/dust produce an explosive atmosphere		NO	
Is the flashpoint below 32 °C for any of the substances identified		NO	
What to do in the event of a fire			
	Use water spray, alcohol-resistant foam, dry chemical or carbon dioxide. Special hazards arising from the substance or mixture: Nature of decomposition products not known. Promptly isolate the scene by removing all persons from the vicinity of the incident if there is a fire. No action shall be taken involving any personal risk or without suitable training. Do not allow run-off from fire-fighting to enter drains or water courses. Do not inhale explosion and combustion gases. Use caution when applying carbon dioxide in confined spaces. Carbon dioxide can displace oxygen. Use water spray jet to protect personnel and to cool endangered containers. Fire-fighters should wear appropriate protective equipment and self-contained breathing apparatus (SCBA) with a full face-piece operated in positive pressure mode.		
Other substance that this substance(s) must not come into contact with			
Stable under recommended storage conditions.			
Incompatible materials: Strong oxidizing agents.			
What to do in the event of a spillage			
	Wear respiratory protection. Avoid breathing vapours, mist or gas. Ensure adequate ventilation. Evacuate personnel to safe areas. Soak up with inert absorbent material and dispose of as hazardous waste. Keep in suitable, closed containers for disposal. Approach release from upwind. Prevent entry into sewers, water courses, basements or confined areas. Avoid dispersal of spilled material and runoff and contact with soil, waterways, drains and sewers. Inform the relevant authorities if the product has caused environmental pollution (sewers, waterways, soil or air). Prevent further leakage or spillage if safe to do so. Do not let product enter drains. Discharge into the environment must be avoided.		

How dispose of substances associated with this process



Dispose according to LHS waste policy. The information presented only applies to the material as supplied. The identification based on characteristic(s) or listing may not apply if the material has been used or otherwise contaminated. It is the responsibility of the waste generator to determine the toxicity and physical properties of the material generated to determine the proper waste identification and disposal methods in compliance with applicable regulations. Disposal should be in accordance with applicable regional, national and local laws and regulations.

The generation of waste should be avoided or minimized wherever possible. Waste packaging should be recycled. Incineration or landfill should only be considered when recycling is not feasible.

Offer surplus and non-recyclable solutions to a licensed disposal company.

Health / Medical Surveillance to be undertaken when using these substances



Not Specified

Are hazards to health adequately controlled with all the above control measures in place?

Yes

Additional Notes / Summary

Current Risk

To the best of our knowledge, the chemical, physical, and toxicological properties have not been thoroughly investigated.

For non-emergency personnel upon accidental release: No action shall be taken involving any personal risk or without suitable training. Evacuate surrounding areas. Keep unnecessary and unprotected personnel from entering. Do not touch or walk through spilled material. Provide adequate ventilation. Wear appropriate respirator when ventilation is inadequate. Put on appropriate personal protective equipment.

LOW/MEDIUM RISK

Overall Residual Risk

LOW/MEDIUM RISK



Photo Gallery

NOTICE

There are currently no photographs associated with the assessment.



Record Notes / History



NOTICE

There are currently no notes associated with the assessment.

Ethanol














Description of the work area and/or process activity	Persons Affected
Use and storage of Ethanol in Wetlab, MB334, MB524.	Cleaners x 6 Postgraduate Student x 5 Staff x 5 Students x 5
Company	Aston University
Site	Life and Health Sciences
Branch	Biology

Substance Name	Emergency Tel No.	Usage Information	MSDS Date	Cat
 Ethanol Substance Form: Liquid	+ 	Method of use: Used as organic solvent. Duration 3 Hours(s) Frequency When Required	09/07/2015	A

Hazard Labelling
  <div>harmful (caution) flammable</div>

Can a less hazardous substance(s) be used to do the same job	NO
--	----

Control Measures
Use explosion-proof ventilation equipment. Use adequate general or local exhaust ventilation to keep airborne concentrations below the permissible exposure limits. Facilities storing or utilizing this material should be equipped with an eyewash facility and a safety shower. Handle in accordance with good industrial hygiene and safety practice. Wash hands before breaks and at the end of workday.

Personal Protective Equipment		First Aid Measures	
	Eye Protection Face shield and safety glasses Use equipment for eye protection tested and approved under appropriate government standards such as NIOSH (US) or EN 166(EU).		Eye Contact Rinse thoroughly with plenty of water for at least 15 minutes and consult a physician.
	Hand Protection Handle with gloves. Gloves must be inspected prior to use. Use proper glove removal technique (without touching glove's outer surface) to avoid skin contact with this product. Dispose of contaminated gloves after use in accordance with applicable laws and good laboratory practices. Wash and dry hands. The selected protective gloves have to satisfy the specifications of EU Directive 89/686/EEC and the standard EN 374 derived from it. Type: butyl-rubber, 0.3mm thickness, 480min break through time (full contact) nitrile, 0.2mm thickness, 38min break through time (splash contact)		Ingestion Do NOT induce vomiting. Never give anything by mouth to an unconscious person. Rinse mouth with water. Consult a physician.
	Clothing Impervious clothing, Flame retardant antistatic protective clothing., The type of protective equipment must be selected according to the concentration and amount of the dangerous substance at the specific workplace.		Skin Contact Wash off with soap and plenty of water. Consult a physician.
	Mask / Respirator Where risk assessment shows air-purifying respirators are appropriate use a full-face respirator with multi-purpose combination (US) or type ABEK (EN 14387) respirator cartridges as a backup to engineering controls. If the respirator is the sole means of protection, use a full-face supplied air respirator. Use respirators and components tested and approved under appropriate government standards such as NIOSH (US) or CEN (EU).		Inhalation If breathed in, move person into fresh air. If not breathing, give artificial respiration. Consult a physician.
			Injection Seek medical attention.
How the substances associated with this process should be stored			
	Keep away from heat, sparks, and flame. Keep away from sources of ignition. Store in cool place. Keep container tightly closed in a dry and well-ventilated place. Containers which are opened must be carefully resealed and kept upright to prevent leakage. Storage class (TRGS 510): Flammable liquids		
Have persons undertaking this process been provided with information or training?			YES
Could the release of vapour/gas/dust produce an explosive atmosphere		YES	
Is the flashpoint below 32°C for any of the substances identified		YES	
What to do in the event of a fire			
	Use water spray, alcohol-resistant foam, dry chemical or carbon dioxide. Use water spray to cool unopened containers. As in any fire, wear a self-contained breathing apparatus in pressure-demand, MSHA/NIOSH (approved or equivalent), and full protective gear. Use water spray to keep fire-exposed containers cool. Containers may explode in the heat of a fire.		
Other substance that this substance(s) must not come into contact with			
Ignition sources, excess heat Incompatible materials: Alkali metals, Oxidizing agents, Peroxides			
What to do in the event of a spillage			
	Use personal protective equipment. Avoid breathing vapours, mist or gas. Ensure adequate ventilation. Remove all sources of ignition. Evacuate personnel to safe areas. Beware of vapours accumulating to form explosive concentrations. Vapours can accumulate in low areas. Prevent further leakage or spillage if safe to do so. Do not let product enter drains. Contain spillage, and then collect with an electrically protected vacuum cleaner or by wet-brushing and place in container for disposal according to local regulations.		
How dispose of substances associated with this process			
	Dilute in sink with excess water.		

Health / Medical Surveillance to be undertaken when using these substances



Not Specified

Are hazards to health adequately controlled with all the above control measures in place?

Yes

Additional Notes / Summary

Current Risk

Reproductively toxic to females through ingestion.
Can cause newborn drug dependance.

LOW/MEDIUM RISK

Overall Residual Risk

LOW/MEDIUM RISK



DSEAR Assessment Details for COSHH Assessment - 2304CA

1. Does a activity need to be assessed under DSEAR

Could the release of vapour/gas/dust produce an explosive atmosphere	YES
Is the flashpoint below 32 °C	YES

2. Assessing Possible Failures:

List any work systems or activities that could fail resulting in a fire or explosion, e.g. valves, gaskets, etc	List any sources of ignition
Accidental spillage in lab.	Electric.

3. Existing control measures for identifying hazards:

Has the quantity of substance being held/ used been reduced to a minimum?	YES
APPROXIMATE QUANTITY	
2.5L	
Have steps been taken to avoid or minimise intentional or unintentional release	YES
DETAILS	
Reagent is stored in a sealed bottle within a ventilated metal cabinet.	
Reagent is used within an efficient chemical fume cupboard.	
Have steps been taken to control release at sources	YES
DETAILS	
Reagent is purchased in limited quantity and used in an efficient chemical fume cupboard with no local source of ignition.	
Have steps been taken to prevent the formation of an explosive atmosphere?	YES
DETAILS	
Substance is handled in an efficient chemical fume cupboard.	
Have steps been taken to collect, contain and remove any releases to a safe place, e.g. by ventilation?	YES
DETAILS	
Substance is handled in an efficient chemical fume cupboard.	
Have steps been taken to avoid adverse conditions, e.g. exceeding temperature limits, control settings?	YES
DETAILS	
Substance is handled in an efficient chemical fume cupboard.	
The substance is used according to accepted synthetic chemical procedures.	
Are incompatible substances kept apart in storage and in use, so far as is practicable, e.g. flammables and oxidisers?	YES
DETAILS	
The substance is stored separately to oxidisers.	
Have the number of employees exposed to the dangerous substances or explosive atmosphere been reduced to the minimum	YES
DETAILS	
Substance is only used by experienced operators.	
Has plant been supplied that is explosion resistant	N/A
Is there explosion suppression or relief provided on equipment	N/A
DETAILS	
No Details Given	
Have adequate measures been taken to control or minimise the spread of fire or explosion	YES
DETAILS	
Substance is handled in an efficient chemical fume cupboard.	
Has suitable PPE been provided and have operatives been trained on how to use it?	YES
DETAILS	
Substance is only used by experienced operators.	

4. Management Issues

Is the workplace designed, constructed and maintained, so as to provide adequate fire resistance and/or explosion relief?	YES
Is a permit to work scheme used for working with the substance(s) or in the work area and are these strictly enforced?	YES

In the case of explosive atmospheres continue, if not proceed to section 5.

Have all areas been classified into zones in accordance with schedule 2 of the regulations?	Not Specified
Where necessary have all classified zones been marked at their entry points with the specified "EX" hazard warning sign?	Not Specified
DETAILS	
No Details Given	
Are all classified zones appropriately protected from sources of ignition, through the selection of equipment & protective systems compliant with the equipment & protective systems intended for use in potentially explosive atmospheres regulations 1996?	Not Specified
Have classified zones, before their first operation, been verified as being safe, by a person or organisation competent in the field of explosion protection?	Not Specified
Are employees working in classified zones provided with clothing that does not create a risk of electrostatic discharge?	Not Specified
DETAILS	
No Details Given	

5. Storage

Are all flammable substances kept in a suitable fire resistant store?	YES
DETAILS	
Substance is stored in a flameproof ventilated cabinet.	
Are all quantities in excess of 50 litres kept in a dedicated and appropriately protected flammable store?	N/A
DETAILS	
No Details Given	
Are all petroleum spirits or derivatives in excess of 50 litres kept in a dedicated and appropriately protected petroleum store?	N/A
DETAILS	
No Details Given	
Where appropriate have storage areas been designed to provide explosion relief/resistance?	N/A
Are all incompatible substances stored apart, e.g. flammable, oxidisers, LPG, flammable gasses, combustibles, etc?	YES

6. Emergency procedures

Have suitable procedures been developed and communicated to staff to deal with

Adverse process conditions, e.g. exceeding temperature limits, control settings, etc?	N/A
LOCATION / REFERENCE OF THE PROCEDURE DOCUMENTATION	
No Details Given	
Fire and evacuation?	YES
LOCATION / REFERENCE OF THE PROCEDURE DOCUMENTATION	
See university evacuation procedure	
The spillage of dangerous substances	YES
LOCATION / REFERENCE OF THE PROCEDURE DOCUMENTATION	
See COSHH assessment	

7. Waste disposal

Have suitable procedures been developed and communicated to staff to deal with the safe transport of dangerous substances?	YES
Have suitable procedures been developed and communicated to staff to deal with the safe disposal of dangerous substances and contaminated materials?	YES

8 Information, instruction, supervision and training

Have the product details been communicated to all staff?	YES
Has the safe system of work been communicated to all staff	YES
Are only trained and competent persons involved in work with dangerous substances	YES
PLEASE PROVIDE DETAILS	
The substance is used in the medicinal chemistry research laboratory.	

Photo Gallery

NOTICE

There are currently no photographs associated with the assessment.

Record Notes / History



NOTICE


There are currently no notes associated with the assessment.



Pennicillin/Streptomycin










Description of the work area and/or process activity	Persons Affected
Pennicillin/Streptomycin is routinely used as an antibiotic component of media for tissue culture in MB334, MB524 and wetlab.	Cleaners x 6 Postgraduate Student x 5 Staff x 5 Students x 4
Company	Aston University
Site	Life and Health Sciences
Branch	Biology

Substance Name	Emergency Tel No.	Usage Information	MSDS Date	Cat
 PEN-STREP, LIQ., 10,000 Substance Form: Liquid		Method of use: This substance is used in small volumes and transferred from one vessel to another by using a serological pipette. Duration 5 Minute(s) Frequency When Required	15/04/2010	C

Hazard Labelling
 irritant

Can a less hazardous substance(s) be used to do the same job	NO
--	----

Control Measures
Only authorised personnel to enter the laboratory. Only trained personnel to use the substance. Ensure adequate ventilation, especially in confined areas. Handle in accordance with good industrial hygiene and safety practice

Personal Protective Equipment		First Aid Measures	
	Eye Protection safety glasses with side-shields		Eye Contact Rinse immediately with plenty of water, also under the eyelids, for at least 15 minutes
	Hand Protection impervious gloves.		Ingestion Never give anything by mouth to an unconscious person
	Clothing Lab coat buttoned up.		Skin Contact Wash off immediately with plenty of water
	Mask / Respirator In case of insufficient ventilation wear suitable respiratory equipment		Inhalation Move to fresh air
			Injection Not Specified


How the substances associated with this process should be stored

	Keep in properly labelled containers
--	--------------------------------------

Have persons undertaking this process been provided with information or training?	YES
---	-----

Could the release of vapour/gas/dust produce an explosive atmosphere	Not Specified
Is the flashpoint below 32°C for any of the substances identified	Not Specified

What to do in the event of a fire

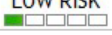
	dry chemical. Wear self-contained breathing apparatus and protective suit.
--	---

What to do in the event of a spillage

	Use personal protective equipment Soak up with inert absorbent material.
--	---

How dispose of substances associated with this process

	Dispose of in accordance with local regulations.
--	--

Are hazards to health adequately controlled with all the above control measures in place?	Yes
Additional Notes / Summary	Current Risk
This substance presents no risk to health as long as good chemical practice is observed.	LOW RISK 

Overall Residual Risk

LOW RISK




Photo Gallery

NOTICE



There are currently no photographs associated with the assessment.


NOTICE

There are currently no notes associated with the assessment.










Teepol Bleach - Storage and Use WETLAB_MB334_MB524

Description of the work area and/or process activity	Persons Affected
The use of bleach for cleaning.	Cleaners x 2 Postgraduate Student x 4 Staff x 4 Students x 3
Company	Aston University
Site	Life and Health Sciences
Branch	Biology

Substance Name	Emergency Tel No.	Usage Information	MSDS Date	Cat
 Teepol Multipurpose Detergent Substance Form: Liquid		Method of use: Use only as directed on the container or label. Provide good ventilation in working area. Wash hands after use and do not allow to enter surface water drains. Store only in original containers out of reach of children. Storage temperature should be between 5°C and 30°C. Duration 10 Minute(s) Frequency Weekly	28/02/2007	C


Hazard Labelling
 


Can a less hazardous substance(s) be used to do the same job	NO
Control Measures	
Not Specified	


Personal Protective Equipment		First Aid Measures	
	Eye Protection Tightly fitting safety goggles.		Eye Contact Irrigate with water for 10 to 15 minutes until irritation subsides. If irritation persists seek medical attention.
	Hand Protection Handle with gloves. Use proper glove removal technique to avoid skin contact.		Ingestion If conscious, give plenty of water to drink, do not induce vomiting, obtain medical attention immediately.
	Clothing Complete suit protecting against chemicals.		Skin Contact Wash splashes from skin immediately. If skin becomes sore or inflamed seek medical attention.
	Mask / Respirator Provide adequate ventilation.		Inhalation Ensure supply of fresh air and seek medical attention.
			Injection Not Specified


How the substances associated with this process should be stored	
	Store only in original containers out of reach of children. Storage temperature should be between 5°C and 30°C.

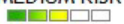
Have persons undertaking this process been provided with information or training?		YES
Could the release of vapour/gas/dust produce an explosive atmosphere	NO	
Is the flashpoint below 32°C for any of the substances identified	NO	

What to do in the event of a fire	
	Wear self-contained breathing apparatus and protective clothing as appropriate to the associated fire.

What to do in the event of a spillage	
	Remove contaminated clothing. Small spillages may be flushed to a foul drain. Wash splashes from skin immediately. If skin becomes sore or inflamed seek medical attention. Irrigate with water for 10 to 15 minutes until irritation subsides. If irritation persists seek medical attention.

How dispose of substances associated with this process	
	When disposing of surplus or waste product use suitable PPE etc. ensuring empty containers are rinsed out and disposed of safely. Do not allow product to enter land or surface water drains. Dispose of in accordance with local authority regulations. Do not mix with other waste materials.

Health / Medical Surveillance to be undertaken when using these substances	
	Not Specified

Are hazards to health adequately controlled with all the above control measures in place?	Yes
Additional Notes / Summary	Current Risk
Should pose no risk to health as long as good chemical practice is observed and the specific instructions given in this COSHH Assessment are adhered to.	MEDIUM RISK 

Overall Residual Risk

MEDIUM RISK



[Photo Gallery](#)

NOTICE

There are currently no photographs associated with the assessment.

[Record Notes / History](#)

NOTICE

There are currently no notes associated with the assessment.

B

Non Cataractous eye surgery feedback

Non cataractous porcine eye

Year of Training:		No. of Cases performed:
2		0-50 50-100 100-200 X 200-300 300-500 500-1000 1000 +
Surgical Step/Tissue	Score 1 – 5 (worst to best)	Comments
Cornea	4	Clear, thicker and slightly tougher than human cornea. Need to adjust incision architecture.
Incisions	4	
Iris	2	Iris is slightly floppy and pupil is generally small. It may respond to intracameral mydriatic like phenylephrine. Would work well as model for floppy iris cases.
Lens capsule	4	Thicker and tougher than human capsule. Very elastic like young human capsule. Although it is not close to routine senile cataract cases it does simulate a tense and elastic capsule well and would be good to challenge these skills.
Continuous Curvilinear Capsulorhexis	4	
Hydro Dissection	2	Lens is soft and essentially normal so hydrodissection is easier. It is therefore difficult to judge how good your technique is.
Phacoemulsification	2	The lens is soft and no phaco-power is required to remove the lens, however this is a good simulation where a young patient may require cataract surgery.
Soft Lens Matter Removal	1	Essentially no soft lens matter remnants as nucleus is so soft.
Intra ocular lens insertion	5	Very realistic anatomical dimensions therefore very realistic.
General/Other		Anatomical dimensions are close to human so it is a good simulation tool.

C

Cataractous eye surgery feedback

Cataractous porcine eye

Year of Training:		No. of Cases performed:
2		0-50 50-100 100-200 X 200-300 300-500 500-1000 1000 +
Surgical Step/Tissue	Score 1 – 5 (worst to best)	Comments
Cornea	2	The cornea appeared to be decompensating, view became difficult during procedure
Incisions	4	
Iris	2	Iris is slightly floppy and pupil is generally small. It may respond to intracameral mydriatic like phenylephrine. Would work well as model for floppy iris cases.
Lens capsule	4	Brittle and easy to create a capsulorhexis. More similar to a senile lens capsule.
Continuous Curvilinear Capsulorhexis	4	As above
Hydro Dissection	2	Not able to perform effectively likely due to the posterior nature of the induced cataract.
Phacoemulsification	2	Posterior cataract. Anterior of lens was quite soft with the posterior aspect being very dense and difficult to phacoemulsify.
Soft Lens Matter Removal	1	Minimal soft lens matter, however difficult to judge extent as the corneal view was compromised.
Intra ocular lens insertion	5	Very realistic anatomical dimensions therefore very realistic.
General/Other		The cataract model does indeed provide a new challenge. It is difficult to gauge the utility in view of the poorer corneal view.